NEUROPROTECTIVE STUDIES ON THE MPTP AND SOD1 MOUSE MODELS OF NEURODEGENERATIVE DISEASES

Christine V. Fontanilla

Submitted to the faculty of the University Graduate School
in partial fulfillment of the requirements
for the degree
Doctor of Philosophy
in the Department of Medical Neurosciences,
Indiana University

February 2012

Accepted by the Faculty of Indiana University, in partial
fulfillment of the requirements for the degree of Doctor of Philosophy.

Martin R. Farlow, M.D., Chair

Yansheng Du, Ph.D.

Doctoral Committee

Xiaoming Jin, Ph.D.

December 19, 2011

Zao C. Xu, M.D., Ph.D.

DEDICATION

This dissertation work is dedicated to my family, who has been my emotional anchor and source of encouragement throughout my life: my wonderful parents, Dr. Abraham Fontanilla and Dr. Angelita Fontanilla, who emphasized the importance of education, hard work, and perseverance; my awesome brother, Anthony, who showed me the importance of getting more out of life and following your life's passion.

I love you!

ACKNOWLEDGEMENTS

I would like to thank my advisor, Dr. Yansheng Du, who is a great mentor and a good friend. His guidance, teachings, and trust have helped me grow as a scientist and have given me the confidence and strength to accomplish my career goals. I would next like to thank Dr. Martin Farlow, who has always provided an invaluable clinical perspective, allowing me to constantly keep in mind the “bigger picture” of my project and the purpose of scientific research. I would also like to thank my committee members: Dr. Xiaoxi Qiao, Dr. Xiaoming Jin, and Dr. Joe Xu. Their insightful comments and advice were instrumental in the success of my project’s progress and completion.

I would like to thank the past members of the Du Laboratory, Dr. Zhizhong Ma and Dr. Liming Zhao, for their technical expertise and training for my project. I want to especially thank Dr. Xing Wei and Dr. Huiying Gu for not only being fantastic co-workers but extremely supportive friends. I will greatly miss our daily conversations.

I would like to thank everyone in the Medical Neurosciences Program, the Department of Neurology, and the IUPUI Graduate Office, especially Dr. Gerry Oxford, Dr. Sherry Queener, Nastassia Belton, and Debra Barker.

Last but not least, I would like to thank my family: my parents and role models, Abe and Angie, and my brother, Anthony. Without them, none of this would be possible.

ABSTRACT

Christine V. Fontanilla

NEUROPROTECTIVE STUDIES ON THE MPTP AND SOD1 MOUSE MODELS OF NEURODEGENERATIVE DISEASES

The main, underlying cause of neurodegenerative disease is the progressive loss of neuronal structure or function, whereby central and/or peripheral nervous system circuitry is severely and irreversibly damaged, resulting in the manifestation of clinical symptoms and signs. Neurodegenerative research has revealed many similarities among these diseases: although their clinical presentation and outcomes may differ, many parallels in their pathological mechanisms can be found. Unraveling these relationships and similarities could provide the potential for the discovery of therapeutic advances such that a treatment for one neurologic disease may also be effective for several other neurodegenerative disorders. There is growing awareness that due to the complexity of pathophysiological processes in human disease, specifically targeting or inactivating a single degenerative process or a discrete cellular molecular pathway may be ineffective in the treatment of these multifaceted disorders. Rather, potential therapeutics with a multi-target approach may be required to successfully and effectively control disease progression. Recent advances in neurodegenerative research involve the creation of animal disease models that closely mimic their human counterparts. The use of both toxin-

exposure and genetic animal models in combination may give insight into the underlying pathologic mechanisms of neurodegenerative disorders (target identification) leading to the development and screening of prospective treatments and determination of their neuroprotective mechanism (target validation). Taken together, ideal candidates for the treatment of neurodegenerative disease would need to exert their neuroprotective effect on multiple pathological pathways. Previous studies from this laboratory and collaborators have shown that the naturally-occurring compound, caffeic acid phenethyl ester (CAPE), is efficacious for the treatment against neurodegeneration. Because of its versatile abilities, CAPE was chosen for this study as this compound may be able to target the pathogenic pathways shared by two different animal models of neurodegeneration and may exhibit neuroprotection. In addition, adipose-derived stem cell conditioned media (ASC-CM), a biologically-derived reagent containing a multitude of neuroprotective and neurotrophic factors, was selected as ASC-CM has been previously shown to be neuroprotective by using both animal and cell culture models of neurodegeneration.

Martin R. Farlow, M.D., Chair

TABLE OF CONTENTS

Page

Page

Page

Page

Page

Page

LIST OF TABLES

Page

LIST OF FIGURES

Page

Page

Page

Page

Page

LIST OF ABBREVIATIONS

6-OHDA	6-hydroxydopamine
AIF	apoptosis-inducing factor
ALS	amyotrophic lateral sclerosis
ALS-TDI	ALS Therapy Development Institute
AMPA	α-amino-3-hydroxy-5-methyl-4-isoxazolepropionic acid
ANOVA	analysis of variance
ARE	antioxidant response element
ASC-CM	adipose-derived stem cell conditioned media
ATP	adenosine triphosphate
BDNF	brain-derived neurotrophic factor
BME	basal media Eagle
CAPE	caffeic acid phenethyl ester
CGN	cerebellar granule neurons
CNS	central nervous system
COMT	catechol-O-methyltransferase
CSF	cerebrospinal fluid
DA	dopamine
DAB	3,3′-diaminobenzidine tetrahydrochloride
DAT	dopamine transporter
DHE	dihydroethidium
DHR	dihydrorhodamine

EAAT	excitatory amino acid transporter
EDTA	ethylenediaminetetraacetic acid
EGTA	ethylene glycol tetraacetic acid
ER	endoplasmic reticulum
GFAP	glial fibrillary acidic protein
GPe	external globus pallidus
GPi	internal globus pallidus
GTP	guanosine triphosphate
H_2O_2	hydrogen peroxide
HO-1	heme oxygenase-1
HPLC	high-performance liquid chromatography
HRP	horseradish peroxidase
Iba-1	ionized calcium binding adaptor molecule
IGF-1	insulin-like growth factor
IκB	inhibitor of kappaB
IL-1β	interleukin-1beta
IL-6	interleukin-6
Keap1	Kelch-like ECH-associated protein 1
L-dopa	L-3,4-dihydroxyphenylalanine
MAO-B	monoamine oxidase B
MAP2	microtubule-associated protein 2
MAPK	mitogen activated protein kinase
$MgCl_2$	magnesium chloride

MPP^+	1-methyl-4-phenylpyridinium
$MPDP^+$	1-methyl-4-phenyl-2,3-dihydropyridinium
$MPPP^+$	1-methyl-4-phenyl-4-propionoxypiperidine
MPTP	1-methyl-4-phenyl-1,2,3,6-tetrahydropyridine
NF-κB	nuclear factor kappa-light-chain-enhancer of activated B cells
NMDA	N-methyl D-aspartate
Nrf2	nuclear factor E2-related factor 2
iNOS	inducible nitric oxide synthase
PBS	phosphate buffered saline
PD	Parkinson's disease
PEG-400	polyethylene glycol-400
RIPA	radio-immunoprecipitation assay
RMN	rostral mesencephalic neurons
ROS	reactive oxygen species
SEM	standard error of the mean
SNpc	substantia nigra pars compacta
SOD1	[copper, zinc] superoxide dismutase 1
TH	tyrosine hydroxylase
TNF-α	tumor necrosis factor-alpha
VMAT	vesicular monoamine transporter
WT	wild type

CENTRAL HYPOTHESIS

If two neurodegenerative disorder animal models share the same downstream underlying pathogenic pathways, then a compound targeting those pathways should be beneficial for both animal models.

EXPLORATORY STUDY: If two different classes of reagents target the same downstream pathogenic pathways involved in neurodegenerative disease, then these two reagents should be beneficial in the same neurodegenerative animal model.

SECTION 1: To determine if administering a compound that has effects on multiple downstream pathways in beneficial in a neurotoxin-induced animal model of neurodegenerative disease. This section tested the first sub-hypothesis that CAPE is beneficial in a toxin model of neurodegeneration.

SECTION 2: To determine if administering the same compound is beneficial in a genetic animal model of neurodegenerative disease. This section tested the second sub-hypothesis that CAPE is beneficial in a genetic model of neurodegeneration.

SECTION 3: To determine if administering a biologically-derived reagent is an effective treatment in that genetic animal model of neurodegenerative disease. This section is comprised of the pilot study experiments for the proposed Exploratory Study, the effect of adipose-derived stem cell conditioned media on a genetic animal model of neurodegeneration.

CHAPTER 1: Caffeic Acid Phenethyl Ester Prevents 1-Methyl-4-phenyl-1,2,3,6-tetrahydropyridine-induced Neurodegeneration

1.1. Rationale

Previous studies and preliminary experiments by this laboratory and collaborators have demonstrated the efficacy of utilizing a propolis-isolated component, caffeic acid phenethyl ester (CAPE), for the treatment of neurodegenerative disease by using animal models (Wei *et al.*, 2004); and, the exploration of CAPE's neuroprotective mechanisms have been documented with the use of cell culture systems of neuronal death (Wei *et al.*, 2004; Noelker *et al.*, 2005; Ma *et al.*, 2006). CAPE is posited to be neuroprotective by way of a host of protective abilities against neuronal cell death mechanisms commonly shared among neurodegenerative disease etiology and progression, including anti-inflammatory, anti-oxidant, and immunomodulatory properties (Scapagnini *et al.*, 2011). Because of CAPE's multi-faceted protective abilities during the disease or injured state, the present research in Chapter 1 sought to examine the effects of CAPE treatment on an animal model of Parkinson's disease (PD). The 1-methyl-4-phenyl-1,2,3,6-tetrahydropyridine (MPTP) mouse model of PD was utilized to examine the effects of CAPE, as this model exhibits consistent neurodegeneration and dopaminergic cell loss specific to the brain area of interest with minimal-to-no collateral damage to surrounding brain regions, as neuronal cell death due to systemically-administered MPTP is found to be restricted to the nigrostriatal circuit and not other dopaminergic systems

(Langston and Irwin, 1986). There are currently a very limited number of effective treatments available for the human PD patient to curb disease development or progression. Additionally, with a projected over-65 U.S. population doubling by 2030 (http://www.census.gov/population/www/projections/usinterimproj, Accessed September 2011) and aging being a significant risk factor for PD (Hickey and Stacy, 2011), the development of effective treatments for PD becomes increasingly important with every upcoming decade. Results from this study would provide evidence for the potential of CAPE treatment for PD-associated neurodegeneration and determine CAPE's targets and mechanisms of action to further its prospective use in the PD patient.

1.2. Abstract

Parkinson's disease is associated with the loss of dopaminergic neurons in the substantia nigra and decreased striatal dopamine levels. This study now reports that caffeic acid phenethyl ester (CAPE), an active component of propolis, attenuated dopaminergic neurodegeneration and dopamine loss in an MPTP mouse model of Parkinson's disease. The neuroprotective effect of CAPE was associated with marked reductions in iNOS and caspase-1 expression. Additionally, CAPE inhibited MPP^+-induced neurotoxicity *in vitro* and directly inhibited MPP^+-induced release of cytochrome *c* and apoptosis inducing factor (AIF) from mitochondria. Thus, CAPE may have beneficial effects in slowing or preventing the progression of Parkinson's disease and other neurodegenerative disorders.

CV Fontanilla, Z Ma, X Wei, J Klotsche, L Zhao, P Wisniowski, W Lee, RC Dodel, MR Farlow, WH Oertel, Y Du. 2011. Caffeic acid phenethyl ester prevents 1-methyl-4-phenyl-1,2,3,6-tetrahydropyridine-induced neurodegeneration. *Neuroscience* 188:135-41.

1.3. Introduction

1.3.1. Parkinson's Disease

In 1817, *An Essay on the Shaking Palsy* by James Parkinson (Parkinson, 1817) was the first written work describing "paralysis agitans" in 6 patients afflicted with this disease (Eyles, 1955) that was renamed by Jean-Martin Charcot 60 years later as "Parkinson's disease" (PD; Morris *et al.*, 1955). PD is a common neurodegenerative disorder, second in incidence only to Alzheimer's disease (http://ninds.nih.gov/disorders/parkinsons_disease, Accessed September 2011), that is characterized by a progressive loss of dopaminergic neurons in the substantia nigra pars compacta (SNpc; Pakkenberg *et al.*, 1991), which results in the extrapyramidal motor dysfunction leading to the hallmark clinical symptoms of PD – resting tremor, bradykinesia, rigidity, and postural instability, including cognitive impairment at later stages of the disease (Antal *et al.*, 1998; Leenders and Oertel, 2001; Galvin 2006; Stacy 2009; Hickey and Stacy, 2011; Yokoyama *et al.*, 2011).

PD is strongly associated with aging and incidence increases with age (Hickey and Stacy, 2011). Incidence rates of PD quadruple with age when comparing individuals between 55 – 65 years of age versus those 85 years and older (Baldereschi *et al.*, 2000). The average age of onset is 60 years. Although 1% of the population older than 60 years are affected (over 1.2 million individuals; Fahn and Przedborski, 2010) and nearly 50,000 new cases per year are diagnosed in the U.S. alone (http://ninds.nih.gov/disorders/parkinsons_disease, Accessed September 2011),

it has been difficult to get an accurate number as diagnoses is hampered by the lack of definitive tests for PD as well as the presence of misdiagnoses. PD is diagnosed in approximately 50% more males than females (Baldereschi *et al.*, 2000), however aging is the greatest risk factor (http://ninds.nih.gov/disorders/parkinsons_disease, Accessed September 2011; Hickey and Stacy, 2011).

1.3.2. Neurochemical and Neuropathological Changes in PD

The neuropathology of PD is characterized by death of dopaminergic neurons residing in the SNpc. Within these degenerating cells, there is accumulation of cytoplasmic inclusions (Lewy bodies) that were shown to contain alpha-synuclein, parkin, ubiquitin, chaperone proteins, and phosphorylated components of the neuronal cytoskeleton (Jellinger, 2009). When approximately 50% cell death of dopaminergic neurons and 80% depletion of striatal dopamine occurs, manifestation of the characteristic primary motor symptoms of PD begins (German *et al.*, 1989; Marsen, 1990; Agid, 1991). PD pathophysiology involves the progressive disruption of the normal function and anatomy of the basal ganglia (Hickey and Stacy, 2011). Under normal, physiologic conditions and regardless of the presence of body movements, there is a continuous and constant firing of dopaminergic neurons in the SNpc resulting in steady levels of dopamine in the striatum, which leads to persistent activation of striatal dopamine receptors (Grace and Bunney, 1983, 1984; Venton *et al.*, 2003). In PD, the progressive loss of dopaminergic neurons in the SNpc (Hirsch *et al.*, 1988;

Fearnley and Lees, 1991) decreases nigro-striatal dopaminergic content and signaling via D1 and D2 receptors, resulting in the disinhibition of the external globus pallidus (GPe), which leads to disinhibition of the subthalamic nucleus. Progressive disruption and degeneration of the dopaminergic nigro-striatal pathway permanently alters the neural circuitry of the basal ganglia, causing the primary motor symptoms of PD to manifest (Fig 1.1; Hamani and Lozano, 2006; Blandini *et al.*, 2000).

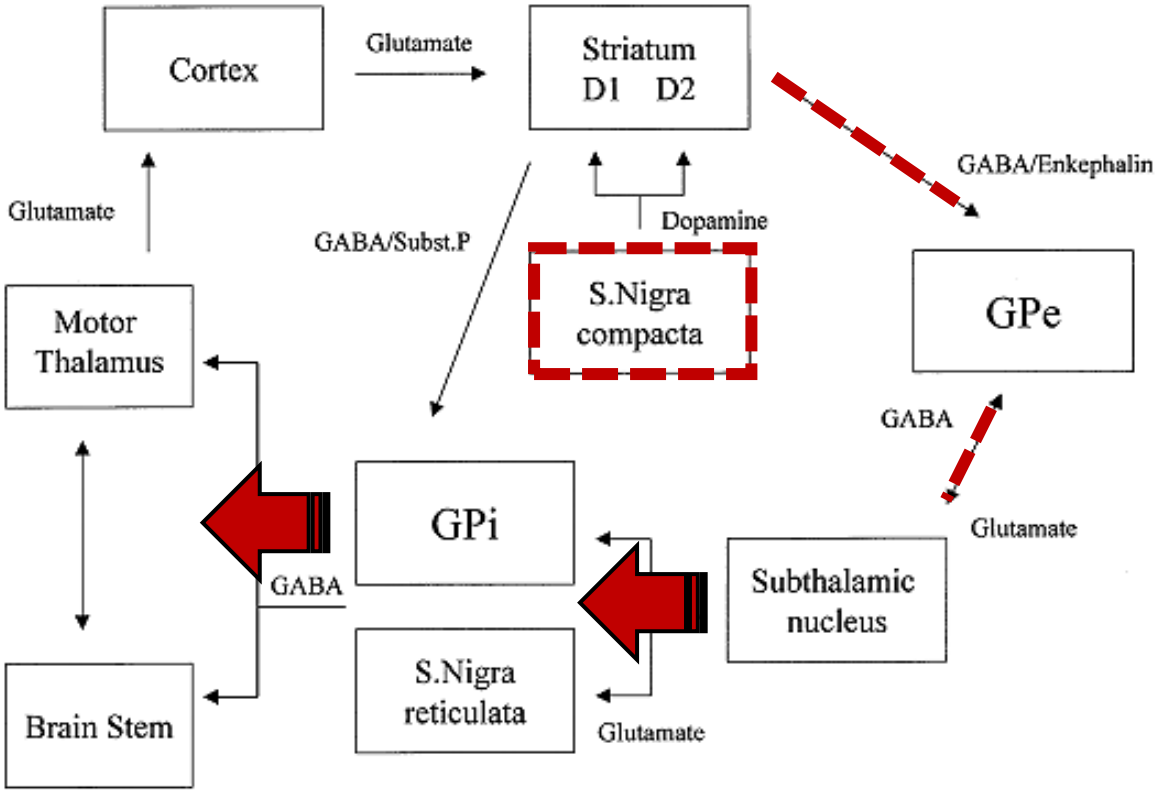

Adapted from Hamani and Lozano, 2006

Figure 1.1. Schematic of the proposed neural network affected by PD.

In PD, neurodegeneration begins in the substantia nigra pars compacta, where significant dopaminergic cell death occurs, leading to a decrease in dopamine release to the striatum. The characteristic dopamine (DA) loss affects both the direct and indirect pathways involving output from the external globus pallidus (GPe) and internal globus pallidus (GPi) and substantia nigra reticulata, respectively. Disruption of these neural outputs ultimately results in the characteristic movement disorders observed in PD. Dotted lines and large block arrows represent the major neural pathways affected in PD.

1.3.3. Current Treatments for PD

Currently, there is no neuroprotective drug available to alter, reverse, or slow disease onset or progression (Quinn, 1998). PD drug development is immensely challenged due to the expected population doubling of the over-65 age group by 2030 in the U.S. alone (http://ninds.nih.gov/disorders/parkinsons_disease, Accessed September 2011) and the lack of specific disease biomarkers or etiology. Because the causes of PD initiation are yet unknown, present treatments can only be applied after disease onset, when primary motor symptoms have increased in severity and significant, irreversible dopaminergic neuronal death has occurred. Since the initial description and first diagnosis of PD almost 200 years ago (Parkinson, 1817; Eyles, 1955; Morris *et al.*, 1955), the currently available treatments for this disease are only directed towards the alleviation of both the primary motor and/or late-stage non-motor symptoms of the PD patient.

The search for novel therapeutics as well as definitive management of disease remains elusive at both the basic science and clinical levels. In addition, most available treatments are currently unable to address the permanent neuronal death that occurs in PD, and a majority only target one aspect of the disease's neuronal death mechanisms. Nevertheless, drug discovery research over the years continues to add to the repertoire of information on PD and its underlying neuronal death mechanisms.

1.3.3.1. *Drug Treatments*

1.3.3.1.1. *L-3,4-dihydroxyphenylalanine*

L-3,4-dihydroxyphenylalanine (L-dopa) therapy is currently the most widely used and most successful treatment for PD, especially for patients in the early stages of the disease (Hoehn, 1992). L-Dopa can be administered intravenously, via enteral infusion, or orally. Active transport allows this dopamine precursor to cross the blood-brain barrier (Kincses and Vescei, 2011). L-Dopa is usually given concurrently with a peripheral decarboxylase inhibitor and/or a cathechol-O-methyl transferase inhibitor in order to block conversion of L-dopa to dopamine in the periphery and peripheral inactivation of L-dopa, respectively, resulting in the maintenance of dopamine bioavailability (Hoehn, 1992; Lyons and Pahwa, 2006; Wichers *et al.*, 2008). Although treatment with L-dopa alleviates the motor symptoms of PD by way of providing a peripherally-administered source of dopamine to a dopamine-depleted environment, this treatment was found to be associated with motor and psychiatric side effects (Merello *et al.*, 1996). Most importantly, it is unable to prevent the death of dopaminergic neurons.

1.3.3.1.2. *Monoamine Oxidase B Inhibitors*

The physiologic function of monoamine oxidases is to catalyze the oxidative deamination of monoamines, such as dopamine. These enzymes are embedded in the outer membrane of the mitochondrion, where they play key roles in dopamine degradation (Edmondson *et al.*, 2004; Tipton *et al.*, 2004). The

B isoenzyme, monoamine oxidase B (MAO-B), is the more prevalent form of monoamine oxidase present in the neurons and glial cells of the human central nervous system (Edmondson *et al.*, 2007). Irreversible inhibitors of MAO-B, selegiline and rasagiline, were found to have neuroprotective effects in animal models of PD (Kupsch *et al.*, 2001; Blandini *et al.*, 2004) via blockage of monoamine oxidase activity. However, most drugs targeting preservation of dopamine levels in the brain do not prevent the neuronal death observed in PD.

1.3.3.1.3. *Dopamine Agonists*

Dopamine agonists directly stimulate dopamine receptors by binding to them in place of dopamine (Stacy and Galbreath, 2008). This functional aspect presents a clear advantage over therapies such as L-dopa as dopaminergic receptors can be directly activated in the absence of dopamine and the effects of these agonists is independent of the existing population of dopaminergic neurons and dopamine metabolism (Kincses and Vecsei, 2010). Dopamine agonists have demonstrated neuroprotection in animal and cell culture models of neurodegeneration by reducing components responsible for oxidative stress, such as free radicals, via upregulation of enzymes with anti-oxidative function (Kondo *et al.*, 1994; Ogawa *et al.*, 1994; Nishibayashi *et al.*, 1996; Finotti *et al.*, 2000; Yoshioka *et al.*, 2002). However, regarding treatment of the PD patient, there is modest benefit for symptoms versus L-dopa and a higher incidence of impulse control disorders, which can have significant negative consequences on the life of the PD patient (Driver-Dunckley *et al.*, 2003; Weintraub *et al.*, 2006;

Evans *et al.*, 2009; Weintraub *et al.*, 2010). Although dopamine agonists can help maintain the dopaminergic neurocircuitry in the PD patient regardless of the presence of dopamine level reduction and the amount of dopaminergic neuron loss, these compounds do not alter or block the underlying neuronal death.

1.3.4. Caffeic Acid Phenethyl Ester

Caffeic acid phenethyl ester (CAPE) is a naturally-derived polyphenolic compound and the biologically active component isolated from propolis, which is a popular folk medicine derived from conifer tree bark and is utilized by honeybees for hives (Grunberger *et al.*, 1988; Natarajan *et al.*, 1996; Nagai *et al.*, 2003; Scapagnini *et al.*, 2011). CAPE is small and lipid soluble with structural similarity to the flavonoids (Spencer, 2008; Korish and Arafa, 2011). Because of its lipophilicity, CAPE can easily cross cell membranes and enter cells upon systemic administration, such as intraperitoneal injection (Yildiz *et al.*, 2009). Several studies have shown that CAPE has anti-inflammatory, anti-oxidant, and immunomodulatory properties (Grunberger *et al*., 1988; Su *et al*., 1991, 1994; Michaluart *et al.*, 1999; Russo *et al.*, 2002; Son and Lewis, 2002; Wei *et al*., 2004; Tan *et al.*, 2005; Iraz *et al.*, 2006; Gokce *et al.*, 2009; Aygun *et al.*, 2011; Gocer and Gulcin, 2011; Korish and Arafa, 2011).

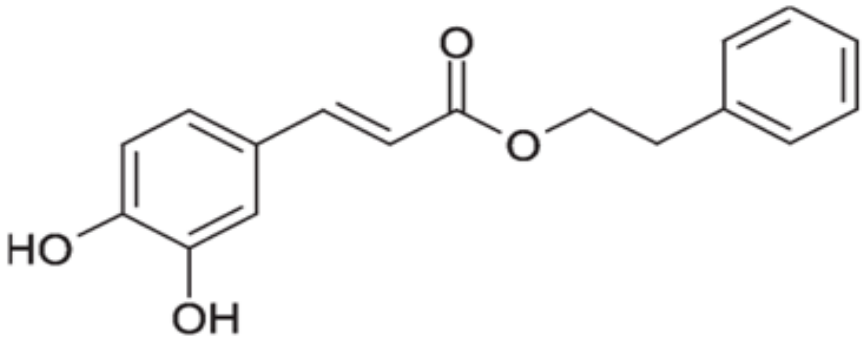

Figure 1.2. CAPE chemical structure.

Studies utilizing fluorine substitution for hydrogens in CAPE were designed to evaluate CAPE derivatives and their cytoprotective activity. It was observed that the 3' and 4' hydroxyl (-OH) groups within CAPE's catechol ring were important for the compound's anti-oxidant ability (Wang *et al.*, 2010).

One posited property underlying CAPE's numerous protective biological activities is its ability to inhibit the nuclear transcription factor, nuclear factor kappa-light-chain-enhancer of activated B cells (NF-κB; Natarajan *et al.*, 1996; Orban *et al.*, 2000; Lee *et al.*, 2010). The exact mechanism by which CAPE inhibits NF-κB is currently unknown. NF-κB plays an important transcriptional role in the regulation of genes involved in inflammation and immune function (Li and Verma, 2002). Under non-pathologic conditions, the NF-κB protein heterodimer (Urban *et al.*, 1991) is sequestered in the cytosol in an inactive state and bound to inhibitor of κB (IκB). Upon stimulation by pathogenic signals, such as pro-inflammatory or oxidative stress conditions outside the cell, IκB is phosphorylated by IκB kinase and subsequently degraded, allowing for the release and nuclear translocation of NF-κB (Natarajan *et al.*, 1996). Within the nucleus, NF-κB activity

leads to the production of biological mediators responsible for immune function and inflammation, such as pro-inflammatory cytokines, acute phase proteins, chemokines, and enzymes including nitric oxide synthase (Li and Verma, 2002; Liu and Malik, 2006). The ability of CAPE to inhibit NF-κB activation (Natarajan *et al.*, 1996) makes it an attractive candidate for therapeutic intervention of immune and inflammatory responses in disease or injured states (Calzado *et al.*, 2007; Korish and Arafa, 2011).

Another ability posited to be responsible for CAPE's protective effects is the induction of heme oxygenase-1 (HO-1; Scapagnini *et al.*, 2002; Wang *et al.*, 2010; Scapagnini *et al.*, 2011). Activation of the Keap1/Nrf2/ARE pathway by CAPE results in HO-1 upregulation (Wang *et al.*, 2010). As with NF-κB inhibition, the specific mechanism by which CAPE activates the Keap1/Nrf2/ARE pathway is not clearly defined; however, it is suggested that CAPE may directly react with Kelch-like ECH-associated protein 1 (Keap1), whose normal function is bind to and sequester nuclear factor E2-related factor 2 (Nrf2) in the cytosol, thereby inhibiting Nrf2's function as a nuclear transcription factor (Itoh *et al.*, 1999). Posited reaction of CAPE with Keap1 could create a conformational change in Keap1, allowing for the release of Nrf2 and its nuclear translocation and binding to the antioxidant response element (ARE). Upon binding of Nrf2 to ARE, activation of transcription for phase II antioxidant genes, such as the HO-1 gene, occurs (Dinkova-Kostova *et al.*, 2002; Wakabayashi *et al.*, 2004). HO-1 plays a key role in the cell's response against oxidative stress and is highly inducible in astrocytes and neurons. The HO-1 system exerts its protective effects against

neuronal death via anti-inflammatory and anti-oxidative events (Le *et al.*, 1999; Chen *et al.*, 2000). HO-1 induction results in the release of bioactive agents that have been shown to have powerful anti-oxidant behavior (Stocker *et al.*, 1987; Baranano *et al.*, 2002; Otterbein *et al.*, 2003).

1.3.4.1. *CAPE and Neuroprotection*

This laboratory has previously demonstrated that CAPE blocks hypoxia-ischemia-induced neuronal death through inhibition of neuroinflammation and mitochondrial cytochrome *c* release (Wei *et al*., 2004). Additional studies from this laboratory have shown the efficacy of *in vitro* CAPE treatment in the 6-hydroxydopamine (6-OHDA) cell culture model of neurodegeneration, whereby neuroprotection is reflected in the reduction of free radical generation, a hallmark of this neurotoxin culture model and its underlying neuropathologic events (Noelker *et al*., 2005; Ma *et al*., 2006).

Previous studies (See 1.3.3. Caffeic Acid Phenethyl Ester) have demonstrated that CAPE protects cells through its anti-inflammatory properties via inhibition of NF-κB and its anti-oxidant ability by way of HO-1 induction. Despite CAPE's success with reducing injury-induced neuronal cell death as demonstrated in an animal model of hypoxia-ischemia (Wei *et al.*, 2004) and confirmation of its neuroprotection using cell culture systems of neuron cell death (Noelker *et al*., 2005; Ma *et al*., 2006), to date, CAPE's effects in a PD animal model of neurodegeneration have not been tested. Because PD and other neurodegenerative diseases, such as amyotrophic lateral sclerosis and hypoxia-

ischemia, share common downstream degenerative pathways leading to neuronal death, including neuroinflammation and oxidative damage, it is of interest to this lab to explore the effects of CAPE in a PD animal model and to determine whether its anti-oxidant and anti-inflammatory ability play roles in its neuroprotection.

1.3.5. Animal Models of PD

Animal models of disease serve two major purposes; they have mechanistic value for examination of disease etiology and/or progression and they are also the first line of testing for a prospective treatment. Prior to the 1980s, the development of experimental animal models of PD focused on decreasing the levels of dopamine in the striatum as a pathological hallmark of the disease is dopamine depletion in the brain (Scherman *et al.*, 1989). The major disadvantage of these models was that although they allowed for the alteration of dopamine content in the brain via chemical or mechanical manipulation, which was known to result in the development of the primary motor dysfunction observed in the PD patient, and paved the way for use of L-dopa in PD patients (Carlsson *et al.*, 1957), these models did not accurately reproduce PD brain pathology (Bezard and Przedborski, 2011), such as the death of dopaminergic neurons (Marsden 1990; Fearnley and Lees, 1991). Although these earlier pharmacological animal models produced behavioral changes reminiscent of PD without the associated neuronal death (Carlsson *et al.*, 1957; Windle and Cammermayer, 1958; Bezard *et al.*, 1998), they paved the way for

present neurotoxin-related research by demonstrating that a greater than 60% loss of striatal dopamine led to motor behavioral changes (Bezard and Przedborski, 2011).

To date, there is no animal model that fully recapitulates all of the features of clinical PD, such as the neuroanatomical, neurochemical, and neurobehavioral changes. Additionally, PD is an aging disorder that progresses over a time period of decades. Because of these obstacles and the etiology of PD is still unknown, there is currently no perfect animal model for this disease. However, PD animal model development has significantly advanced with the application of neurotoxin-induced models, whereby a majority of primary motor symptoms, brain biochemical changes, and associated neuropathology of PD became reproducible. In addition to inducing dopamine depletion, with these models, scientists are now able to induce dopaminergic neuronal death, a key PD feature absent in previous animal models.

1.3.5.1. *Neurotoxin Models of PD*

Previous animal models of PD were successful in replicating the neurochemical changes and behavioral symptoms observed in PD, but none of these models were able to reproduce dopaminergic neuronal death (Bezard and Przedborski, 2011). Although discovery of the 6-hydroxydopamine-lesioned rat garnered attention in the 1970s (Ungerstedt, 1968; Ungerstedt and Arbuthnott, 1970), it was not until the 1980s that neurotoxin-induced animals entered prominence in the modeling of PD. The advantage of neurotoxin models is that

they can specifically alter or induce the degeneration of a selected region of neuronal populations. If a brain area is known to be affected by a particular neurologic disease, that region can then be targeted for degeneration by a neurotoxin. Additionally, there are reports supporting neurotoxin use to induce neurodegeneration as environmental toxin exposure has been found to play a role in development of sporadic PD (Hageman *et al.*, 1999; Di Monte, 2001; Gash *et al.*, 2008; Tanner *et al.*, 2009; Cannon and Greenamyre, 2010).

1.3.5.1.1. *6-Hydroxydopamine Model*

The 6-hydroxydopamine (6-OHDA) is one of the oldest, and widely used, PD models still in use today (Dauer and Przedborski, 2003; Cannon and Greenamyre, 2010). It is also the first animal model demonstrating neurotoxin-induced dopaminergic neuronal death in the substantia nigra pars compacta (SNpc; Ungerstedt, 1968).

The chemical structure of 6-OHDA is similar to that of dopamine and this neurotoxin is selective for monoamine neurons via uptake by dopamine and noradrenergic transport systems (Schwarting and Huston, 1996; Luthman *et al.*, 1998; Bezard *et al.*, 1998). The additional hydroxyl group contributes to its toxicity to monaminergic neurons. 6-OHDA cannot cross the blood-brain barrier, and in order to target the nigrostriatal pathway, local stereotaxic infusion into the striatum or median forebrain bundle, or directly into the substantia nigra, is required for its neurotoxic ability (Javoy *et al.*, 1976; Schwarting and Huston, 1996; Cannon and Greenamyre, 2010). Upon entry into catecholaminergic

neurons, 6-OHDA accumulates in the cytosol where it is auto-oxidized and damages cells via reactive oxygen species (ROS) formation and oxidative stress (Deumens *et al.*, 2002; Orth and Tabrizi, 2003).

The advantage of the 6-OHDA model is that the stereotaxic lesion can be applied unilaterally, such that the contralateral, unlesioned side serves as an internal control for each animal. Another appealing feature is that the extent of unilateral lesion-induced damage can be assessed behaviorally by observing asymmetric circling of the injected animal (Przedborski *et al.*, 1995). A disadvantage of the 6-OHDA model is that it must be directly administered to the target site or a distal site with projections to the brain region of interest. Additionally, administration of 6-OHDA requires stereotaxic surgery, which may be difficult to perform in smaller animals, such as mice (Cannon and Greenamyre, 2010). Despite the potential technical difficulties of neurotoxin administration, the 6-OHDA model can exhibit dopaminergic neuron death, depletion of striatal dopamine, and some motor deficits associated with PD (Schwarting and Huston, 1996).

1.3.5.1.2. *1-Methyl-4-phenyl-1,2,3,6-tetrahydropyridine Model*

Because Chapter 1 of this thesis work is focused on the MPTP model, please see Section 1.3.7. 1-Methyl-4-phenyl-1,2,3,6-tetrahydropyridine Mouse Model of PD.

1.3.5.1.3. *Rotenone Model*

The rotenone model was the first animal model that provided a link between environmental toxin exposure and α-synuclein-containing Lewy body-like inclusions in surviving dopaminergic neurons (Betarbet *et al.*, 2000). Rotenone is found in the roots of several tropical plant species and a widely used pesticide and fish poison (Cannon and Greenamyre, 2010). Rotenone is highly lipophilic and rapidly and readily crosses the blood-brain barrier (Talpade *et al.*, 2000). This neurotoxin was shown to inhibit mitochondrial complex I and binds to the same site as MPP^+. However, unlike MPTP, rotenone-induced inhibition of complex I is systemic and not specific to catecholaminergic neurons (Betarbet *et al.*, 2000). In addition, the produced lesions were not specific for dopaminergic neurons (Ferrante *et al.*, 1997; Cannon and Greenamyre, 2010). The major disadvantages of the rotenone model are that it exerts a more widespread, nonspecific inhibition of mitochondrial complex I, its use in small animals can be technically difficult (Betarbet *et al.*, 2000), and a link between environmental rotenone exposure and development of PD in humans remains unclear.

1.3.5.1.4. *Paraquat Model*

Paraquat is a widely used herbicide. Because of its presence in the environment, paraquat gained attention as a possible contributor to the development of or increased risk for sporadic PD (Liou *et al.*, 1997). Paraquat has a structure similar to MPP^+, except that paraquat has an additional N-methyl-pyridinium group instead of the phenyl group found on MPP^+ (Dauer and

Przedborski, 2003). Unlike MPP^+, paraquat's neuron damaging action is not through inhibition of mitochondrial complex I (Richardson *et al.*, 2005), but via superoxide formation and oxidative stress (Day *et al.*, 1999; Chun *et al.*, 2001). The advantage of using paraquat for modeling PD neurodegeneration is that systemic administration results in dopaminergic neuron death and the formation of α-synuclein-containing proteinaceous inclusions in the substantia nigra (Manning-Bog *et al.*, 2002; McCormack *et al.*, 2002). However, current epidemiological evidence and experimental data do not provide support for a clear link between paraquat exposure and the development of PD or higher risk for PD in humans or that paraquat directly causes brain lesions (Berry *et al.*, 2010).

1.3.6. *In Vitro* Models To Study Neurodegenerative Mechanisms

While animal models of PD can provide information on the effectiveness of a potential treatment and are more appropriate for addressing the complex features of clinical disease, cell culture systems are better suited for determining the mechanisms of disease and/or a prospective treatment's mode of action. As with animal models, there is presently no *in vitro* system that fully recapitulates the cellular population and microenvironment within the human PD patient brain. Despite each culture system's limitations and disadvantages, the mechanistic data afforded by these models can still function as predictors of what occurs *in vivo* in animal models of PD. This allows for both the identification and pre-

screening of potential treatments as well as examination of the treatments' mechanisms of action.

Dopaminergic cell lines, such as human neuroblastoma SH-SY5Y (Biedler *et al.*, 1978) and murine mesencephalon-derived MN9D cells (Choi *et al.*, 1992), are advantageous as they comprise a uniform population of cells and provide a relatively easy and replenishable source of dopaminergic neurons. As a good alternative to primary neuronal cultures, cell lines allow for certain biochemical analyses and other cell number-dependent assays, which would be difficult to accomplish with primary cultures as dopaminergic neurons make up less than 5% of the primary culture population (Collier *et al.*, 2003).

Studies using the SH-SY5Y cell line have demonstrated that exposure to MPP^+ (Veech *et al.*, 2000; Gomez *et al.*, 2001) and rotenone (Sherer *et al.*, 2001; Borland *et al.*, 2008) resulted in inhibition of mitochondrial complex I of the electron transport chain and neuronal death. Treatment with the dopamine agonist, pramipexole, was neuroprotective against MPP^+-induced toxicity (Cassarino *et al.*, 1998; Presgraves *et al.*, 2004), indicating that this cell line exhibits similar neuronal death responses to complex I-inhibiting neurotoxins as observed in animal models of PD (Langston *et al.*, 1983; Nicklas *et al.*, 1987; Gerlach *et al.*, 1991). In addition, treatment with a dopamine transporter (DAT) inhibitor, GBR12909 (Presgraves *et al.*, 2004), prevented MPP^+-induced neuronal death, providing evidence for functional DAT in these immortalized cells. Incubation with protein aggregates of α-synuclein induced cell death in cultured SH-SY5Y (El-Agnaf *et al.*, 1998) and exposure of these cells to MPP+

increased α-synuclein expression (Gomez-Santos *et al.*, 2002), providing evidence for the role of abnormal protein aggregation in PD neuronal death. These reports further validate the use of dopaminergic cell lines for exploring the mechanisms of PD and the screening of compounds for PD treatment as they can replicate the cellular responses to neurotoxins as found in animal model brains. However, the major disadvantage of dopaminergic cell lines is inherent in their experimentally-manipulated proliferative nature (Collier *et al.*, 2003). These cell lines are undifferentiated and require differentiation and have the ability for continuous expansion in culture, unlike primary dopaminergic neurons, which are terminally differentiated and post-mitotic. While these cell lines behave similarly to and express the cellular features characteristic of dopaminergic neurons in primary cultures, their undifferentiated (versus differentiated) states remain in question when utilizing these cells as a culture model of PD or neurodegeneration (Schule *et al.*, 2009).

Primary cell cultures are directly obtained from brain tissue of embryonic or postnatal animals. Primary neuronal cultures derived from animal mesencephalon, such rostral mesencephalic neurons (RMN), are advantageous over those comprised of specific cell lines as they are authentic and unaltered dopaminergic and non-dopaminergic neurons that are cultured in the presence of other cell types, including glial cells, normally found within that brain region. Additionally, the culturing of primary neurons allows for the isolation of neuronal areas containing specific populations of dopaminergic neurons based on the dissected brain area (Collier *et al.*, 2003). Culturing dopaminergic neurons within

the cellular context of their naturally-occurring microenvironment is of great advantage when exploring the effects of neurotoxins and neuroprotective compounds on neuronal survival.

Several studies have demonstrated the use of RMN to examine the effects of neurotoxin-induced neuronal death. Mammalian primary neuronal cultures isolated from mouse mesencephalon and incubated with MPP+ (Heyer *et al.*, 1986; Sanchez-Ramos *et al.*, 1986; Lotharius *et al.*, 1999; Du *et al.*, 2001; Carrasco and Werner, 2002) or 6-OHDA (Michel and Hefti, 1990; Lotharius *et al.*, 1999; Von Coelln *et al.*, 2001; Carrasco and Werner, 2002; Ma *et al.*, 2005) resulted in neuronal death. Exposure of RMN to MPP^+ in culture media also reduced endogenous dopamine levels and dopamine uptake in these cells (Mytilineou and Cohen, 1985; Beck *et al.*, 1991). These data demonstrate that primary neuronal cultures of mesencephalic origin are representative of the functional and neurochemical changes occurring in the dopaminergic neurons of the neurotoxin-exposed animal brain.

In addition to primary culture of RMN, cerebellar granule neurons (CGN) are also used as a cell culture system of neurodegeneration. CGN cultures, like dopaminergic cell lines, are a homogenous population of cells; however, unlike cell lines, CGN are primary neuronal cultures derived from brain tissue. Thus, the advantage of utilizing CGN for mechanism studies and *in vitro* screening of neuroprotective compounds is that it is an enriched and authentic neuronal population.

In the MPTP *in vivo* model, attention has not been focused on the cerebellum, as the neurotoxin's mode of action mainly involves the dopamine neuron and its DAT (See also Section 1.3.7.1. 1-Methyl-4-phenyl-1,2,3,6-tetrahydropyridine). However, there are several reports demonstrating the involvement of the cerebellum in MPTP neurotoxicity. In MPTP-exposed mice, there is significant loss of Purkinje cells located in the cerebellar cortex (Takada *et al.*, 1988). Tracing studies using tritium (^{3}H)-labeled MPTP have shown that levels of bound ^{3}H-MPTP are equal to or greater than striatal levels (Bocchetta *et al.*, 1985); in addition, cerebellar ^{14}C-MPP^{+} levels equaled those observed in the substantia nigra in monkeys administered ^{14}C-MPTP (Yang *et al.*, 1988). Previous studies have reported the sensitivity of CGN to MPP^{+} (Marini *et al.*, 1989; Marini and Paul, 1992; Du *et al.*, 2001) and 6-OHDA neurotoxicity (Noelker *et al.*, 2005; Ma *et al.*, 2006), such that these toxins were able to induce CGN death in culture. Experiments using glial-neuronal co-cultures exposed to MPTP demonstrated that while astrocytic viability remained unaffected by MPTP exposure or MPP^{+} formed in the co-culture, the neurotoxins induced CGN death (Marini *et al.*, 1989). Because CGN do not express a DAT, it is posited that MPP^{+} may be entering CGN by using the cell's glutamate uptake system (Balcar and Johnston, 1972; Balcar *et al.*, 1977; Young *et al.*, 1988; Marini *et al.*, 1989). These *in vivo* and *in vitro* data suggest that the cerebellum and its CGN may be an under-examined area of MPTP and MPP^{+} neurotoxicity.

1.3.7. 1-Methyl-4-phenyl-1,2,3,6-tetrahydropyridine Mouse Model of PD

The 1-methyl-4-phenyl-1,2,3,6-tetrahydropyridine (MPTP) mouse model was utilized in the present study. MPTP is a mitochondrial complex I inhibitor with selectivity for dopaminergic neurons (Vila and Przedborski, 2003). MPTP administration has been shown to result in significant dopaminergic neuronal death that is primarily observed in the substantia nigra pars compacta, a midbrain area severely affected in PD, as well as a profound loss of striatal dopamine (Heikkila *et al.*, 1984), causing the neurointoxicated mice to replicate most motor deficits observed in clinical PD (Vila and Przedborski, 2003). This mouse model has been studied extensively and remains one of the most widely used neurotoxin animal models of PD. To date, there have been no *in vivo* studies reporting the use or benefit of caffeic acid phenethyl ester in this mouse model.

1.3.7.1. *1-Methyl-4-phenyl-1,2,3,6-tetrahydropyridine*

1-Methyl-4-phenyl-1,2,3,6-tetrahydropyridine (MPTP) is a neurotoxin that is a byproduct of the synthesis of an opioid analgesic drug, 1-methyl-4-phenyl-4-propionoxypiperidine (MPPP), a meperidine analog (Przedborski and Vila, 2001). MPTP first garnered recognition as a neurotoxin in 1982 when the California neurologist, J. William Langston, discovered the link between a contaminant, later identified as MPTP, which was found in illicitly-synthesized MPPP, and the development of a parkinsonian syndrome in a group of young drug addicts (Langston *et al*., 1983).

Upon systemic administration, conversion of MPTP to MPP^+ by glia cells and serotonergic neurons within the central nervous system (CNS) is required for this protoxin to induce neurotoxicity. Its highly lipophilic nature allows it to cross the uncompromised blood-brain barrier (Przedborski and Vila, 2003). Once inside the CNS, MPTP is taken up by non-dopaminergic cells, where it is metabolically converted into the intermediate, 1-methyl-4-phenyl-2,3-dihydropyridinium ($MPDP^+$), by the enzyme, monoamine oxidase B (MAO-B; Tipton and Singer, 1993). Presumed spontaneous oxidation of $MPDP^+$ then facilitates the final conversion of $MPDP^+$ to the polar molecule and active neurotoxin, 1-methyl-4-phenylpyridinium (MPP^+), which is then released from the MAO-B-containing cell into the extracellular space by a currently unknown mechanism (Fig 1.3; Przedborski and Jackson-Lewis, 1998; Przedborski and Vila, 2003). Because MPP^+ is a polar molecule, it cannot easily pass the cell membrane and gain entry into the cell. MPP^+ has a high affinity for the dopamine transporter (DAT) and depends on the DAT for uptake into the dopaminergic neuron, where it can then exert its neurotoxic effects and lead to neurodegeneration (Przedborski and Vila, 2003).

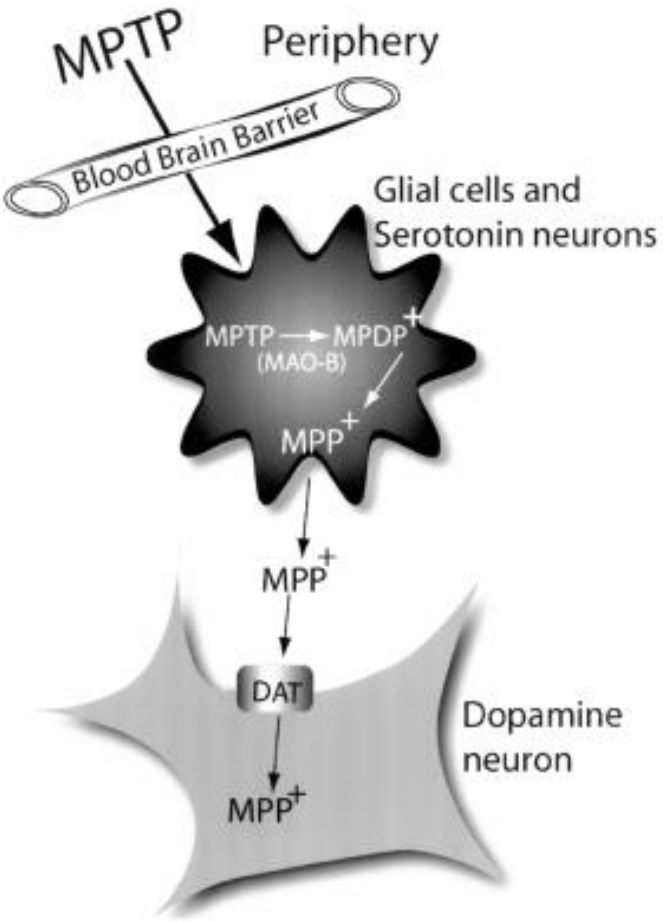

Przedborski and Vila, 2003

Figure 1.3. Action of MPTP within the central nervous system.

Systemically-administered MPTP readily crosses the blood-brain barrier due to its high lipophilicity and enters the brain where it is taken up by non-dopaminergic neurons and enzymatically converted to $MPDP^+$ by MAO-B. $MPDP^+$ is spontaneously oxidized into MPP^+, which then leaves the cell by an unknown mechanism. MPP^+ gains entry into dopaminergic neurons via the DAT. Once inside the cell, MPP^+ induces neurotoxicity by way of a variety of pathogenic mechanisms leading to dopaminergic cell death and the characteristic signs of clinical PD.

1.3.7.2. *MPTP and Neurodegeneration*

MPTP selectively destroys dopaminergic neurons in the SNpc, resulting in a Parkinson-like syndrome in humans, monkeys, and mice (Tolwani *et al*., 1999). Upon MPTP conversion to MPP^+ within the brain, the neurotoxin enters dopaminergic neurons where MPP^+ is available to bind to vesicular monoamine transporters (VMATs) leading to MPP^+ sequestration and accumulation within synaptic vesicles, bind to and disrupt enzymes in the cytosol, and concentrate within mitochondria thus altering the dopaminergic neuron's adenosine triphosphate (ATP) formation (Fig 2.3; Przedborski and Vila, 2003). It is suggested that neuronal apoptosis is involved in the acute MPTP model (Viswanath *et al*., 2001) and that mitochondria, cytochrome *c*, as well as apoptosis inducing factor (AIF) play important roles in the MPTP and MPP^+ models (Du *et al*., 1997; Mogi *et al*., 1998; Offen *et al*., 1998). Recently, it has been shown that MPTP administration results in robust gliosis in the SNpc, accompanied by upregulation of interleukin-1β (Liberatore *et al*., 1999) and inducible nitric oxide synthase (iNOS) (Knott *et al*., 2000). Interestingly, mice with inhibition of caspase-1 and iNOS were found to be resistant to MPTP neurotoxicity (Dehmer *et al*., 2000; Klevenyi *et al*., 1999; Liberatore *et al*., 1999).

Previous studies from this and other laboratories using the acute MPTP mouse model have demonstrated that after 7 days of MPTP exposure, there is a significant and stable decrease in the number of neurons positive for tyrosine hydroxylase (TH) in the midbrain (Du *et al*., 2001). It is important to note for the present study that a duration of 7 days of MPTP exposure was used as several

reports have indicated that the loss of dendritic processes of striatal and nigral TH-positive neuronal cell bodies were not permanent and that the recovery of striatal and nigral TH-immunoreactivity was observed after MPTP is eliminated systemically within 7 days (Ricaurte *et al*., 1986).

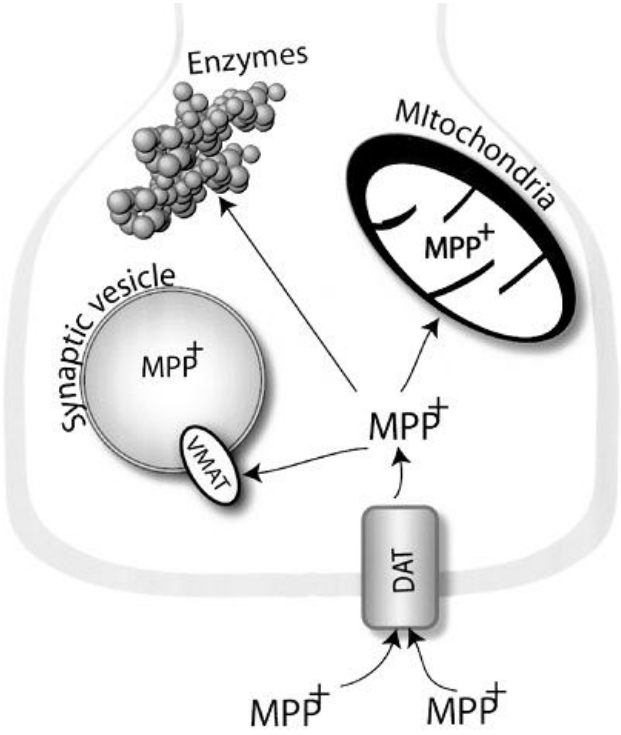

Przedborski and Vila, 2003

Figure 1.4. Consequences of MPP^+ entry into dopamine (DA) neurons.

Within the dopamine (DA) neuron, MPP^+ binds to a vesicular monoamine transporter (VMAT), interacts with cytosolic enzymes, or accumulates within the mitochondrion. These processes lead to the degeneration of the DA neuron.

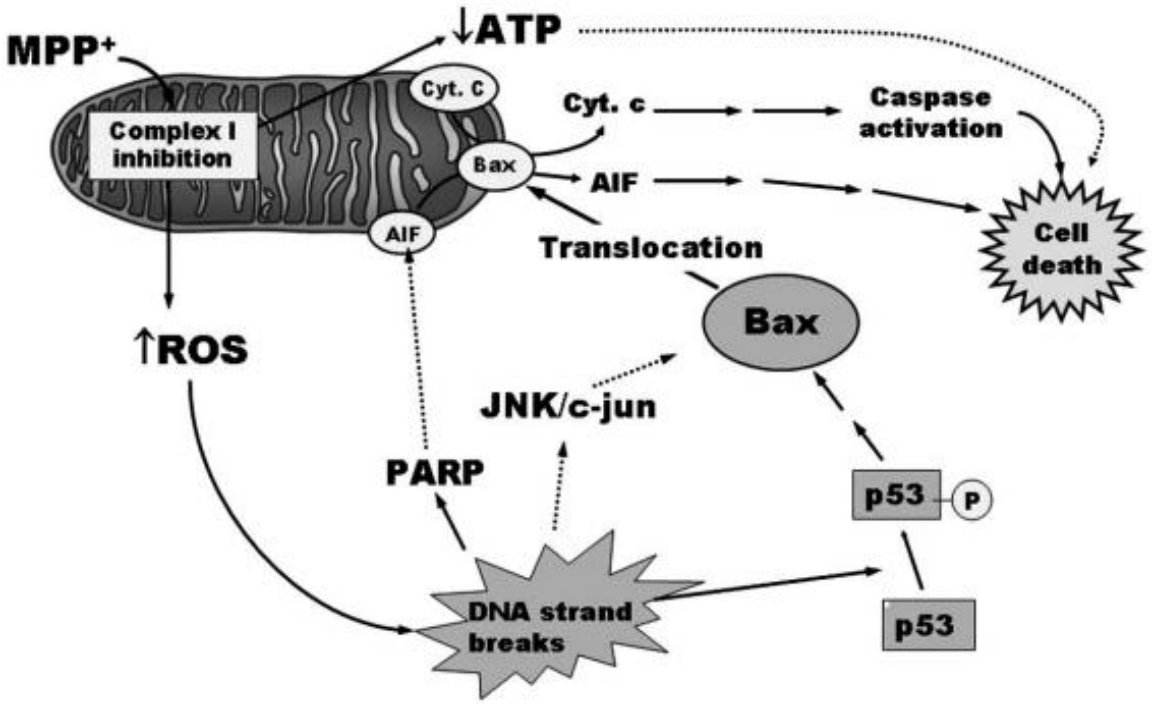

Przedborski *et al*., 2004

Figure 1.5. Proposed mitochondrial-dependent mechanisms of MPTP action leading to cell death.

MPP^+ concentrates within the mitochondrion and binds to and disrupts activity of complex I of the electron transport chain. The resulting inhibition of the respiratory chain decreases ATP formation and increases ROS production with both major events leading to DA neuronal cell death.

1.3.8. Mechanisms of PD

With the advancement of PD animal model development and the comparisons of experimental reports to clinical data, several key mechanisms of PD neurodegeneration have been revealed and posited to be responsible for the development and progression of PD. These major pathways may act in concert or occur separately in succession, but these neuropathogenic mechanisms ultimately converge toward the shared outcome of neuronal death.

1.3.8.1. *Mitochondrial Dysfunction and Oxidative Stress*

Oxidative phosphorylation is the metabolic process by which the mitochondrion produces energy in the form of adenosine triphosphate (ATP) from nutrients, molecular oxygen, and a series of coupled reduction-oxidation reactions within the inner mitochondrial membrane, where the necessary machinery (electron transport chain) is located and exchange of electrons occurs (Kincses and Vecsei, 2011). The electrons transported down the electron transport chain may reduce molecular oxygen, resulting in the formation of mitochondrial respiration by-products – reactive oxygen species (ROS), such as superoxide and hydrogen peroxide, which can then react with other molecules to produce damaging hydroxyl radicals or peroxynitrite (Davies, 1995; Dauer and Przedborski, 2003; Valko *et al.*, 2007).

Studies examining the effects of MPTP in animals have shown that systemic administration of this neurotoxin results in the inhibition of complex I of the mitochondrial electron transport chain. Inhibition of this complex can lead to

increased production of ROS, resulting in a cycle of cellular damage, further disruption of the mitochondrial electron transport chain, and even more ROS formation and oxidative stress within the cell (Langston *et al.*, 1983; Nicklas *et al.*, 1987; Gerlach *et al.*, 1991). Additionally, when these events occur within a dopaminergic neuron, the potential oxidative stress produced can be compounded by the metabolism of dopamine. This physiological event, along with dopamine oxidation, has been found to produce ROS and equally-damaging quinones (Graham, 1978; Dauer and Przedborski, 2003). Therefore, dopaminergic neurons may be inherently more at risk for oxidative damage resulting from the actions of mitochondrial respiration by-products, as well as the possible resultant reduction in energy/ATP production, and dopamine metabolism.

Clinical data have been correlated with the mitochondrial dysfunction and oxidative damage reported in animal models of PD. Decreased complex I activity was observed in the PD brain, platelets, and skeletal muscle (Parker *et al.*, 1989; Schapira I *et al.*, 1990; Blin *et al.*, 1994; Swerdlow *et al.*, 1996; Greenamyre *et al.*, 2001). Additionally, in the SNpc of PD patients, reduced levels of anti-oxidants, such as glutathione, have been reported (Sian *et al.*, 1994), which could lead to aberrant handling or clearing of ROS and subsequent oxidative injury. Taken together, the potential susceptibility of dopaminergic neurons to oxidative stress and decreased anti-oxidant levels in the brain could contribute to dopaminergic neuron death in PD.

1.3.8.2. *Neuroinflammation*

Although the role of neuroinflammation in PD is not yet fully understood, there are increasing reports evidencing that neuroinflammation may contribute to PD pathogenesis and neuronal death. Microglial activation was found to be increased in the substantia nigra of MPTP-exposed humans (McGeer *et al.*, 1988; Langston *et al.*, 1999). Interestingly, brain microglial cells, the resident CNS macrophages, are found in highest density within the substantia nigra (Kim *et al.*, 2000). In the presence of damage to the CNS, activated microglia and astrocytes proliferate quickly, migrate to the site of injury, exhibit changes in their morphology ("resting" versus "reactive" shapes), and upregulate a variety of cell surface molecules (Floyd, 1999; Raivich *et al.*, 1999a; Raivich *et al.*, 1999b). Upon reaching the injured area, reactive microglia and astrocytes release pro-inflammatory cytokines, which serve to coordinate the immune response within the brain. These inflammatory mediators can then induce the production of oxidative stress-related molecules, such as ROS and nitric oxide, in other glial cells (Hunot *et al.*, 1999).

Studies utilizing the MPTP model of PD report robust microglial activation in substantia nigra and striatum of affected mice (Kohutnicka *et al.*, 1998; Kurkowska-Jastrzebska *et al.*, 1999). Increased levels of inducible nitric oxide synthase (iNOS), pro-inflammatory cytokines, such as interleukin-6 (IL-6), interleukin-1β (IL-1β), cyclooxygenase-2, were observed along with glial activation in the brains of MPTP animals (Kohutnicka *et al.*, 1998; Mogi *et al.*, 1998; Liberatore *et al.*, 1999). Additionally, previous studies from this laboratory

(Du *et al.*, 2001) have demonstrated that minocycline, a tetracycline antibiotic with anti-inflammatory effects, was able to block the degeneration of nigrostriatal dopaminergic neurons in MPTP-exposed mice by preventing glial activation, IL-1β production, and iNOS induction. These data suggest that neuroinflammation may play an important role in neuronal death in the MPTP mouse model of PD.

In PD, several post-mortem studies have reported the activation of astrocytes and microglia (McGeer *et al.*, 1988; Mirza *et al.*, 2000), which was associated with significant elevations in the levels of pro-inflammatory cytokines in the brain and cerebrospinal fluid (CSF). Some of these inflammation mediators included tumor necrosis factor-alpha (TNF-α), IL-6, IL-1β (Mogi *et al.*, 1994a; Mogi *et al.*, 1994b; Blum-Degen *et al.*, 1995; Mogi *et al.*, 1996; Hunot *et al.*, 1999; Nagatsu *et al.*, 2000), which were also increased in the MPTP mouse brain. In particular, an increase in TNF-α-positive glial cells located in the substantia nigra were observed in PD post-mortem; this increase in TNF-α immunoreactivity was found in conjunction with elevations of this pro-inflammatory cytokine in the PD striatum (366%) and CSF (432%; Boka *et al.*, 1994; Mogi *et al.*, 1994b; Hunot *et al.*, 1999). Additionally, there was an inverse correlation with PD severity and IL-6 levels in the CSF of patients (Muller *et al.*, 1998).

Studies of the MPTP animal model and post-mortem PD patient tissues demonstrate a correlation between neuroinflammation, oxidative damage, and the subsequent dopaminergic neuronal death characteristic of this disease. However, *in vivo* studies on the use of anti-inflammatory drugs for the treatment of the MPTP mouse model have been reported with variable outcomes and

effectiveness (Aubin *et al.*, 1998; Kurkowska-Jastrzebska *et al.*, 1999; Mohanakumar *et al.*, 2000; He *et al.*, 2001; Teismann and Ferger, 2001; Kurkowska-Jastrzebska *et al.*, 2002; Wu *et al.*, 2002). This suggests that blockade or attenuation of a single downstream event or the inflammatory process alone is not sufficient to prevent dopaminergic neuron death observed in PD. A potential candidate for the treatment of this disease would require a wide range of neuroprotective action.

1.3.8.3. *Excitotoxicity*

Upon its release from a pre-synaptic cell, glutamate binds to N-methyl D-aspartate (NMDA) and α-amino-3-hydroxy-5-methyl-4-isoxazolepropionic acid (AMPA) receptors, resulting in their activation and excitatory neurotransmission (Dingledine *et al.*, 1999). Glutamate is the key excitatory neurotransmitter in the vertebrate CNS. Under normal physiologic conditions and in addition to excitatory neurotransmission, the interaction between glutamate and its receptors leads to activation of voltage-gated ion channels and the influx of extracellular calcium into the cell and its mitochondria (McCormack *et al.*, 1990). This influx allows for calcium homeostasis during cellular metabolism and oxidative phosphorylation within the mitochondria (Greenamyre and Porter, 1994).

Excitatory amino acid transporters (EAATs) located on neurons and surrounding astrocytes are responsible for terminating excitatory neurotransmission by removal of glutamate from the synapse and extracellular space in order to keep glutamate below excitotoxic levels (Clements *et al.*, 1992;

Shigeri *et al.*, 2004). In neurodegenerative disease, the glutamate concentration in the synaptic cleft reaches high levels due to abnormalities in glutamate clearance (Ankarcrona *et al.*, 1995). Elevations in glutamate levels can lead to increased stimulation of NMDA receptors. This intensified excitatory stimulation can result in a higher influx of calcium into the cell and its mitochondria as well as calcium release from endoplasmic reticular stores (Hertz, 2007). Elevations in intracellular and mitochondrial calcium levels have been shown to cause abnormalities in the mitochondrial permeability transition pore, leading to the neuronal death cascade (Stavrovskaya and Kristal, 2004; Chan *et al.*, 2009).

In PD, it is posited that dopamine depletion in the midbrain ultimately leads to disinhibition of the subthalamic nucleus, which contains excitatory, glutamatergic output neurons that project to the dopaminergic neurons of the substantia nigra that express glutamate receptors (Rodriguez *et al.*, 1998; See also 1.3.2. Neurochemical and Neuropathological Changes in PD). Constant excitatory neurotransmission from the subthalamic nucleus could induce excitotoxicity in the substantia nigra, particularly in the pars compacta area, resulting in the neuronal death of dopaminergic neurons (Blandini *et al.*, 2000; Johnson *et al., 2009*). Studies using the MPTP primate models have shown that treatment with excitatory amino acid receptor antagonists is neuroprotective (Beal, 1998; Bonsi *et al.*, 2007), further suggesting the role of excitotoxicity in the PD neuronal death mechanism.

1.3.8.4. *Aggregation of Protein*

The significance and focus of attention towards protein aggregation in PD neuropathogenesis came about when components of Lewy bodies in PD, namely α-synuclein, were revealed. Mutations in the genes of these Lewy body constituents were found in association with the development of familial forms of PD, allowing for the engineering of transgenic mouse models of PD (See also 1.3.5. Mouse Models of PD). Mutations in the α-synuclein gene caused autosomal dominant PD (Polymeropoulos *et al.*, 1997) and mutations in parkin and DJ-1 were associated with autosomal recessive PD (Kitada *et al.*, 1998; Bonifati *et al.*, 2003). Although familial PD makes up a much smaller percentage of total PD cases (PD is primarily sporadic; Siderowf and Stern, 2003) and none of the transgenic animal models of PD fully recapitulate the disease, these studies brought great attention towards the key role of protein aggregation in PD neuronal death.

α-Synuclein has currently unknown physiologic function and exists unfolded and in the α-helix conformation (George, 2002). Unlike its β and γ counterparts, under pathological conditions, α-synuclein can fold into a β-sheet conformation. The assembly of these β-sheets into filaments leads to α-synuclein accumulation in nerve tissue and causes neurodegeneration (El-Agnaf *et al.*, 1998; Lee *et al.*, 2002). Additionally, elevations in α-synuclein protein aggregates lead to oligomer formation, which can be toxic to neurons by disrupting normal functioning of the lysosome and proteosome (Maguire-Zeiss 2008; Chau *et al.*,

2009). Malfunctioning of the lysosome and proteosome then results in accumulation of proteins within the neuron.

Proteinaceous aggregates of α-synuclein have been shown to promote the aberrant folding of other proteins (Olanow, 2009), such as the microtubule-associated protein, tau (Giasson *et al*., 2003). Interestingly, tau gene polymorphisms have been associated with a higher risk for developing PD (Martin *et al.*, 2001), suggesting that significant protein aggregation plays a key role in the neuronal death observed in PD. Studies with MPTP have documented the critical role of α-synuclein and protein aggregation in neuronal death as α-synuclein null mice exhibited resistance against MPTP-induced dopaminergic neurodegeneration (Dauer *et al.*, 2002). Additionally, it has been shown that mitochondrial complex I inhibition and oxidative damage following neurotoxin (MPTP, rotenone, or paraquat) exposure contribute to α-synuclein relocation from the synapse and aggregation and build-up of inclusions within degenerating neurons (Fig 1.6; Kowall *et al.*, 2000; Manning-Bog *et al.*, 2002; Sherer *et al.*, 2003), further suggesting that protein aggregation involving α-synuclein plays a critical role in the PD neuronal death pathway.

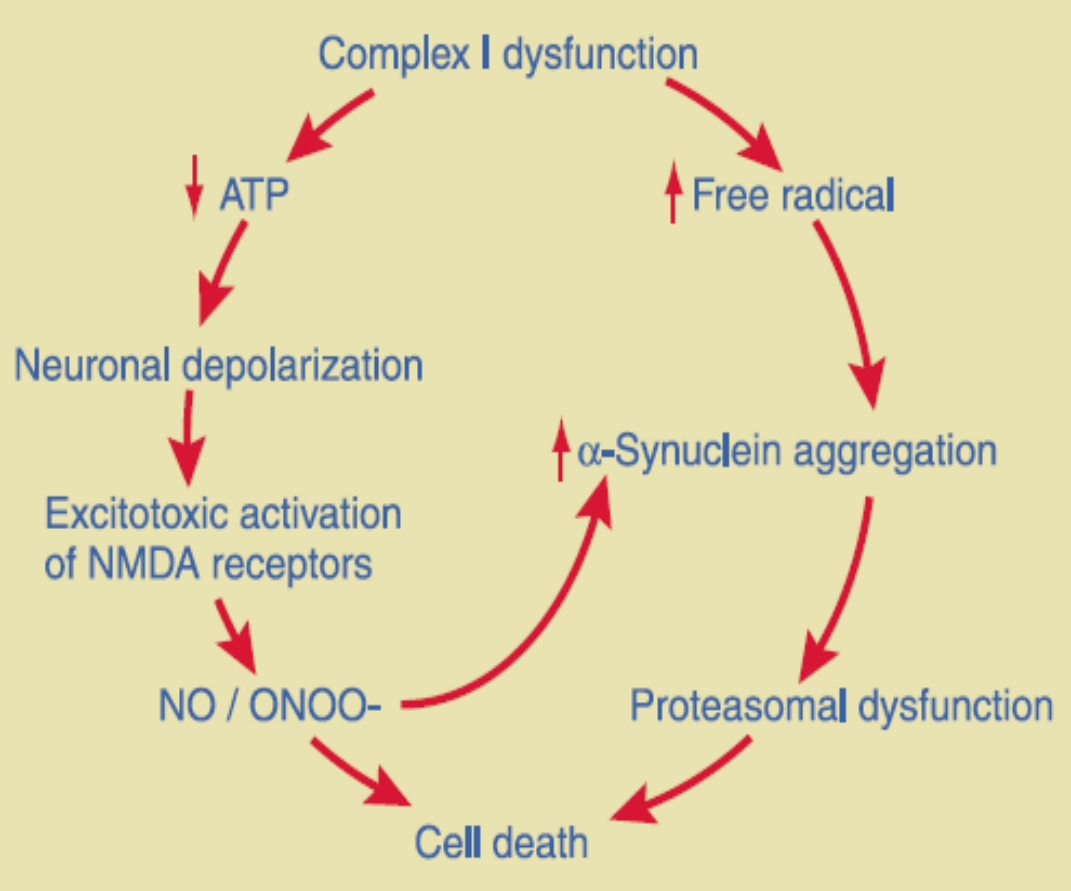

Adapted from Dawson and Dawson, 2003

Figure 1.6. The key role of mitochondrial dysfunction and complex I inhibition in PD.

Reports on the MPTP, rotenone, paraquat animal models of PD reveal that the mode of pathogenic action of these neurotoxins is inhibition of complex I. Disruption of this mitochondrial component sets off a chain of events contributing to the neuronal death observed in PD. Complex I inhibition results in excitotoxicity and oxidative stress via activation of NMDA receptors and increased ROS production, respectively. Further excitotoxicity-induced oxidative damage leads to increased protein aggregation and dysfunction of the proteosome. The resulting consequence is cell death.

1.4. Experimental Procedures

1.4.1. Animals and Animal Treatment Protocol

Eight-week-old male C57BL/6 mice (Taconic Farms, Inc., Cambridge City, IN, USA) were used with procedures and materials approved by the IACUC at the Indiana University School of Medicine (Indianapolis, IN, USA). Mice (vehicle, n = 15; MPTP, n = 14; 2 mg/kg CAPE, n = 6; 5 mg/kg CAPE, n = 7; 10 mg/kg CAPE, n = 9) were administered caffeic acid phenethyl ester (CAPE; 2, 5, or 10 mg/kg/day; molecular weight = 284.31, Sigma-Aldrich Corp., St. Louis, MO, USA) in 33% PEG-400 vehicle (polyethylene glycol-400 diluted in deionized H_2O; molecular weight = 400, Sigma-Aldrich Corp.) by oral gavage (p.o.) once only at 1 hour prior to exposures to 1-methyl-4-phenyl-1,2,3,6-tetrahydropyridine (MPTP). Vehicle-only, CAPE-only, and MPTP-only groups were included. The MPTP-treated groups (MPTP-only and MPTP-CAPE mice) received four intraperitoneal (i.p.) injections of 20 mg/kg MPTP-HCl (1-methyl-4-phenyl-1,2,3,6-tetrahydropyridine hydrochloride; molecular weight = 209.72, Sigma-Aldrich Corp.) in 0.9% saline at 2-hour intervals in a single day (4 injections total) as previously described (Du *et al*., 2001) and sacrificed at 7 days after the last MPTP injection (a total of 7 days and 1 hour after CAPE administration). The vehicle group received four injections of 0.9% saline in the same time interval as MPTP-treated animals. CAPE-only animals (2, 5, or 10 mg/kg/day) were not administered MPTP injections.

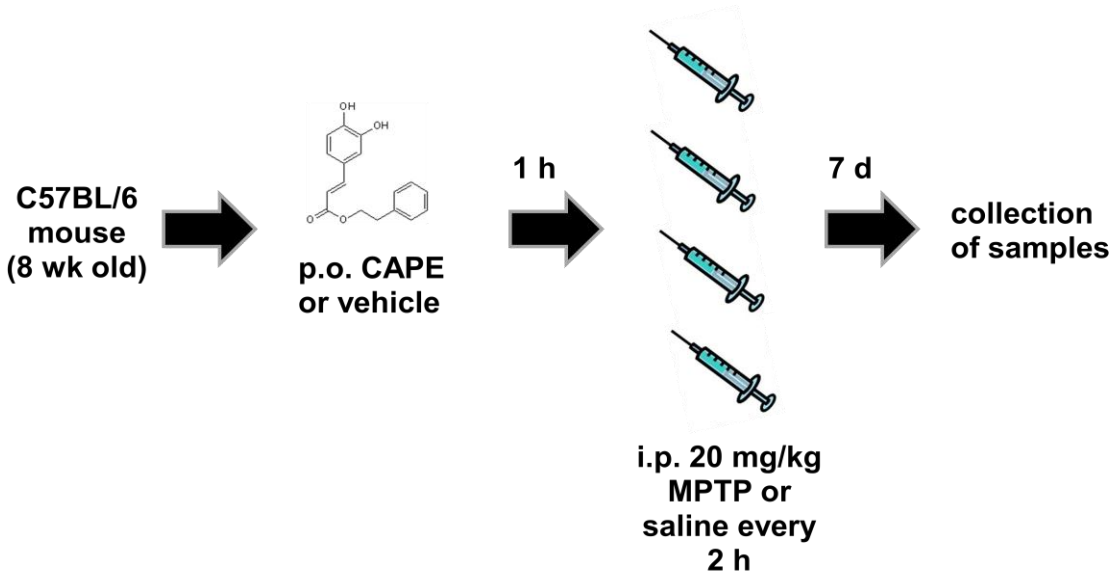

Figure 1.7. Diagram of the Animal Treatment Protocol used for this study.

1.4.2. TH-immunohistochemistry and Stereological Quantitation of TH-positive Neurons

After perfusion-fixation with 4% paraformaldehyde in 0.1 M phosphate buffer (pH 7.4) and cryoprotection in 30% sucrose/phosphate buffer, the brains were frozen in liquid nitrogen and serially sectioned (40 µm) through the entire midbrain. Tissue sections were incubated successively with rabbit polyclonal anti-tyrosine hydroxylase (anti-TH) antibody (1:2,500; Calbiochem, Cincinnati, OH, USA), goat biotinylated-conjugated polyclonal anti-rabbit antibody (1:250; Vector Laboratories, Inc., Burlingame, CA, USA) and horseradish-peroxidase conjugated avidin/biotin complex (Vector Laboratories, Inc.). Sections were then exposed to 3,3′-diaminobenzidine tetrahydrochloride (DAB) for detection. To

quantify TH-positive neurons, we utilized the nuclear counterstain, methyl green (Vector Laboratories) and the stereological method for counting TH-positive neurons as previously described by Du and colleagues (2001).

1.4.3. Measurement of Dopamine Levels in the Striatum

Following the specified animal treatments, the striatum was dissected in ice-cold 1X phosphate buffered saline (PBS), frozen on dry ice, and stored at -80°C. High-performance liquid chromatography (HPLC) with electrochemical detection was used to simultaneously measure the concentration of dopamine in each sample (Du *et al*., 2001).

1.4.4. Measurement of Caffeic Acid Phenethyl Ester in Mouse Tissue

C57BL/6 mice were given 10 mg/kg CAPE by oral gavage. Whole brain and blood were collected after 1 hour. Levels of CAPE in harvested tissues were measured by using HPLC with electrochemical detection as previously described (Du *et al*., 2001).

1.4.5. Measurement of Monoamine Oxidase Activity in Mouse Brain

Monoamine oxidase (MAO) activity was examined in brain samples using the Amplex Red Monoamine Oxidase Assay kit (Molecular Probes, Carlsbad, CA, USA). Brain tissue was homogenized on ice in a buffer containing 0.3% dithiothreitol, 1 mM ATP, 0.1 mM GTP, 0.1 mM Pipes, 0.5 mM $MgCl_2$, 2 mM EGTA, 0.1 mM EDTA, pH 7.2. The homogenate was then treated with 0.5%

Triton X-100 at 4°C for 2 hours and centrifuged at 15,000 rpm with an Eppendorf microcentrifuge (Fisher Scientific, Pittsburgh, PA, USA) at 4°C for 10 minutes. The supernatant was taken as the enzyme source for MAO and was evaluated for total protein content (Pierce protein assay kit; Pierce, Rockford, IL, USA). The amine oxidase containing 160 µg of supernatant protein was diluted in 1X Reaction Buffer and 100 µL of this mixture was used for each reaction. CAPE was then added to this mixture at 1 µM, 10 µM, 50 µM, or 100 µM. A positive control was prepared by using 10 µM H_2O_2 in 1X Reaction Buffer. A negative control contained 1X Reaction Buffer but no H_2O_2. A working solution of 400 µM Amplex Red reagent with 1 U/mL horseradish peroxidase (HRP) and 2 mM substrate was made and added to each microplate well containing the brain samples and controls. The reaction microplate was incubated for 30 minutes at room temperature and protected from light. Fluorescence was measured using excitation at 530 nm and emission at 590 nm.

1.4.6. Measurement of CAPE and MPP^+ Levels in the Midbrain

CAPE and MPP^+ were determined in brain samples using liquid chromatography. The liquid chromatograph utilizes two Water 510 pumps with a 484 UV detector (Waters, Milford, MA, USA). For CAPE, a 10 µL sample was injected into a Beckman ultrasphere C18 column (2.0 x 250 mm; Beckman Coulter, Inc., Brea, CA, USA). The mobile phase consisted of 0.1% TFA in water (Buffer A) and acetonitrile (Buffer B). The separation used a linear gradient segment of 0 minutes 100% A and 12 minutes 52% A. From 13 minutes to 20

minutes the mobile phase consisted of 2% A and 98% B. The flow rate was 1.0 mL/min and the eluent was monitored at 295 nm. For MPP^+ (Du *et al*., 2001), a 10-µL sample was injected into a Whatman partisil 10 SCX column (2.0 x 250 mm; Whatman, Inc., Piscataway, NJ, USA). The mobile phase consisted of 90% of a solution (pH 2.35) of 0.1 M acetic acid and 75 mM triethylamine and 10 % acetonitrile. The flow rate was 1.5 mL/min for the eluent, which was monitored at 295 nm. Clearly delineated chromatographic peaks with the retention time of authentic standards and expected molecular weights were seen after injection of brain extracts from treated animals. Analytes were quantified based on the areas of these peaks.

1.4.7. Neuronal Cell Cultures and Assessment of Neuronal Viability

1.4.7.1. *Cerebellar Granule Neuronal Primary Culture*

Cerebellar granule neurons (CGN) were prepared from 8-day-old Sprague-Dawley rat pups (Harlan Laboratories, Inc., Indianapolis, IN, USA) as previously described (Du *et al*., 2001). Briefly, freshly dissected cerebella were dissociated and the cells seeded at a density of 1.2 to 1.5 x 10^6 cells/mL on poly-L-lysine-coated dishes in Basal Medium Eagle supplemented with 10% fetal bovine serum (FBS), 25 mM KCl, and gentamicin (0.1 mg/mL). Cytosine arabinoside (10 µM) was added to the culture medium 24 hours after initial plating. All experiments utilized CGN after 7 – 8 days in vitro (DIV). Viable CGN were quantified by counting fluorescein (green) positive cells following staining with fluorescein diacetate. Propidium iodide, which interacts with nuclear DNA

and produces a red fluorescence, was used to identify dead neurons (Du *et al*., 2001).

1.4.7.2. *Rostral Mesencephalic Neuronal Primary Culture*

Primary cultures of rostral mesencephalic neurons (RMN) dissected from embryonic day-15 rat embryos (Harlan) were prepared as previously described (Du *et al*., 2001). Briefly, RMN were dissociated using trypsin and DNase I (Gibco) and the cells were suspended in Dulbecco's Modified Eagle Medium supplemented with Ham F12 nutrient mixture (1:1; Gibco) and 10% FBS. Cells were plated in poly-L-lysine (10 µg/mL; Sigma) pre-coated 24-well plates at a density of 1 x 10^5 cells/cm^2. After 24 hours, the medium was supplemented with 10 µM cytosine arabinoside to inhibit glial cell proliferation. Cultures were used 2 days after preparation. Dopaminergic neurons in primary cultures were visualized by TH-immunohistochemistry (Du *et al*., 2001) and quantified using a Leitz inverted microscope (x 200).

1.4.8. Immunoblot

Western blot analysis was performed on brain extracts from selected regions and cell cytoplasmic extracts (Du *et al*., 2001). Extracts were prepared by lysing tissues/cells in a buffer containing 1% Nonidet P-40, 0.1% SDS, 50 mM Tris (pH 8.0), 50 mM NaCl, 0.05% deoxycholate, and protease inhibitor (Roche Diagnostics Corp., Indianapolis, IN, USA). Proteins were size fractionated on a 4 – 12% polyacrylamide gradient gel (SDS-NuPAGE) and transferred onto

nitrocellulose (Hybond N; Amersham Biosciences, Piscataway, NJ, USA). Blots were then probed with polyclonal or monoclonal antibodies (1:500; iNOS, nNOS, and caspase-1; Santa Cruz Biotechnology Inc., Santa Cruz, CA, USA), followed by a secondary antibody conjugated with horseradish peroxidase (Santa Cruz Biotechnology Inc.) and visualized utilizing enhanced chemiluminescence.

1.4.9. Mitochondrial Isolation and Cytochrome *c* and AIF Assay

Brain mitochondria were prepared from adult C57BL/6 mice. Briefly, brains were homogenized in ice-cold buffer (pH 7.4) containing 250 mM mannitol, 75 mM sucrose, 10 µM K-HEPES and homogenates were centrifuged at 1,000 x *g* for 10 minutes. Supernatants were then centrifuged at 10,000 x *g* for 15 minutes. Pellets were washed three times and immediately used in experiments (Du *et al*., 2001). For the *in vitro* cytochrome *c*/AIF assay, an aliquot of 12.5 µg brain mitochondria (25 µl) was pretreated with CAPE for 5 minutes following challenge with 100 µM MPP^+ for 30 minutes at 30°C. After centrifugation, the supernatant was evaluated by Western blot.

To assay *in vitro* neuronal cytochrome *c* release, CGN were washed once with ice-cold PBS and harvested in 500 µL ice-cold Buffer A (50 mM Tris-HCl, pH 7.4; 1 mM EDTA; 1 mM DTT; complete EDTA-free Protease Inhibitor Cocktail Tablets, Roche Diagnostics Corp.; 250 mM sucrose). The cells were disrupted by douncing 10 times with a pestle in a 7-mL Wheaton douncer. After centrifugation in a microcentrifuge at 1,000 x *g* for 10 minutes at 4°C, the supernatants were

further centrifuged at 12,000 x *g* for 40 minutes. The resulting supernatants were used for immunoblot analysis.

1.4.10. Assessment of the Effect of CAPE on MPP^+-induced Free Radicals and Peroxynitrite Formation

To assess superoxide ($O_2^{\cdot -}$) production and peroxynitrite in the cultures, CGN were treated with MPP^+ (70 µM) in the absence or the presence of CAPE (2-hour pretreatment) for 24 hours and 48 hours. Neurons were washed twice with PBS and 1 mL of PBS containing 10 µg/mL dihydroethidium (DHE; Molecular Probes) or 50 µM dihydrorhodamine 123 (DHR; Molecular Probes) was then added. After an additional 30 minutes of incubation at 37°C, luminescence was measured in a Cytofluor fluorimeter with an excitation wavelength of 485 nm (both dyes) and a detection wavelength of 610 nm (DHE) or 530 nm (DHR; Ma *et al*., 2006).

1.4.11. Statistical Analysis

Statistical analysis was performed by linear models. Between groups comparisons were conducted by post-hoc tests (F-tests) after model estimation. Groups were defined by CAPE dosages (0, 2, 5 and 10 mg/kg p.o.) and experiment (Control, C, CA, MPTP/MPP, MPTP/MPP-CA). All data are reported as mean ± standard error of the mean. *p* values less than 0.05 were considered significant. All statistical analyses were performed with STATA 11.1 (STATA Corp, 2009).

1.5. Results

1.5.1. MPTP-induced neurotoxicity of midbrain dopaminergic neurons is blocked by CAPE

C57BL/6 mice were treated with CAPE (2, 5, or 10 mg/kg, p.o.) daily for 7 days to evaluate a dose response and determine the most effective CAPE dosage against MPTP neurotoxicity. Based on these studies, it was observed that the doses of 5 mg/kg and 10 mg/kg CAPE significantly preserved DA neurons in mice with MPTP exposure. On day 0, mice were administered a single CAPE treatment prior to administration of MPTP (4 x 20 mg/kg, i.p.). Seven days following the last dose of MPTP, mice that received daily treatments of CAPE at either 5 or 10 mg/kg and MPTP showed an increased percentage of TH-positive neurons in the SNpc, ranging from 46% of control (no CAPE treatment, $F(1,32) = 0.89$; $p = 0.351$, Fig 1.8Aa) to 73% (5 mg/kg, $F(1,32) = 34.89$, $p < 0.001$, Fig 1.8Ab) and 92% (10 mg/kg, $F(1,32) = 87.73$, $p < 0.001$, Fig 1.8Ac) of control (Fig 1.8B). CAPE alone (103% of control ± 7.0%) did not alter the number of TH-positive neurons significantly (Fig 1.8B). Additionally, HPLC analysis of tissues detected 5 µg/mg brain CAPE and 300 g/mL blood CAPE from C57BL/6 mice given 10 mg/kg CAPE orally, demonstrating successful uptake of the compound and systemic distribution at 1 hour after oral gavage.

1.5.2. CAPE blocks MPTP-induced loss of striatal dopamine

Mice that received 10 mg/kg of CAPE had striatal dopamine levels that were 32.6% of untreated controls, compared to only 6.6% in the MPTP (alone)-treated group ($F(1,6) = 9.48$, $p = 0.022$; Fig 1.9).

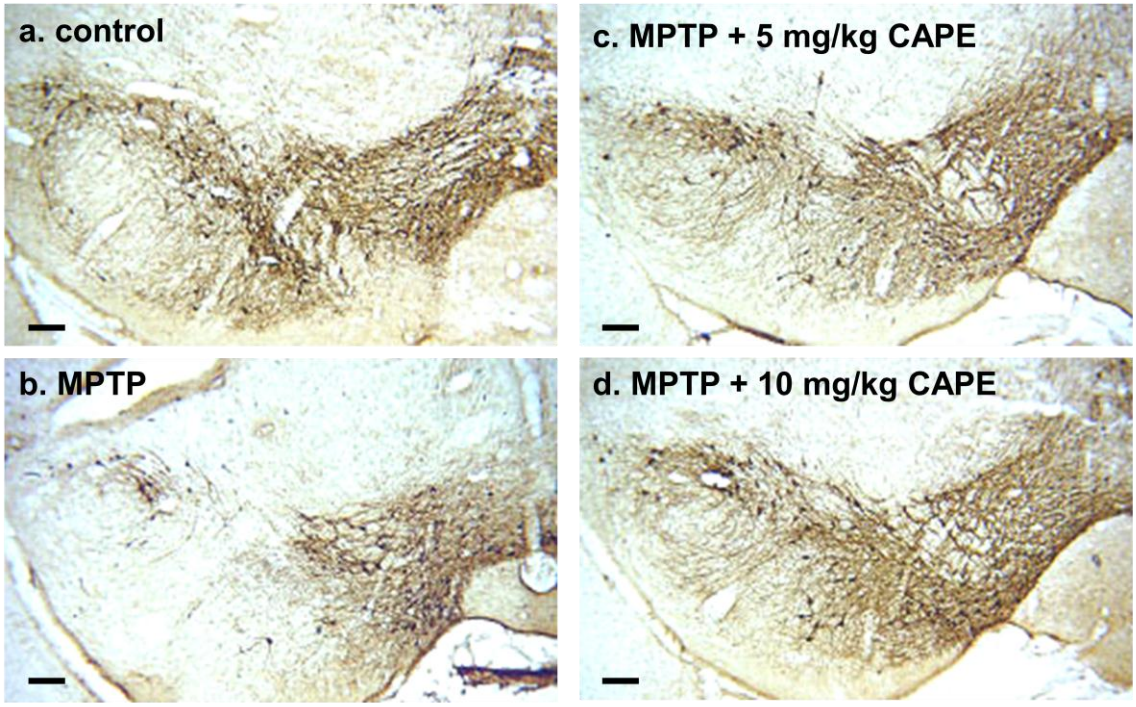

Figure 1.8A. CAPE treatment prevented the loss of TH-positive neurons in the midbrain following MPTP administration.

C57BL/6 mice were exposed to MPTP and given CAPE treatment as described in Experimental Procedures. Whole brains were removed and prepared for immunohistochemical analysis of TH-immunoreactivity 7 days after the last MPTP exposure. Representative images of coronal sections of mouse brain showed that CAPE treatment at 5 mg/kg (c) and 10 mg/kg (d) significantly protected the loss of TH-positive neurons induced by MPTP exposure as compared to (b) MPTP-exposed animals without CAPE treatment. A wild type control without CAPE treatment or MPTP exposure is represented in (a). Scale bars: 100 µm.

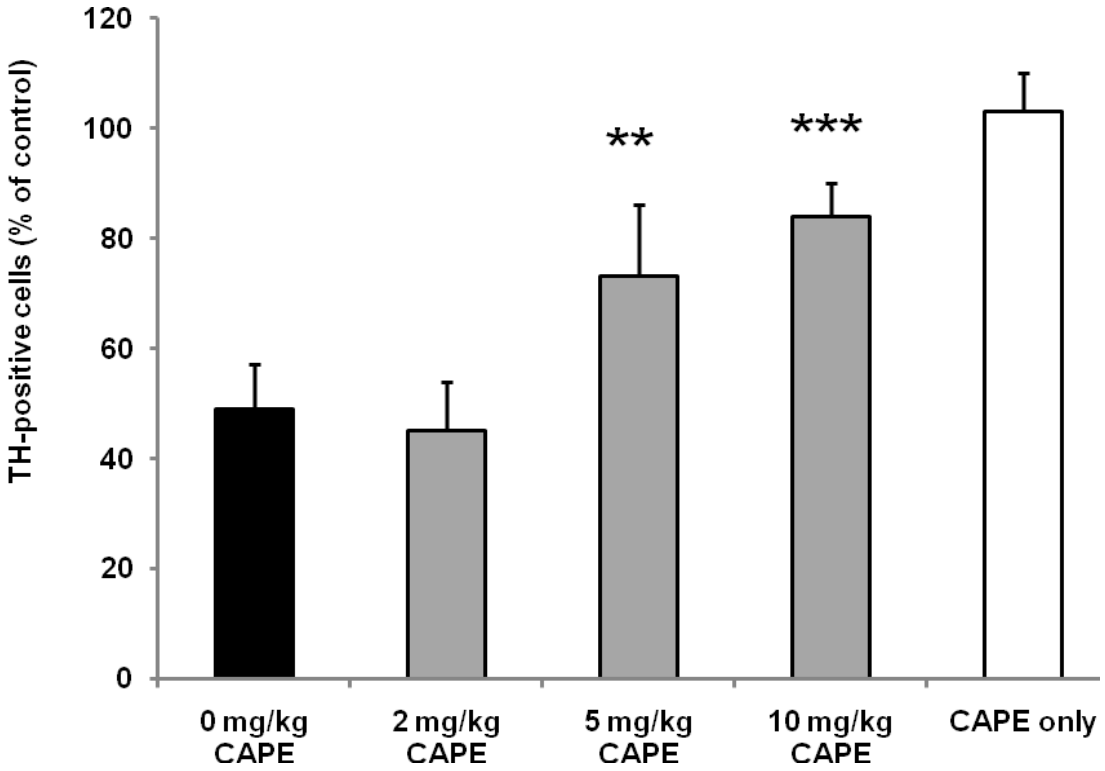

Figure 1.8B. Treatment with CAPE resulted in higher numbers of TH-positive neurons in midbrain after MPTP exposure.

C57BL/6 mice were administered MPTP and CAPE as described in Experimental Procedures. Removal and processing of whole brains was performed at 7 days after the last MPTP exposure. A stereological method for counting TH-positive neurons and methyl green counterstain was used as previously described by Du *et al*. (2001). CAPE treatment significantly protected animals from MPTP-induced dopaminergic cell death. Vehicle, n = 15; 0 mg/kg CAPE (MPTP-alone), n = 14; 2 mg/kg CAPE, n = 6; 5 mg/kg CAPE, n = 7; 10 mg/kg CAPE, n = 9. ** $p < 0.01$, *** $p < 0.001$ versus 0 mg/kg CAPE (MPTP-alone).

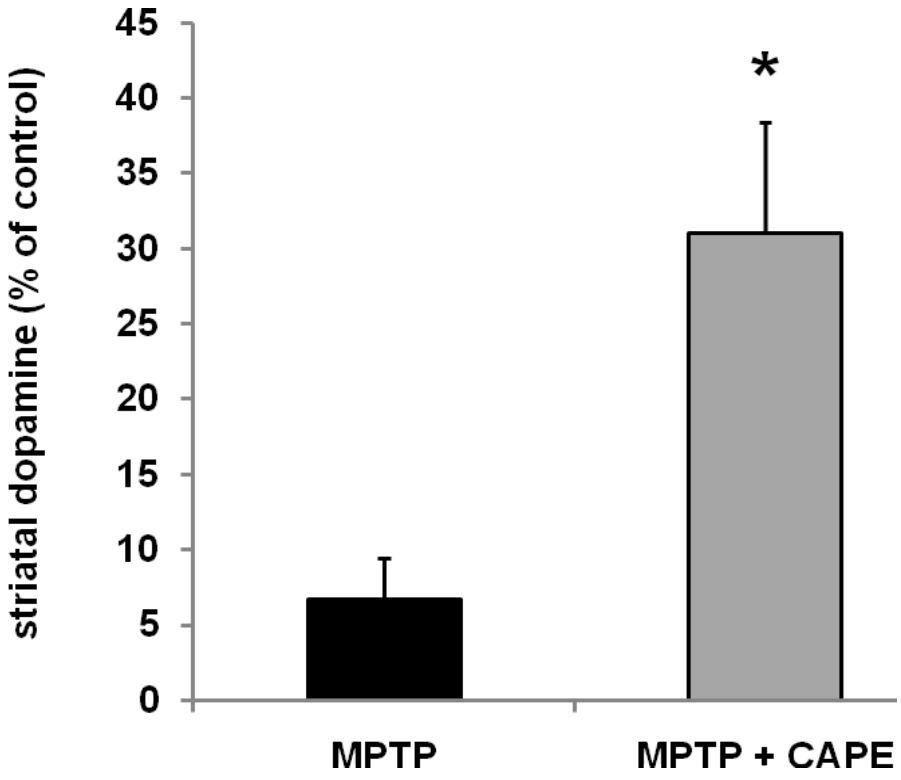

Figure 1.9. Treatment with 10 mg/kg CAPE decreased the loss of striatal dopamine levels in MPTP-exposed mice.

Brains from MPTP-exposed C57BL/6 mice with or without CAPE treatment were dissected at 7 days following the last MPTP exposure and prepared for dopamine measurement via HPLC analysis as described in Experimental Procedures. CAPE treatment resulted in lower reductions in striatal dopamine levels as compared to vehicle. Vehicle, n = 15; CAPE, n = 9. * $p < 0.05$

1.5.3. CAPE does not alter MAO activity and brain MPP^+ levels

CAPE did not inhibit MAO-B at concentrations as high as 100 µM. By comparison, the mixed MAO-A and MAO-B inhibitor, pargyline, inhibited mouse brain MAO-B with pI_{50} values of 8.2 µM. Moreover, MPP^+ levels in midbrain were 4.5 ± 1.6 µg/g in untreated or 5.1 ± 0.6 µg/g in CAPE-treated (10 mg/kg) animals at 3 hours following MPTP treatment ($p = 0.71$). With the same treatments, midbrain levels of CAPE were 0.22 ± 0.024 µg/g. These data suggest that the neuroprotective effect of CAPE is not due to reduced metabolism of MPTP to MPP^+.

1.5.4. CAPE blocks MPTP-induced expression of midbrain iNOS and caspase-1

Measurements of both iNOS and caspase-1 in midbrain homogenates of mice exposed to MPTP were performed (Fig 1.10). At 24 hours following MPTP exposure, both iNOS (Fig 1.10b) and caspase-1 (Fig 1.10c) were upregulated, but were blocked in the presence of CAPE (Fig 1.10b and 1.10c). In contrast, neither MPTP nor CAPE had any effect on nNOS expression in the same samples (Fig 1.10a).

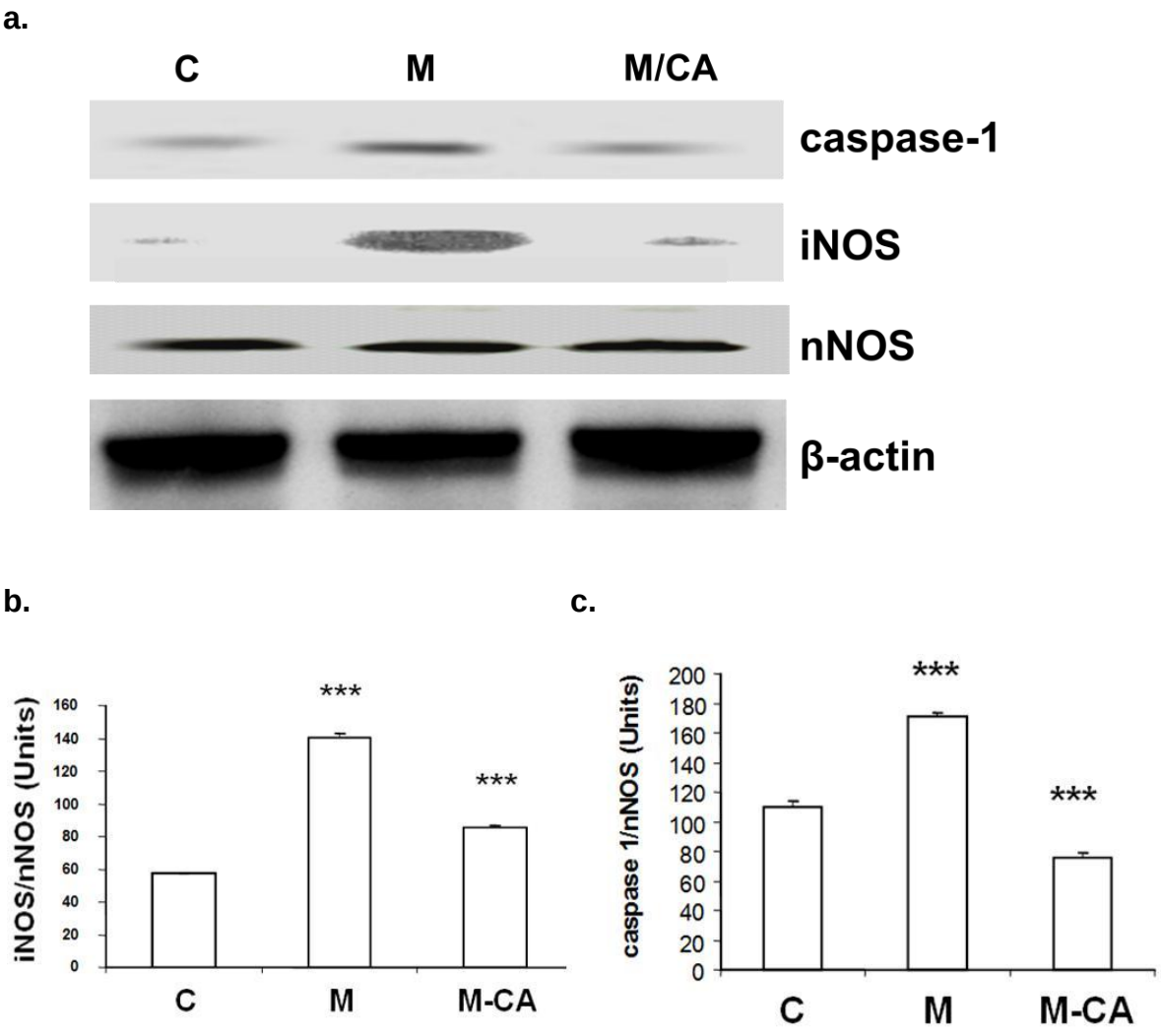

Figure. 1.10. CAPE blocked MPTP-induced *in vivo* expression of iNOS and caspase-1.

Immunoblot analyses were performed with polyclonal antibodies against iNOS, nNOS, and caspase-1. CAPE blocked MPTP-induced expression of (b) iNOS and (c) caspase-1. Note that MPTP and CAPE treatments fail to alter nNOS expression in these same samples (a). β-actin was used as an internal loading control. “C” represents control group; “M” represents MPTP group; “M-CA” represents MPTP + CAPE group. 3 independent experiments (n = 3 per group) with similar results were performed. *** $p < 0.001$

1.5.5. CAPE blocks MPP+ -induced neurotoxicity in both RMN and CGN

Neurons were exposed to MPP^+ (10 µM for RMN and 70 µM for CGN) in the absence or presence of CAPE. CAPE significantly protected RMN ($F(1,12) = 5.04$; $p = 0.039$) (Fig 1.11A and 1.11B) and CGN ($F(1,20) = 146.49$, $p < 0.001$) (Fig 1.12A and 1.12B) against MPP^+ neurotoxicity. Since there is no dopamine transporter (DAT) in CGN, our data indicates that CAPE's inhibition of MPP^+-induced neurotoxicity does not occur via inhibition of DAT activity. Additionally, we did not observe MPP^+-induced (70 µM) free radical formation in cultured CGN (data not shown).

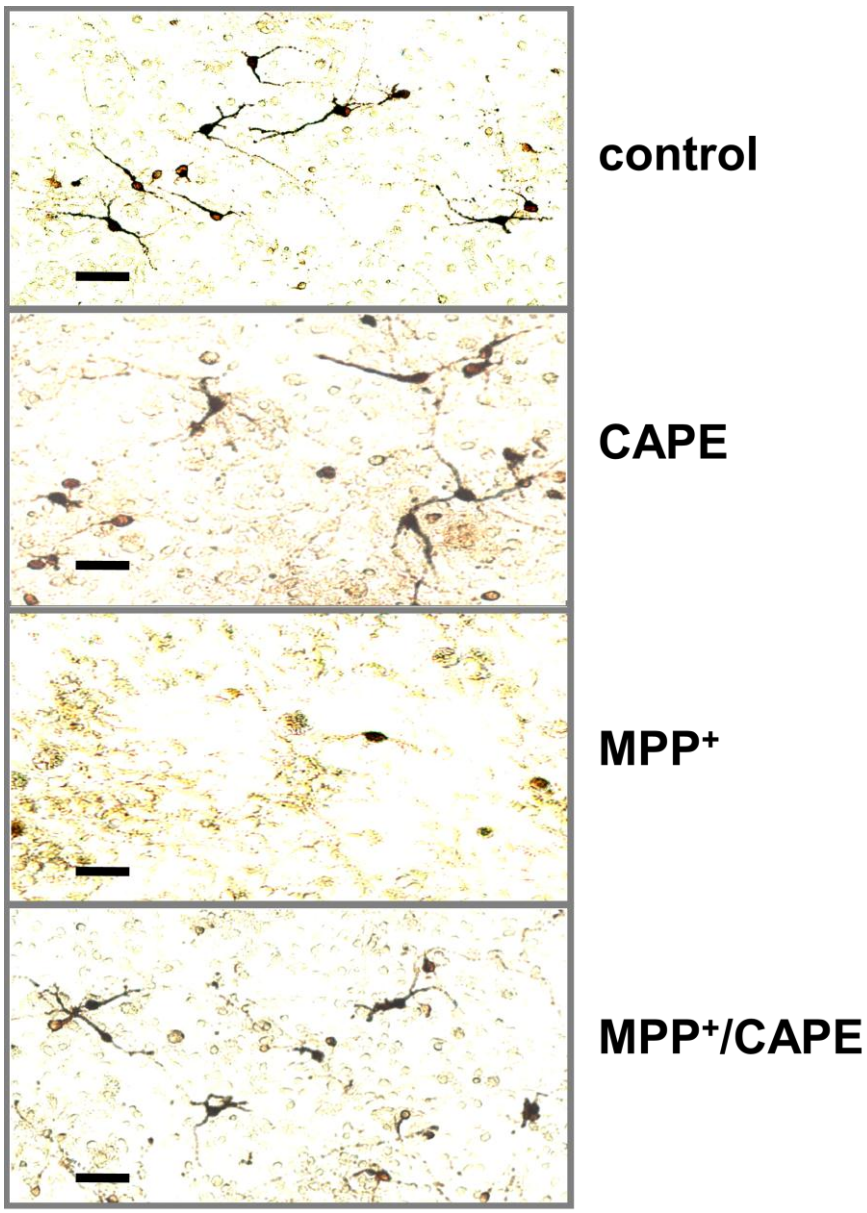

Figure 1.11A. CAPE treatment resulted in reduced RMN cell death induced by MPP^+ exposure.

RMN cell culture was performed as detailed in Experimental Procedures. RMN were pretreated with CAPE (10 µM) for 2 hours followed by MPP^+ exposure (10 µM) for 72 hours. DAB staining with tyrosine hydroxylase antibody was used to detect surviving RMN as previously described in Experimental Procedures. Representative images of primary cell culture plate fields showed a decrease in MPP^+-induced RMN cell death in the absence of CAPE, but reduced MPP^+-induced RMN death in the presence of CAPE. Scale bars: 20µm.

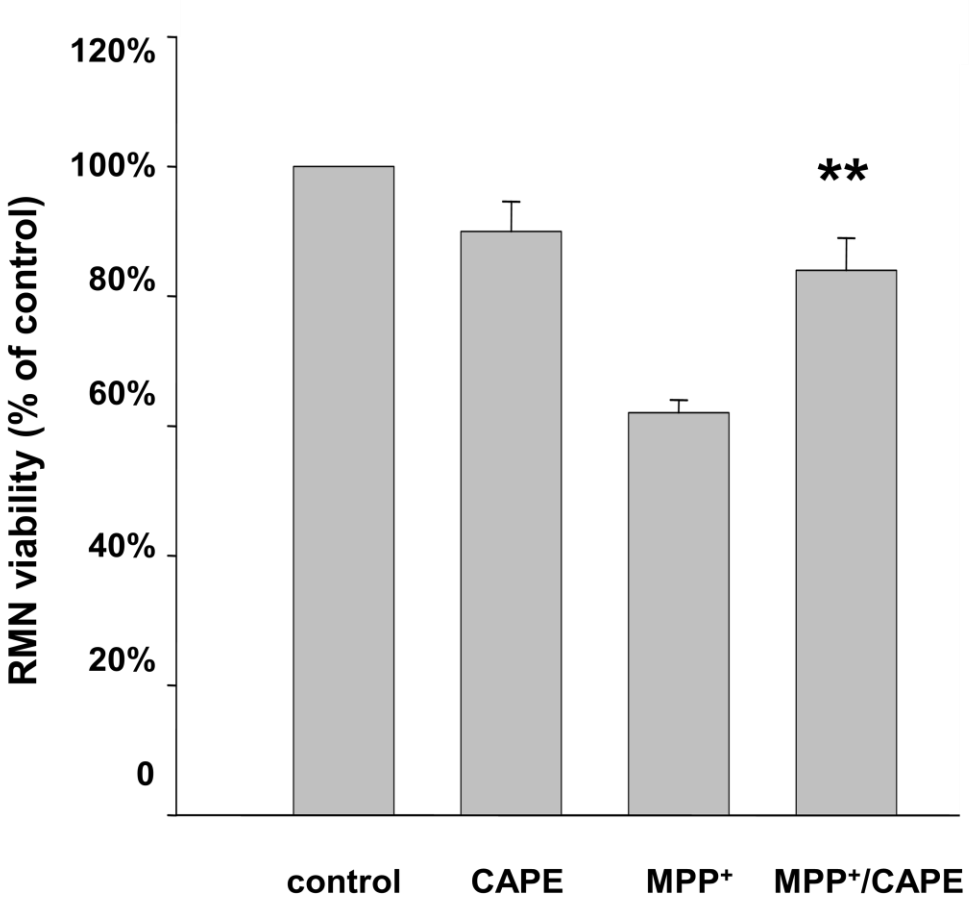

Figure 1.11B. CAPE blocked MPP^+-induced neurotoxicity of cultured RMN.

RMN cell culture was performed and surviving RMN were detected by using DAB staining with tyrosine hydroxylase antibody as previously described in Experimental Procedures. RMN were pretreated with CAPE (10 µM) for 2 hours followed by MPP^+ exposure (10 µM) for 72 hours. A decrease in MPP^+-induced RMN cell death was observed in CAPE-treated cultures as compared to CAPE-lacking cultures. Experiments (n = 3 per group) were repeated 3 times with similar results. ** $p < 0.01$

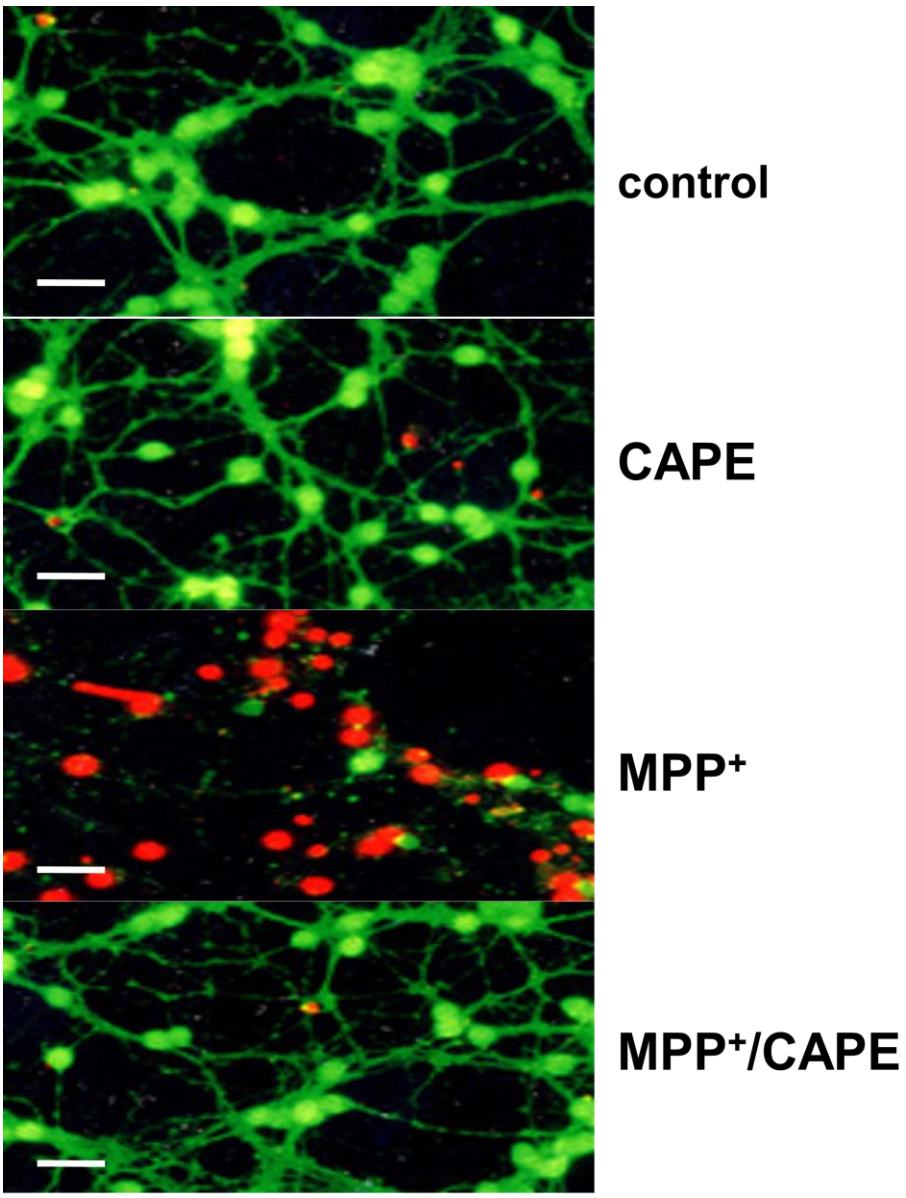

Figure 1.12A. CAPE prevented MPP^+-induced cell death of cultured CGN.

CGN were pretreated with CAPE (10 µM) for 2 hours followed by MPP^+ exposure (70 µM) for a total of 72 hours. Fluorescence staining with fluorescein diacetate (green) and propidium idiode (red) was used to visualize surviving CGN (green) versus dead CGN (red) as previously described in Experimental Procedures. Representative images of primary cell culture plate fields demonstrated a decrease of CGN cell death induced by exposure to MPP^+ in the presence of CAPE. Scale bars: 40µm.

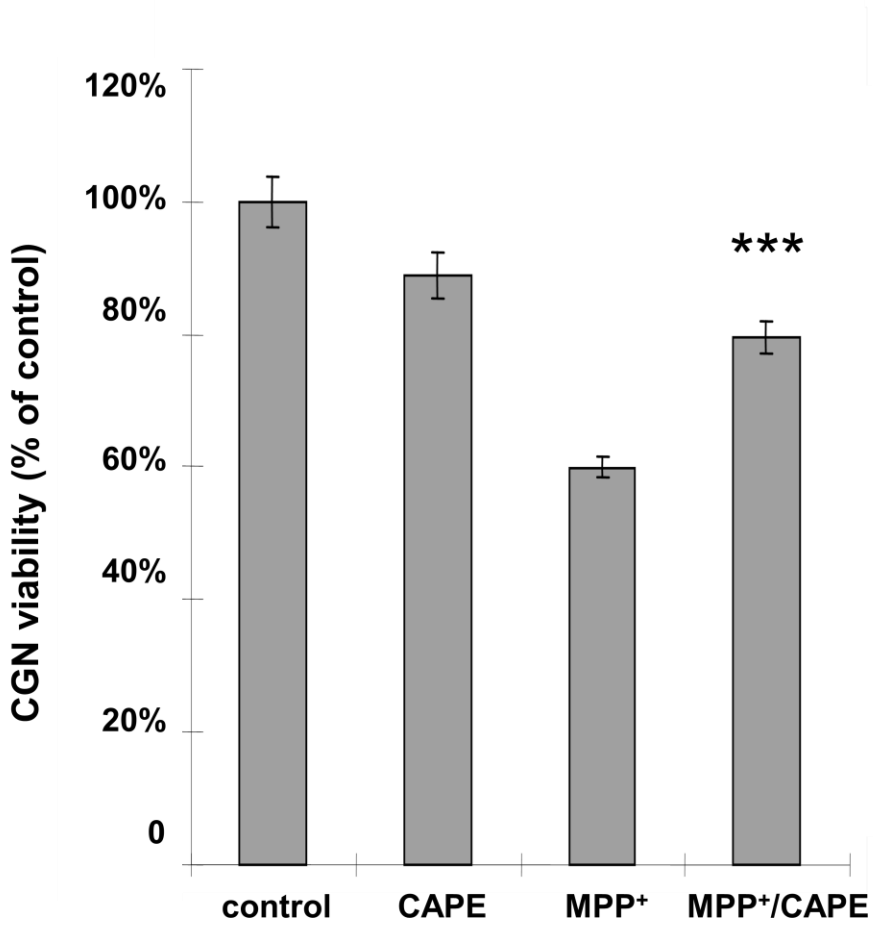

Figure 1.12B. MPP^+-induced neurotoxicity of CGN is blocked by CAPE.

CGN cell culture was performed and surviving CGN were detected by using a fluorescent double-stain technique involving fluorescein diacetate and propidium idiode as previously described in Experimental Procedures. CAPE (10 µM) pretreatment was applied for 2 hours followed by MPP^+ exposure (70 µM) for a total of 72 hours. CAPE treatment resulted in a blockade of MPP^+-induced CGN cell death. Experiments (n = 3 per group) were repeated three times with similar results. *** $p < 0.001$

1.5.6. CAPE blocks MPP^+-induced cytochrome *c* and AIF release

Since cytochrome *c* and AIF were shown to mediate MPP^+-induced neurotoxicity (Chu *et al*., 2005), we examined whether MPP^+-induced release of cytochrome *c* and AIF was the primary target of CAPE action. A concentration of 100 µM MPP+ was able to induce cytochrome *c* and AIF release from brain mitochondria; CAPE significantly blocked this induction at 20 µM (Fig 1.13), a similar observation that was previously shown with Ca^{2+}-induced cytochrome *c* release in previous studies (Wei *et al*., 2004).

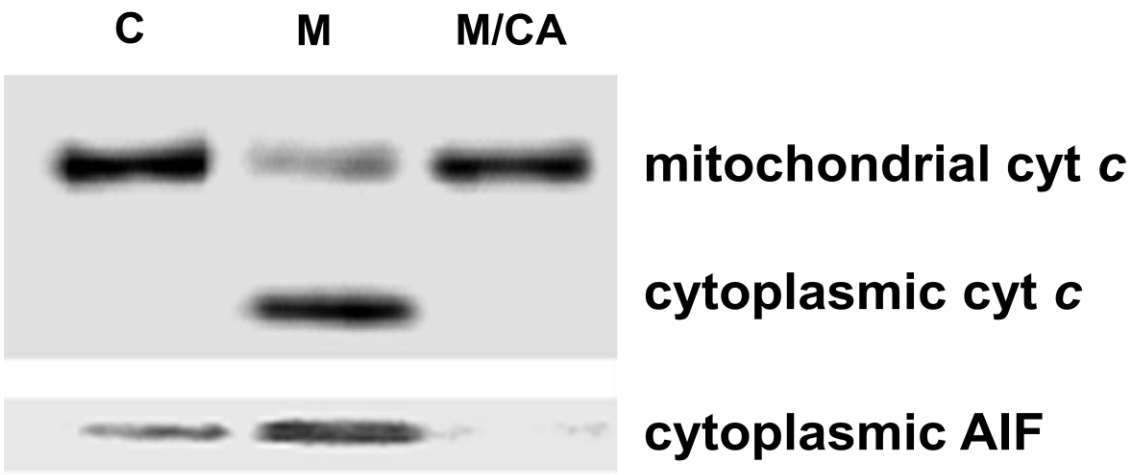

Figure 1.13. CAPE inhibited MPP^+-induced cytochrome *c* and AIF release from isolated mouse brain mitochondria.

30 µg of mouse brain mitochondria was exposed to MPP^+ (100 µM) for 30 minutes at 37°C in the absence (M+) or presence of CAPE (M+/CA, 20 µM). Experiments (n = 3 brain samples per group) were repeated three times with similar results.

1.6. Discussion

Previous studies from this lab using the MPTP mouse model have demonstrated that after 7 days of MPTP exposure, there is a significant decrease in the number of TH-positive neurons in the midbrain (Du *et al*., 2001). The present study sought to determine if CAPE confers neuroprotection at this time point. Furthermore, previous studies from this lab have also shown that treatment with CAPE once daily for 7 days results in prevention of neuronal loss following hypoxia-ischemia-induced brain damage (Wei *et al*., 2004). The present study was designed to determine if CAPE treatment once daily for 7 days would provide protection in another model of neuronal injury (the MPTP model). Our data demonstrate that oral administration of CAPE effectively protects midbrain dopaminergic neurons from the toxic effects of MPTP *in vivo*. Additionally, CAPE treatment results in a marked “protective effect” on the depletion of DA in the striatum following MPTP administration. Moreover, we have also shown that CAPE-induced neuroprotection did not result from alteration of brain MAO activity and MPP^+ levels.

In order to investigate whether CAPE could directly protect neurons against MPTP/MPP^+ neurotoxicity, we used an *in vitro* system and treated both RMN and CGN with MPP^+. We have found that CAPE directly blocks MPP^+-induced neuronal death in both RMN and CGN cultures. Given that CGN completely lack expression of the DAT and MPP^+ induces its neurotoxicity via the organic cation transporter 3 (Shang *et al*., 2003), we suggest that CAPE-induced neuroprotection against MPP^+ neurotoxicity should not result from inhibiting DAT

function. These results are in agreement with previous studies from this laboratory that show CAPE's neuroprotective effect against 6-OHDA exposure *in vitro* (Noelker *et al*., 2005; Ma *et al*., 2006); however, because the 6-OHDA and MPP+ models differ in their mechanisms of neurodegeneration and neuropathology, it can be posited that CAPE is multifaceted in its neuroprotective effects, such that CAPE is effective against neurotoxicity associated with an oxidative damage basis (the 6-OHDA model) or neuroinflammation and neuronal apoptosis (the MPTP model).

CAPE has been shown to have anti-inflammatory properties (Wei *et al*., 2004) and we demonstrate that CAPE inhibits MPTP-induced iNOS and caspase-1 expression in mice. Our data suggest that CAPE could also indirectly protect dopaminergic neurons by attenuating MPTP-induced neuroinflammation that is detrimental to neurons (Dehmer *et al*., 2000; Klevenyi *et al*., 1999; Liberatore *et al*., 1999).

CAPE has anti-oxidant function that may help protect neurons against MPP^+-induced neurotoxicity. However, at least in CGN, we did not find that CAPE induced neuroprotection from MPP^+ neurotoxicity by inhibiting free radical generation. Our CAPE data are consistent with other reports indicating the neuroprotective efficacy of anti-oxidants on the MPTP animal model; however, these data are also contrary to a previous study whereby an antioxidant, minocycline, could not directly block MPP^+-induced neuronal death, but significantly blocked hydrogen peroxide- (H_2O_2-)induced neuronal death (Du *et al*., 2001, Tikka *et al*., 2001). Therefore, we sought to investigate whether CAPE

provides neuroprotection through other mechanisms. Since cytochrome *c* /AIF release contributes to MPP^+ neurotoxicity (Chu *et al*., 2005) and mitochondria are the major target for MPP^+, in this study, we investigated if CAPE directly protects mitochondrial membrane integrity. We treated isolated brain mitochondria with MPP^+ and CAPE. 20 µM CAPE significantly blocked MPP+-induced release of cytochrome *c* and AIF from mitochondria, indicating that this compound directly protects mitochondria from MPP^+ attack. This concentration of CAPE prevents the release of cytochrome *c* either by stimulation due to MPP^+ exposure (present study) or Ca^{2+}-induced (Wei *et al*., 2004), further demonstrating that an underlying pathway of CAPE neuroprotection involves cytochrome c and the mitochondrial membrane. This result indicates that in addition to other anti-inflammatory and antioxidant functions, CAPE is able to directly block MPP^+-induced neuronal death by protecting the integrity of the mitochondrial membrane.

CHAPTER 2: Caffeic Acid Phenethyl Ester Extends Survival of a Mouse Model of Amyotrophic Lateral Sclerosis

2.1. Rationale

Because the previous study of this dissertation (Chapter 1: *Caffeic Acid Phenethyl Ester Prevents 1-Methyl-4-phenyl-1,2,3,6-tetrahydropyridine-induced Neurodegeneration*) demonstrated the effectiveness of caffeic acid phenethyl ester (CAPE) in a neurotoxin-based (1-methyl-4-phenyl-1,2,3,6-tetrahydropyridine, MPTP) mouse model of neurodegeneration, the present report sought to validate the use of CAPE for protection against neuronal cell degeneration and to verify the compound's neuroprotective benefit in a genetically-engineered animal model of neurodegenerative disease, namely amyotrophic lateral sclerosis (ALS).

This dissertation hypothesizes that despite etiology (environmental versus genetic), if two diseases have similar downstream events that are responsible for the degeneration of neurons, then the most effective treatment for both diseases would need to be beneficial in slowing disease progression by way of targeting those shared downstream events. Neurodegenerative diseases share many common pathogenic events that lead to the death of neurons, the subsequent disease state, and ultimately death. Although the target neurons in each disease (dopaminergic neurons in MPTP/PD and motor neurons in ALS) differ, the causal mechanisms responsible for progression are similar. Because the underlying neuronal death pathways in the MPTP mouse model and PD are comparable to

those observed in ALS, the present study was designed to test the effectiveness of CAPE against those neuropathologic mechanisms in a mouse model of ALS as these analyses have not been examined to date. By using the compound, CAPE, that has been shown to host a large array of neuroprotective abilities and can target multiple pathogenic pathways, such as those observed in the MPTP mouse model of PD discussed in Chapter 1, neurodegeneration and disease progression would be slowed, regardless of disease etiology (neurotoxin-based versus an underlying genetic mutation).

2.2. Abstract

There is currently very limited effective pharmacological treatment for amyotrophic lateral sclerosis. Recent evidence suggests that caffeic acid phenethyl ester has strong anti-inflammatory, anti-oxidative, and anti-neuronal death properties; thus, the present study tested the effects of caffeic acid phenethyl ester in mice expressing a mutant superoxide dismutase ($SOD1^{G93A}$) linked to human amyotrophic lateral sclerosis. Administration of caffeic acid phenethyl ester after symptom onset significantly increased the lifespan of $SOD1^{G93A}$ mice by approximately 2 weeks, nearly doubling post-onset survival. Moreover, immunohistochemical analysis detected less activation of microglia and astrocytes and higher motor neuron counts at an early symptomatic stage (7 days following onset) in the spinal cords of $SOD1^{G93A}$ mice given caffeic acid phenethyl ester treatment. Additionally, lower levels of phosphorylated p38, a mitogen-activated protein kinase that is involved in both inflammation and neuronal death, were observed in the spinal cords of $SOD1^{G93A}$ mice treated with caffeic acid phenethyl ester for 7 days. These results indicate that caffeic acid phenethyl ester may represent a novel and effective therapeutic for the treatment of amyotrophic lateral sclerosis and these significant neuroprotective effects observed in a commonly used amyotrophic lateral sclerosis mouse model validate the therapeutic potential of caffeic acid phenethyl ester for slowing disease progression by attenuating the neuroinflammation and motor neuron cell death associated with clinical amyotrophic lateral sclerosis pathology.

Fontanilla CV, Wei X, Zhao L, Johnstone B, Pascuzzi RM, Farlow MR, Du Y. 2011. Caffeic acid phenethyl ester extends survival of a mouse model of amyotrophic lateral sclerosis. Neuroscience, Accepted 2011 Dec 24. [Epub ahead of print]

2.3. Introduction

2.3.1. Amyotrophic Lateral Sclerosis

Amyotrophic lateral sclerosis (ALS) is an incurable, neurodegenerative disorder defined by progressive motor neuron loss, leading to paralysis and ultimately death within 2 to 5 years after diagnosis. The death of motor neurons in the spinal cord results in the atrophy of muscle and eventual paralysis (Tandan and Bradley, 1985). ALS incidence is about 2 per 100,000 persons annually in the United States (Sejvar *et al*., 2005) with the majority being sporadic cases and 5 – 10% familial (Rowland and Shneider, 2001). Because both forms are highly similar in clinical course, pathophysiology, and outcome, the underlying mechanisms of manifestation and progression are posited to be the same (Bruijn *et al*., 2004).

The discovery that inheritable (familial) forms of ALS are linked to mutations in the Zn/Cu superoxide dismutase (Rosen *et al.*, 1993) (SOD1) led to the creation of the $SOD1^{G93A}$ mouse, which is the most extensively-studied animal model of ALS (Gurney *et al*., 1994; Alexander *et al*., 2004). The model exhibits the major ALS hallmarks, including motor neuron pathology leading to progressive paralysis (Gurney *et al*., 1994; Alexander *et al*., 2004). Use of this

model uncovered an array of processes involved in ALS onset and progression, including glutamate excitotoxicity, oxidative damage, glial cell activation, neuroinflammation, mitochondrial dysfunction, and aberrant protein folding and axonal transport (Rowland and Shneider, 2001; Rothstein, 2009).

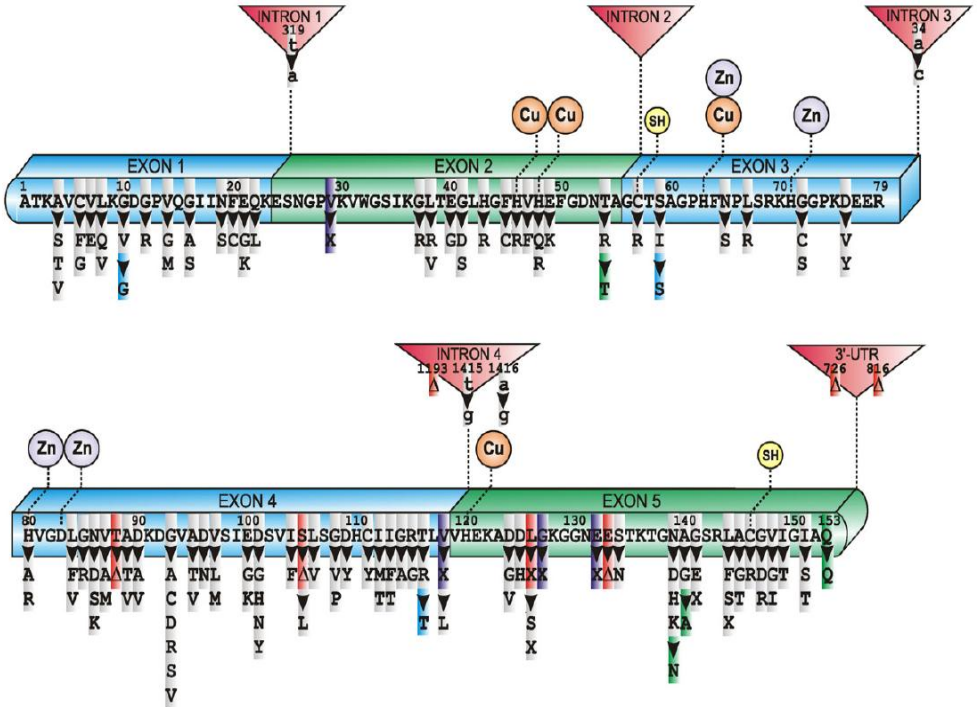

Turner and Talbot, 2008

Figure 2.1 Discovered mutations in the SOD1 human gene.

These mutations were observed in over 13 families with familial forms of ALS (fALS; Rosen *et al*., 1993). At position 93, the SOD1^{G93A} mice have a single glycine (G) to alanine (A) mutation that is required for the animal to develop disease (Gurney *et al*., 1994). To date, there are over 150 mutations found in the Cu, Zn-SOD1 gene (Rosen *et al*., 1993), which have led to the development of mouse models of ALS.

2.3.2. Treatments for ALS

Because multiple neuronal death pathways are implicated in disease development and maintenance, the pathophysiological processes in humans may not be addressable by targeting (inactivating) a single neurodegenerative process; rather, a multi-target approach may be required to effectively control disease progression (Rothstein, 2009). Additionally, as no pre-symptomatic predictors, diagnostic tests, or biomarkers for ALS currently exist, treatment can only be applied after symptom onset (Rowland and Shneider, 2001).

A large number of pharmacologic therapies used in both clinical trials and stringent testing at the ALS Therapy Development Institute (ALS-TDI; Scott *et al.*, 2008) have been unsuccessful in providing protection against the neurodegeneration of motor neurons observed in ALS (Scott *et al.*, 2008). These failures at the pre-clinical or clinical stage may be attributed to the treatment's inability to target more than one neuronal death pathway, resulting in an incomplete or ineffective blocking of motor neuron cell loss and ALS disease progression.

2.3.2.1. *Riluzole (Rilutek®)*

Because excitotoxicity is posited to be involved in the motor neuron death observed in ALS, interest in anti-glutamatergic agents for ALS drug development ensued. To date, the only FDA-approved treatment for the slowing of ALS progression and extending of survival is riluzole (Rilutek®; Gurney *et al.*, 1996, 1998). Riluzole's mode of action was found to involve the inhibition of the release

of glutamate release at the nerve terminal (Martin *et al.*, 1993). One proposed mechanism of inhibition is thought to be related to riluzole functioning as a noncompetitive antagonist at glutamate receptors, specifically of the N-methyl-D-aspartate (NMDA) type (Malgouris *et al.*, 1994). Early treatment with riluzole in $SOD1^{G93A}$ mice with disease onset demonstrated prolonged survival and preserved motor performance, as assessed by wheel running behavior, suggesting that riluzole may be beneficial as a treatment for early stages of ALS (Gurney *et al.*, 1998). In *ex vivo* studies, riluzole exhibited neuroprotection against chronic glutamate-induced neuronal death in spinal cord explants (Rothstein and Kuncl, 1995). Shifted survival times were also observed with treatments with other anti-glutamatergic agents, such as gabapentin (Gurney *et al.*, 1996) and memantine (Wang and Zhang, 2005). Despite its modest effect on patient life extension of 2 – 5 months (Scott *et al.*, 2008), riluzole is currently the only available treatment for the ALS patient.

2.3.3. Caffeic Acid Phenethyl Ester and Neuroprotection

The use of a naturally-derived compound, caffeic acid phenethyl ester (CAPE), for treating an animal model of neurodegenerative disease and examination of the mechanisms underlying its neuroprotective ability were previously investigated by this laboratory (Ma *et al*., 2006; Wei *et al*., 2008). CAPE has numerous potentially beneficial properties, including immunomodulatory, anti-oxidant, and anti-inflammatory activities (Su *et al*., 1991, 1994; Grunberger *et al*., 1988), which this laboratory and collaborators has

previously found to protect against multiple cell death processes *in vitro* in a 6-hydroxydopamine-exposed cell culture model of neuronal death (Noelker *et al*., 2005; Ma *et al*., 2006; Wei *et al*., 2008) and *in vivo* against hypoxia-ischemia injury in neonatal rats (Wei *et al*., 2004). For a further review of CAPE, please see Section 1.3.4. Caffeic Acid Phenethyl Ester located in Chapter 1.

2.3.4. The SOD1^{G93A} Mouse Model of ALS

When discoveries of SOD1 mutations in familial ALS were made, focus was quickly placed on the development of transgenic mouse models of ALS, such as the SOD1^{G93A} mouse. This transgenic mouse model of ALS carries a transgenic construct with a glycine (G) to alanine (A) mutation at position 93 and is driven by the endogenous wild type mouse SOD1 promoter (Gurney *et al.*, 1994). Thus, these mice carry genes for both endogenous wild type mouse SOD1 and the mutated human G93A transgene.

At around 90 days of age, the SOD1^{G93A} mouse develops hind-limb weakness, which progresses to hind-limb hyperreflexia and followed by paralysis and death (Gurney *et al.*, 1994). Spinal cord pathology demonstrates motor neuron death initially detected at the lumbar level and becoming widespread as the disease progresses. In addition to motor neuron degeneration in the spinal cord, astrocytosis and microgliosis is observed (Hall *et al.*, 1998). The SOD1^{G93A} mouse is the most widely used model for ALS and is also the most well-characterized. It is able to exhibit the putative neurodegenerative mechanisms associated with ALS, including glutamate-mediated excitotoxicity, mitochondrial

dysfunction, oxidative damage, neuroinflammation, apoptosis, and ER stress (See Table 2.1) in the spinal cord. However, over a decade after development of the $SOD1^{G93A}$ mouse, the reasons and mechanisms underlying the selectivity of mutant SOD1 for motor neurons is not yet known. The current prevailing theory is that the G → A mutation at position 93 confers an unknown "gain of function" property (Gurney *et al.*, 1994).

2.3.5. Comparison of the Mechanisms of the ALS and MPTP Mouse Models

Below is a table listing the major mechanisms involved in neuronal death in both the MPTP mouse model of PD and the $SOD1^{G93A}$ mouse model of ALS.

Table 2.1. Mechanism Comparison of the ALS and MPTP Mouse Models

Mechanism	MPTP mouse model	$SOD1^{G93A}$ mouse model
mitochondrial dysfunction	inhibition of mitochondrial Complex I (Kindt *et al.*, 1987)	defective mitochondrial respiration (Mattiazzi *et al.*, 2002)
oxidative stress	increased lipid peroxidation and decreased glutathione levels in midbrain (Hung and Lee, 1998)	increased nitrotyrosine levels in spinal cord (Wootz *et al.*, 2004)
neuroinflammation	increased microglia activation and IL-1β and iNOS levels (Wu *et al.*, 2002)	increased microglia and astrocyte activation and ICAM-1 levels (Alexianu *et al.*, 2001)
excitotoxicity	glutamate-induced damage to dopaminergic somata in substantia nigra (Loschmann *et al.*, 1994)	neuron death due to elevated glutamate levels caused by loss of glial glutamate transporters (Rothstein *et al.*, 1996)
protein aggregation	upregulation of synuclein mRNA and protein in DA neurons in SN (Vila *et al.*, 2000)	mutant-mediated toxicity due to aggregation of cellular proteins and mutant SOD1 (Bruijn *et al*., 1998)
programmed cell death	exposure to low MPP^+ concentrations results in apoptosis (Du *et al.*, 1997)	activation of mitochondrial-dependent apoptotic proteins (Guegan *et al.*, 2001)
ER stress	activation of unfolded protein response (UPR) due to protein accumulation in ER (Sado *et al.*, 2009)	increased activation of caspase-12 and UPR (Nagata *et al.*, 2007)

Because the SOD1^{G93A} mouse model of ALS share and its associated human disease share common downstream pathogenic pathways with the MPTP mouse model of PD, CAPE treatment in the former should be neuroprotective against the death of motor neurons in the same manner as the neuroprotection observed in the latter. It is also demonstrated that regardless of disease etiology (neurotoxin-induced versus genetic mutation) and neuron type (dopaminergic versus motor), the shared endpoint is neuronal death.

The present study for Chapter 2 of the dissertation determined the cellular and biochemical responses to CAPE and evaluated its effectiveness against neurodegeneration in the SOD1^{G93A} mouse using clinically-relevant dosing parameters to further validate the use of CAPE for protection against the neuronal cell death occurring in the established disease state.

2.4. Experimental Procedures

2.4.1. Animals

All animal procedures were conducted in compliance with the protocols approved and authorized by the Institutional Animal Care and Use Committee at the Indiana University School of Medicine.

2.4.1.1. *The SOD1^{G93A} mouse model of ALS*

Male and female transgenic mice overexpressing the human SOD1-G93A mutation (SOD1^{G93A} mice) were maintained in-house as hemizygotes on a B6SJL

background by crossing B6SJL-Tg(SOD1-G93A)1Gur/J males (stock #JR2726; The Jackson Laboratory, Bar Harbor, ME, USA; Gurney *et al.*, 1994) with wild type control B6SJLF1/J females (stock #100012; The Jackson Laboratory). Mice carrying the $SOD1^{G93A}$ mutation were identified by performing PCR on tail tissue-derived DNA using a protocol provided by The Jackson Laboratory.

2.4.1.2. *Behavioral Assessment of Animals*

Beginning at 90 days of age, male and female $SOD1^{G93A}$ mice were randomly assigned to either “vehicle” or “CAPE” groups and tested twice a week on a Rotarod apparatus (ENV-575M; Med Associates, Inc., St. Albans, VT, USA) with up to 3 trials per day. Disease onset was determined when the animal became unable to remain on the apparatus for 10 minutes at a speed of 15 rpm. Additionally, Rotarod performance was tested the day after the animal was unable to remain on the apparatus for the defined parameters in order to further verify disease onset. End stage (surrogate death time point) was defined when the animal could not right itself within 20 seconds of being gently rolled on its side. Mice were monitored every morning for morbidity and mortality and every afternoon for the righting reaction.

2.4.1.3. *Animal Treatment Protocol*

CAPE (Sigma-Aldrich Corp., St. Louis, MO, USA) was dissolved in HotRod Formulation (Pharmatek, San Diego, CA, USA) vehicle and orally administered at a single dose of 2.5, 10, or 40 mg/kg, once daily, for optimal

dose determination experiments and a single dose of 10 mg/kg, once daily, for subsequent immunohistochemical and biochemical experiments. Animals in the vehicle group (HotRod alone) were given an equivalent volume according to body weight. Mice received one daily dose of CAPE or vehicle until a humane endpoint near death (survival studies) or for 3 or 7 days after disease onset (biochemical and immunohistochemical studies).

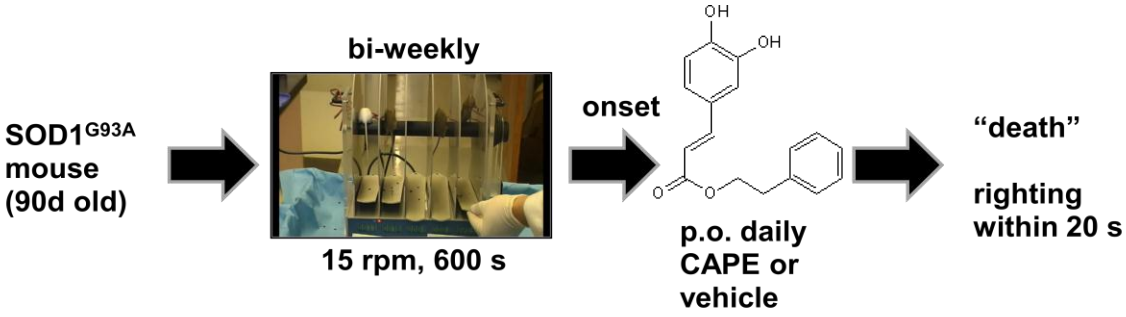

Figure 2.2. Diagram of the Animal Treatment Protocol for the current study.

2.4.2. Immunoblot

Western blot analysis was performed on tissue lysates (15 µg/well) as previously described (Wei *et al*., 2004) after 7 days of treatment with CAPE or vehicle. Spinal cord samples were homogenized in radio-immunoprecipitation assay (RIPA) buffer containing 1% Nonidet P-40, 0.1% SDS, 50 mM Tris (pH 8.0), 50 mM NaCl, 0.05% deoxycholate, and protease inhibitor (Roche Diagnostics Corp., Indianapolis, IN, USA). Proteins were size-fractionated (SDS-NuPAGE) on a 4 – 12% polyacrylamide gradient gel and transferred onto nitrocellulose (Hybond N; Amersham Biosciences, Piscataway, NJ, USA). Blots were incubated with rabbit polyclonal primary antibody specific for

phosphorylated-p38 (1:1000; Millipore, Temecula, CA, USA) followed by horseradish peroxidase-conjugated secondary antibody (Santa Cruz Biotechnology Inc., Santa Cruz, CA, USA), visualized via enhanced chemiluminescence (Amersham Biosciences, Piscataway, NJ, USA), and quantitated by densitometric analysis (ImageJ, http://rsbweb.nih.gov/ij/).

2.4.3. Immunohistochemistry

Following 7 days of treatment with CAPE or vehicle, mice were anesthetized by isofluorane inhalation and perfusion-fixed with 4% paraformaldehyde in 0.1 M phosphate buffer (pH 7.4). Spinal cords were removed, fixed in 4% paraformaldehyde overnight at 4°C, and prepared for paraffin embedding. Samples were serially sectioned (15 µm) through the enlargement of the lumbar spinal cord and immunostained with mouse monoclonal primary antibody against microtubule-associated protein 2 (1:1000, MAP2; Millipore), mouse monoclonal antibody against glial fibrillary acidic protein (1:1000, GFAP; Millipore), or rabbit polyclonal antibody against ionized calcium binding adaptor molecule 1 (1:500, Iba-1; Wako Chemicals USA, Inc., Richmond, VA, USA; Ito *et al*., 2001; Sasaki *et al*., 2001; Voskuhl *et al*., 2009) followed by incubation with biotinylated secondary antibodies (Sigma-Aldrich Corp.). Visualization of the immunoreactions was performed using an avidin-biotin complex kit (Vector Laboratories Inc., Burlingame, CA, USA) with 3,3'-diaminobenzene tetrahydrochloride dehydrate as the chromogen (Sigma-Aldrich Corp.). Immunohistochemical negative control sections were treated with the

same protocol except for incubation with primary antibody and no specific staining was seen. Sections used for motor neuron counting were first observed for defined MAP2-immunoreactive neuronal processes then counterstained using Mayer's hematoxylin (Sigma-Aldrich Corp.) prior to mounting. Large motor neurons were counted in the ventral horn of lumbar spinal cord by using a light microscope with an x40 objective (Nikon, Japan) and were identified by a basophilic cellular outline (containing Nissl substance) and a prominent nucleolus (Grossman *et al.,* 2001; Sato *et al*., 2003). A total of 6 – 8 sections per animal through the lumbar area of the spinal cord were counted and reported as number of motor neurons per section as previously described (Dodge *et al*., 2008). For sections immunostained with Iba-1, as described previously (Ito *et al*., 2001; Sasaki *et al*., 2001; Voskuhl *et al*., 2009), activated microglia were characterized by a rounded cell body with short processes versus a resting or "ramified" morphology.

2.4.4. Statistical Analysis

All data are expressed as mean ± standard error of the mean (SEM). One-way analysis of variance (ANOVA) was used for statistical analyses and comparisons.

2.5. Results

2.5.1. Post-onset CAPE treatment of SOD1^{G93A} mice significantly diminished symptomatic progression and extended life span

The potential for orally administered CAPE to attenuate progression of established disease-like symptoms was assessed in the SOD1^{G93A}-ALS mouse model. Disease onset was determined via bi-weekly Rotarod monitoring of motor function and limb strength. Initial experiments were performed to determine an optimal dose whereby CAPE offers benefit to the SOD1^{G93A} mouse. CAPE-treated animals at all doses (2.5, 10, and 40 mg/kg) showed significant extension of survival time (group means: 26.6 ± 2.8 days, 28.4 ± 2.0 days, and 26.1 ± 3.6 days, respectively) when compared to vehicle-treated mice (14.3 ± 0.63 days, $p < 0.01$; Fig 2.3A), resulting in lengthened lifespan (group means: 132.1 ± 9.4 days, 138.6 ± 11.1 days, and 137.0 ± 14.3 days, respectively; Fig 2.3B) as compared to vehicle (122.1 ± 2.0 days, $p < 0.01$).

HPLC analysis of brain homogenate and whole blood at 1 hour after oral gavage (10 mg/kg CAPE) detected 5 µg CAPE/100 mg brain and 300 µg CAPE/1 mL blood, demonstrating successful uptake by CNS tissues as well as systemic distribution. Additionally, HPLC testing of spinal cord tissue at 1 hour post-gavage revealed detection of 81 ng/g tissue for wild type control and 1,026 ng/g tissue for SOD1^{G93A} mouse with disease onset, suggesting that a compromised blood brain barrier (Garbuzova-Davis *et al*., 2007) allowed for increased spinal cord uptake of CAPE in symptomatic SOD1^{G93A} mice.

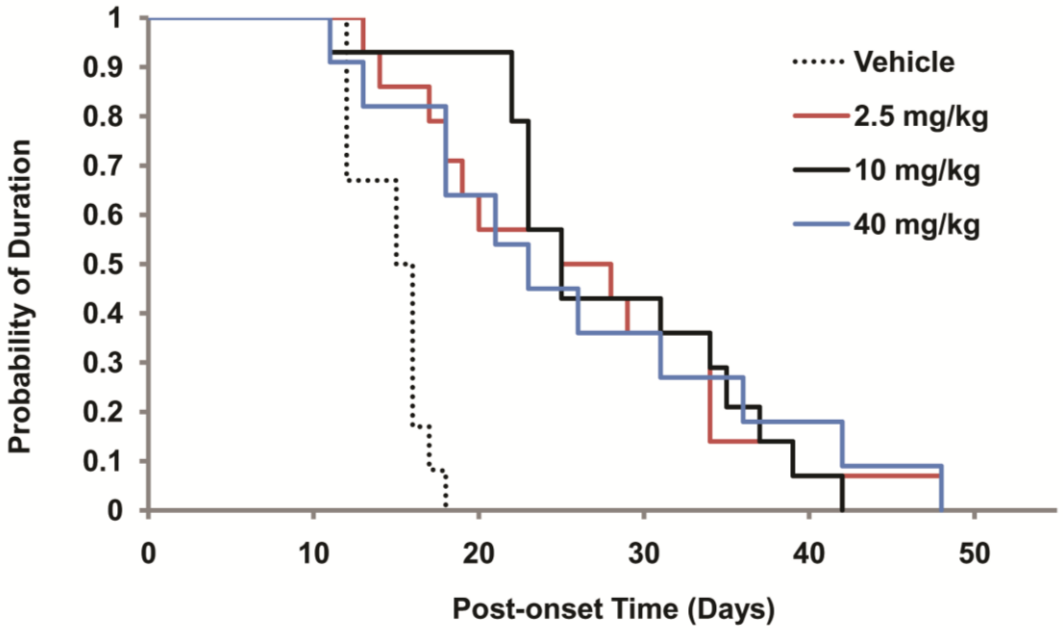

Figure 2.3A. CAPE treatment at increasing doses significantly elongated post-onset survival with disease onset.

Male and female SOD1^{G93A} mice with disease onset were administered CAPE (2.5, 10, or 40 mg/kg) or vehicle until the death endpoint. The number of days between disease onset and a humane endpoint near death were measured and reported as probability of duration. Mice with disease onset who were treated with CAPE at any dose (2.5 mg/kg, n = 14; 10 mg/kg, n = 14; 40 mg/kg, n = 11) had a significant extension of survival time as compared to SOD1^{G93A} mice without CAPE (n = 12).

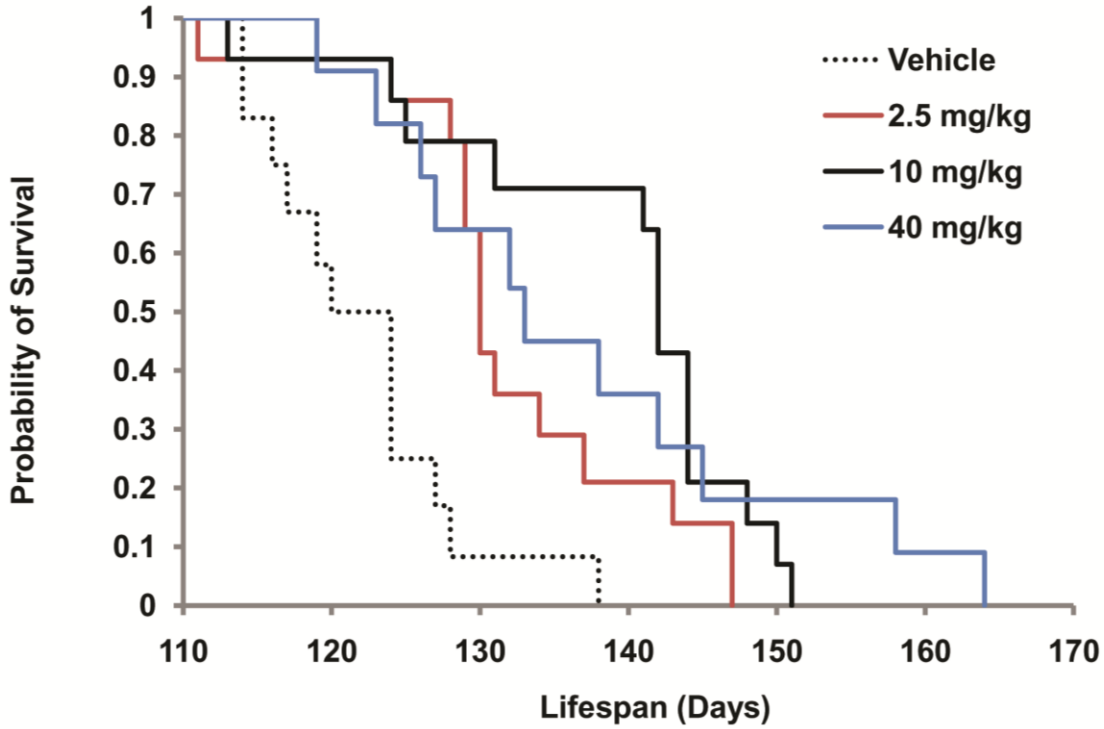

Figure 2.3B. CAPE treatment at increasing doses significantly lengthened lifespan of SOD1^{G93A} mice with disease onset.

Male and female SOD1^{G93A} mice with disease onset were treated with CAPE (2.5, 10, or 40 mg/kg) or vehicle until the death endpoint. The number of days between birth and a humane endpoint near death were measured and reported as lifespan. Mice with disease onset who were treated with CAPE at any dose (2.5 mg/kg, n = 14; 10 mg/kg, n = 14; 40 mg/kg, n = 11) had a significant lifespan extension when compared to SOD1^{G93A} mice with no CAPE treatment (n = 12). Extended post-onset survival times of all CAPE-treated mice (2.5, 10, and 40 mg/kg doses) resulted in the marked lengthening of lifespan relative to vehicle mice.

2.5.2. Daily oral CAPE treatment at a dose of 10 mg/kg is optimal for significantly decreasing disease progression and lengthening life span of symptomatic SOD1^{G93A} mice

For additional subsequent experiments (Fig 2.4), the 10 mg/kg CAPE dose was selected as it was observed that the response of SOD1^{G93A} mice to CAPE treatment had reached a plateau at 10 mg/kg such that there was no significant increase in survival time or lifespan at the 40 mg/kg dose as compared to 10 mg/kg. There was no difference in age of disease onset between CAPE (10 mg/kg) and vehicle groups (group means: 111.3 ± 2.6 days and 107.3 ± 2.6 days, respectively; data not shown). In accordance with initial dose response studies shown in Fig 2.3, additional studies (Fig 2.4) with daily administration of 10 mg/kg CAPE resulted in markedly increased time of post-onset disease duration (29.3 ± 2.0 days, $p < 0.01$; Fig 2.4A) compared to vehicle-treated animals (14.6 ± 0.68 days). This result was qualitatively reflected in total lifespan (Fig 2.4B), with CAPE-treated SOD1^{G93A} mice surviving 140.6 ± 2.4 days compared to 121.9 ± 2.2 days in the vehicle group ($p < 0.01$).

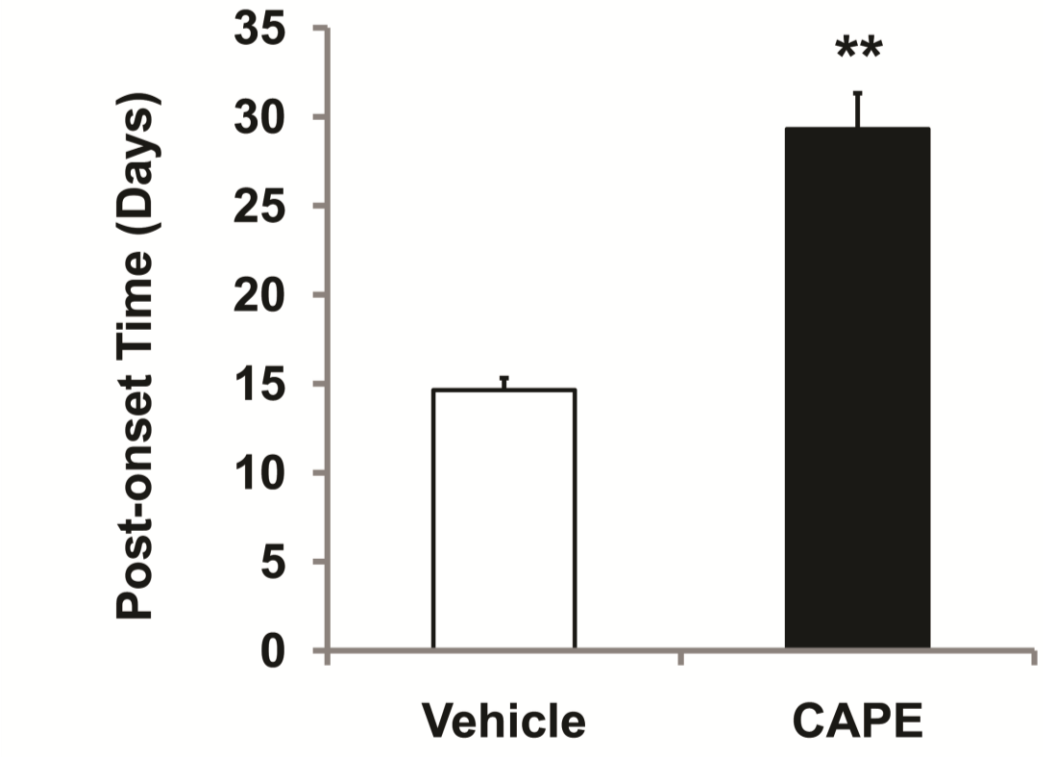

Figure 2.4A. CAPE (10 mg/kg) treatment lengthened disease duration of SOD1^{G93A} mice with disease onset.

Male and female SOD1^{G93A} mice with disease onset were given CAPE (10 mg/kg) or vehicle until a humane endpoint near death. The length of time between onset and the death endpoint was examined, reported as post-onset time, and measured in days of post-onset time. Mice treated with CAPE (n = 13) had longer post-onset survival time compared to vehicle-treated mice (n = 11). The calculated averages (± SEM) of survival post-onset of CAPE-treated mice were significantly greater than the vehicle group. Statistical analysis was performed using one-way ANOVA. **, $p < 0.01$.

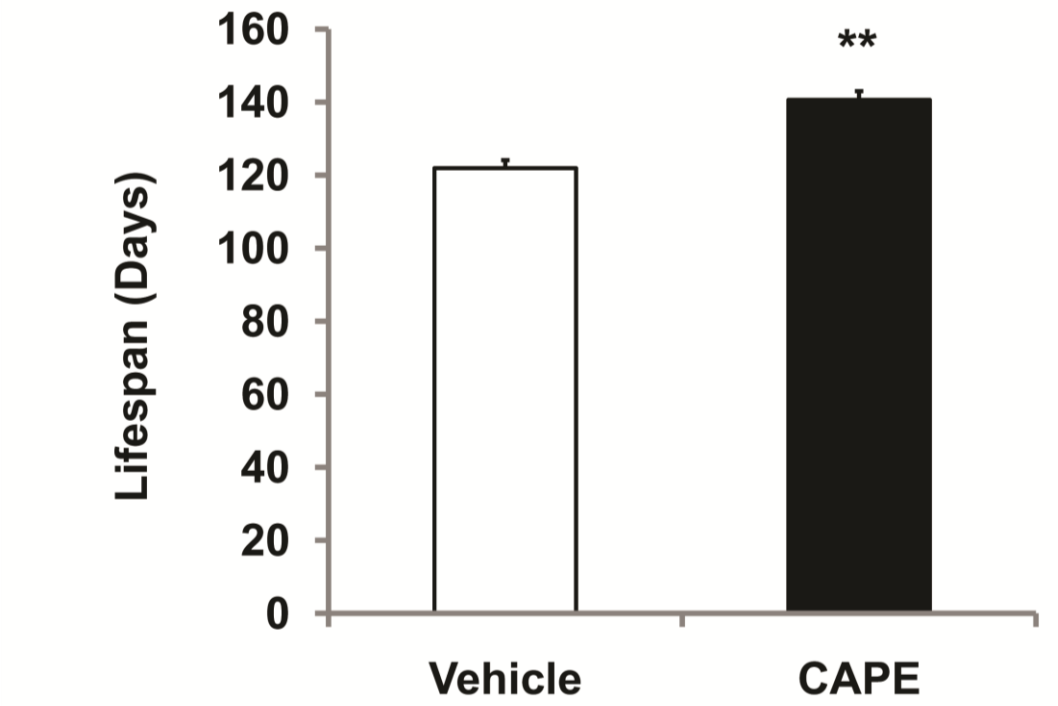

Figure 2.4B. CAPE (10 mg/kg) treatment of symptomatic SOD1^{G93A} mice resulted in elongated lifespans.

Symptomatic male and female SOD1^{G93A} mice were treated with CAPE (10 mg/kg, n = 13) or vehicle (n = 11) until a humane endpoint near death. The length of time between birth and the death endpoint was examined, reported as lifespan, and measured in days of lifespan. The effect of CAPE treatment at onset was sufficiently robust to produce a significantly greater total lifespan extension. Statistical analysis was performed using one-way ANOVA. **, $p < 0.01$.

2.5.3. A greater number of motor neurons in the lumbar spinal cord survived with CAPE treatment

It was determined whether the protective effect of CAPE correlated with prevention of motor neuron loss. Changes in motor neuron density at 7 days post-onset were evaluated in cross-sections of lumbar spinal cords of the $SOD1^{G93A}$ study mice (Fig 2.5A). Vehicle-treated mice exhibited a significant ($p < 0.01$) loss of motor neurons in the ventral horn of the spinal cord lumbar region as compared to age-matched, wild type littermates (group means: 8.48 ± 0.51 and 20.2 ± 0.48, respectively; Fig 2.5B). Motor neuron loss was prevented at this time point by CAPE treatment (18.1 ± 1.4, $p < 0.01$ vs. vehicle) and was not significantly lower than age-matched, wild type mice (Fig 2.5B). Additionally, MAP2-immunoreactive neuronal processes were observed and clearly defined throughout spinal cord sections obtained from wild type and CAPE-treated mice. In contrast, there was very little to no presence of MAP2-positive axons and dendrites in vehicle-treated $SOD1^{G93A}$ mice spinal cord (Fig 2.5A).

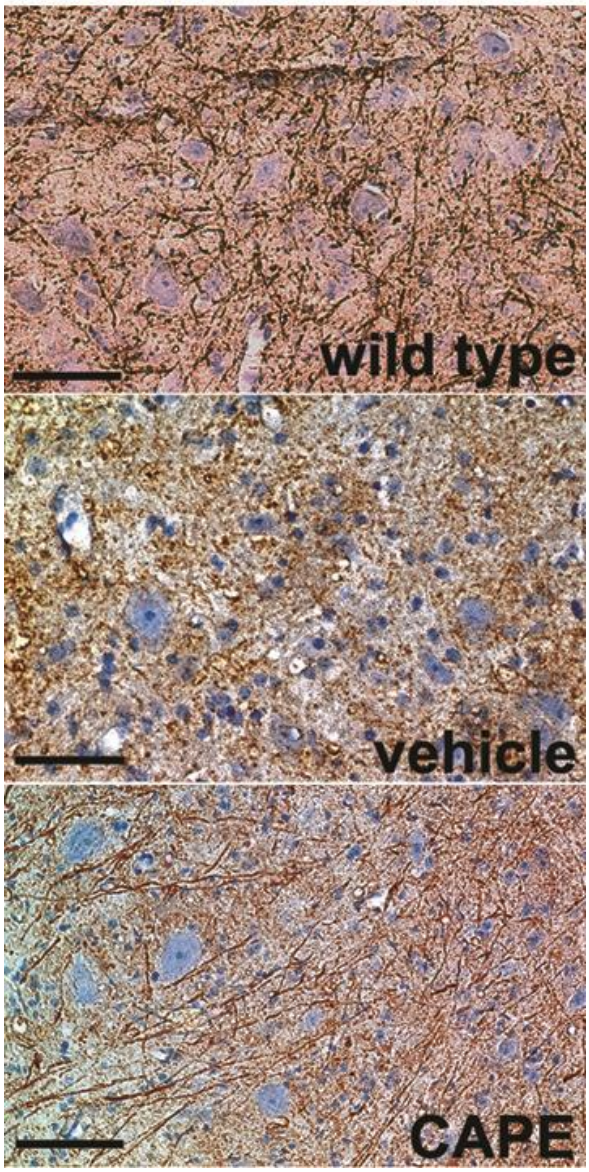

Figure 2.5A. More motor neurons were present in lumbar spinal cords of SOD1^{G93A} mice treated with CAPE upon disease onset.

Symptomatic SOD1^{G93A} mice were treated with or without CAPE (10 mg/kg) for 7 days. Motor neurons in the lumbar spinal cord region were visualized by immunohistochemical staining with antibodies to MAP2 and counterstained with hematoxylin to visualize total nuclei as described in the Experimental Procedures section. Representative immunohistochemical images of lumbar spinal cord sections demonstrated an increase in the presence of MAP2-positive neurons in mice treated with CAPE compared to vehicle. Scale bars: 100 μm.

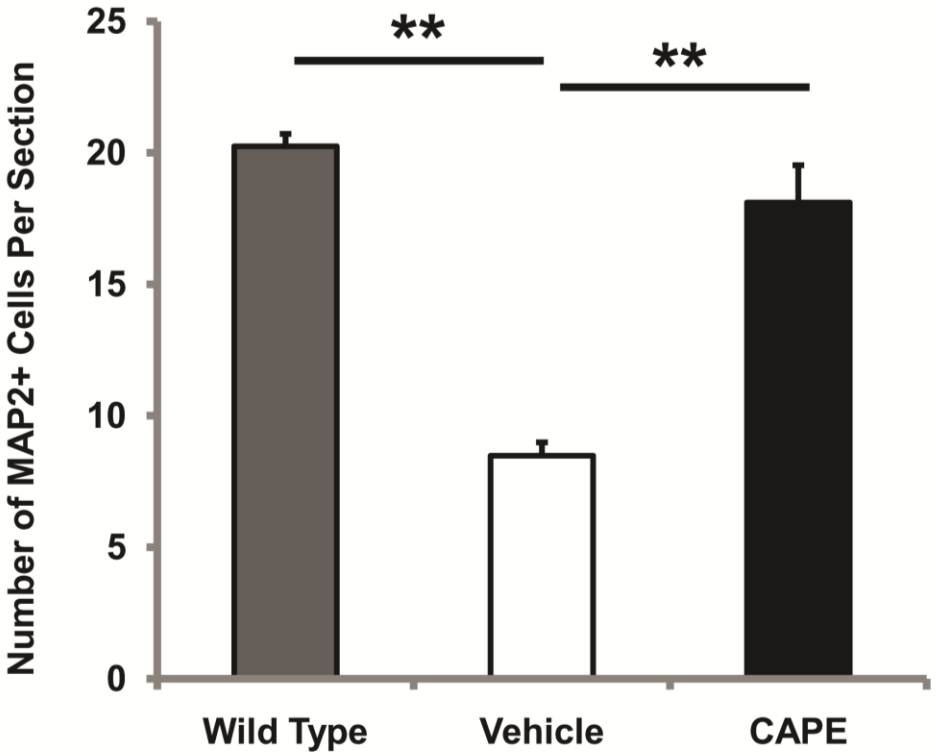

Figure 2.5B. Higher numbers of motor neurons were observed in lumbar spinal cords of SOD1^{G93A} mice treated with CAPE.

SOD1^{G93A} mice with disease onset were treated with or without CAPE (10 mg/kg) for 7 days. Digitized images covering the entire cross-sectional area from 6 – 8 lumbar spinal regions from each mouse in the study were quantitated for staining. CAPE treatment resulted in a greater number of motor neurons in lumbar spinal cord from symptomatic SOD1^{G93A} mice as compared to vehicle. Data for experimental groups are presented as averages (± SEM) of 3 independent tests consisting of 3 animals per group for each test. Data for wild type controls were generated from 4 mice. Statistical analyses were performed using one-way ANOVA. **, $p < 0.01$.

2.5.4. Administration of CAPE had no effect on endogenous mouse SOD1$^{wild\ type}$ and mutant human SOD1^{G93A} expression in spinal cords of SOD1^{G93A} mice

Because the transgene copy number (the copies of the transgene with the G → A at position 93, human mutant form of SOD1) has been shown to affect survival of the SOD1^{G93A} mouse (Alexander *et al.*, 2004b), immunoblot analyses of SOD1 expression were performed on spinal cord homogenates after 7 days of CAPE treatment (Fig 2.6A). Quantitative measurement of band densities revealed that levels of both wild type endogenous mouse SOD1 (mSOD1^{WT}) and mutated human SOD1 (hSOD1^{G93A}) expression showed no differences with or without 7-day CAPE treatment (Fig 2.6B). It is important to note that "wild type/WT" mice express wild type endogenous mouse SOD1 (mSOD1^{WT}) but do not carry the mutated human SOD1 (hSOD1^{G93A}) transgene; "vehicle" and "CAPE" mice are the experimentally-treated SOD1^{G93A} transgenic mice that express wild type endogenous mouse SOD1 (mSOD1^{WT}) as well as the mutated human SOD1 (hSOD1^{G93A}) transgene. There were no differences in expression of actin, which served as an internal loading control for endogenous mouse SOD1 (mSOD1^{WT}). Additionally, no differences were observed in endogenous mouse SOD1 (mSOD1^{WT}) levels, which served as an internal control for mutated human SOD1 (hSOD1^{G93A}) expression.

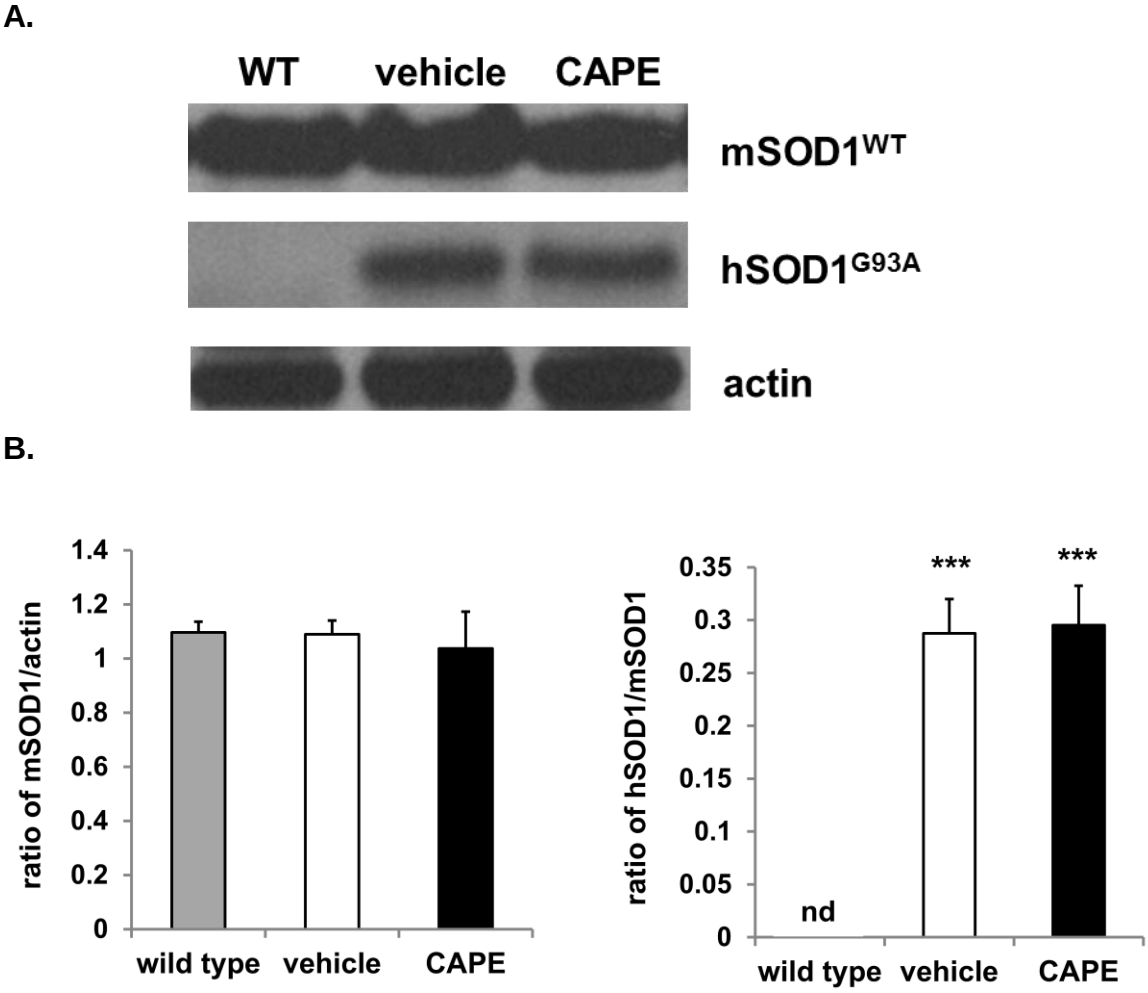

Figure 2.6. CAPE treatment did not affect endogenous mouse wild type SOD1 and mutated human SOD1 transgene expression in spinal cord.

Wild type control ("WT") and SOD1^{G93A} mice ("vehicle" and "CAPE") spinal cords were prepared as detailed in Experimental Procedures. Levels of actin were unchanged and used as an internal loading control for endogenous mouse wild type SOD1 ("mSOD1^{WT}"). There was no difference in mSOD1^{WT} levels, which was the loading control for mutated human SOD1 ("hSOD1^{G93A}"). After 7 days of CAPE treatment, there was no change in expression of either endogenous mouse wild type SOD1 or human SOD1 carrying the G93A mutation in symptomatic SOD1^{G93A} mice. n = 3 per group, ***$p < 0.005$.

2.5.5. Daily CAPE treatment decreased phosphorylation of p38 MAP kinase in spinal cords of SOD1^{G93A} mice

Since motor neuron loss occurs, at least in part, through the action of neighboring activated inflammatory cells (Boillee *et al*., 2006a) and CAPE has demonstrated anti-inflammatory and anti-cell death properties (Wei *et al*., 2004), the effect of CAPE administration on a molecular pathway associated with inflammation and cell death was examined. The levels of activated phosphorylated p38 protein in spinal cords were evaluated at 3 days (Fig 2.7A) and 7 days (Fig 2.7B) following disease onset and with or without CAPE administration during that time period. As demonstrated in other reports with this ALS mouse model (Hu *et al*., 2003; Dewil *et al*., 2007), the phosphorylation status of p38 was elevated in SOD1^{G93A} after disease-like symptoms manifested at both 3 days (0.37 ± 0.11, $p < 0.05$ vs. wild type; Fig 2.7Ab) and 7 days post-onset (0.572 ± 0.11, $p < 0.01$ vs. wild type; Fig 2.7Bb). Conversely, levels of phospho-p38 protein in the spinal cords were significantly reduced with CAPE treatment for 3 days (0.20 ± 0.058, $p < 0.05$ vs. vehicle; Fig 2.7Ab) and for 7 days (0.248 ± 0.057, $p < 0.05$ vs. vehicle; Fig 2.7Bb) as compared to the vehicle groups. However, these phospho-p38 levels observed in CAPE-treated animals were still higher than age-matched, wild type controls at 7 days (0.0457 $\pm$ 0.000010, $p < 0.05$ vs. CAPE group; Fig 2.7Bb).

a.

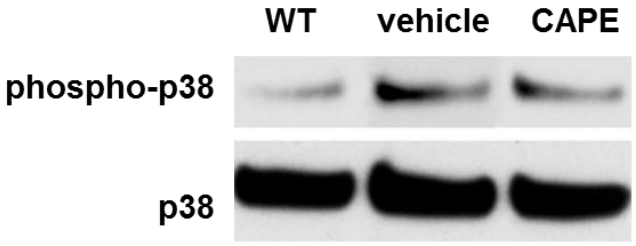

b.

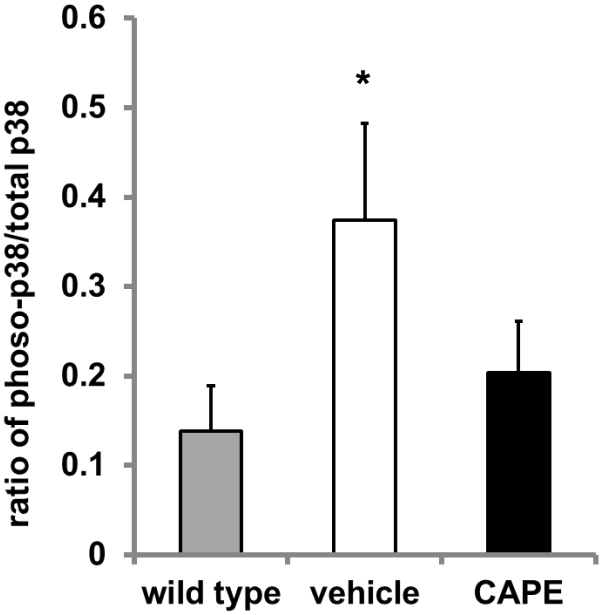

Figure 2.7A. Reduced phosphorylation of p38 in spinal cords of SOD1^{G93A} mice with disease onset was observed after 3 days of CAPE treatment.

SOD1^{G93A} mice with onset received 10 mg/kg CAPE or vehicle for 3 days and spinal cords were prepared for immunoblot analysis as detailed in Experimental Procedures. (a) Representative Western blots and (b) quantitation of band density showed reduced p38 phosphorylation in spinal cords of symptomatic SOD1^{G93A} mice given 3-day CAPE treatment versus vehicle. Total p38 expression remained unchanged and served as an internal loading control. Values are the mean density ± SEM. One-way ANOVA was used for statistical analysis. *, $p < 0.05$; n = 2, WT; n = 3, vehicle; n = 3 , CAPE.

a.

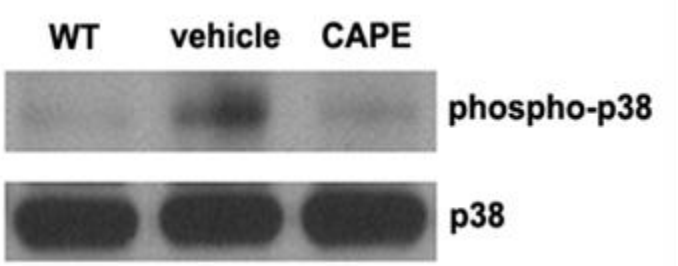

b.

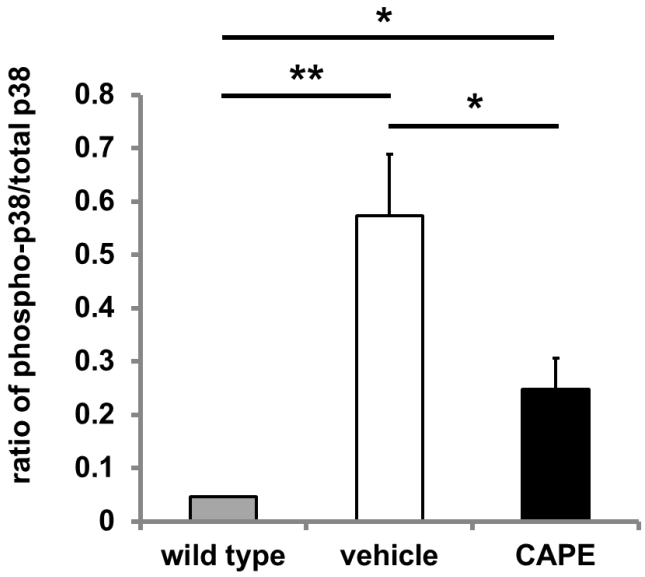

Figure 2.7B. Decreased levels of phospho-p38 in spinal cords of symptomatic SOD1^{G93A} mice were observed after 7 days of CAPE treatment.

Symptomatic SOD1^{G93A} mice were given CAPE (10 mg/kg) or vehicle for 7 days and spinal cords were harvested for Western blotting as described in Experimental Procedures. (a) Representative immunoblots and (b) densitometric quantitation demonstrated reduced phosphorylated p38 expression with CAPE treatment as compared to vehicle-treated animals. Unchanged total p38 levels served as an internal loading control. Values represent the mean density ± SEM. Statistical analysis was performed using one-way ANOVA. *, $p < 0.05$; **, $p < 0.01$; n = 3 , WT; n = 3, vehicle; n = 4 , CAPE.

2.5.6. A reduction in astroglial activation was observed in the spinal cords of symptomatic SOD1^{G93A} mice treated with CAPE

The neuroprotective effect of CAPE was confirmed at the cellular level by determining the astroglia activation state in the spinal cord. Astroglial cell induction within the lumbar spinal cords of SOD1^{G93A} mice was assessed by immunohistochemical analyses (Fig 2.8A). Immunostaining for GFAP expression in the lumbar spinal cord paraffin-embedded sections demonstrated decreased levels of GFAP immunoreactivity with CAPE treatment compared to vehicle-treated controls (Fig 2.8A). For comparison, wild type controls were also analyzed for astroglial activation and showed very little to no GFAP immunoreactivity (representative slide not shown). The density per cross-sectional area of GFAP-positive astrocytes was elevated by over 50-fold in the vehicle-treated group (125.6 ± 9.1, $p < 0.01$ vs. wild type; Fig 2.8B) as compared to wild type control mice (2.25 ± 0.85, Fig 2.8B). In contrast, CAPE-treated SOD1^{G93A} mice exhibited a markedly lower number of GFAP-positive astrocytes (20.3 ± 3.1, $p < 0.01$) compared to the vehicle group (Fig 2.8B). However, the number of GFAP-positive astrocytes in CAPE-treated mice was still significantly higher ($p < 0.01$) compared to wild type controls (Fig 2.8B).

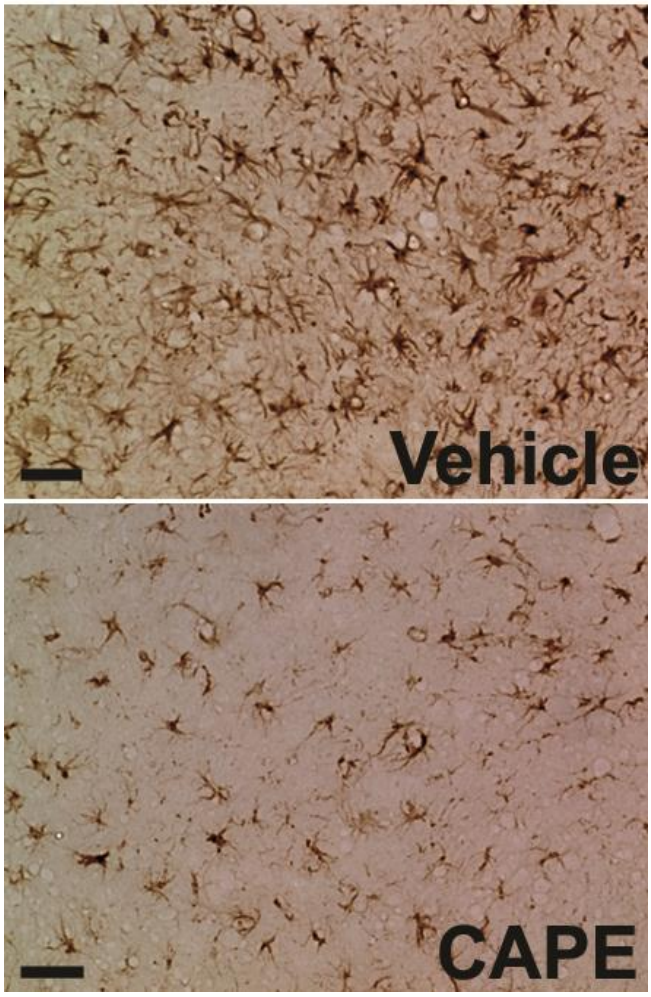

Figure 2.8A. CAPE reduced the presence of activated astrocytes in lumbar spinal cords of symptomatic SOD1^{G93A} mice.

Mice were treated for 7 days with CAPE or vehicle and lumbar spinal cords were removed for analysis and processed as previously described in Experimental Procedures. For comparison, wild type control mice were also analyzed. Representative immunohistochemical images of lumbar spinal cord sections demonstrated a decrease in the presence of GFAP-positive astrocytes in mice treated with CAPE compared to vehicle. Wild type controls showed very little to no GFAP-positive staining (representative section not shown). Scale bars: 50 µm.

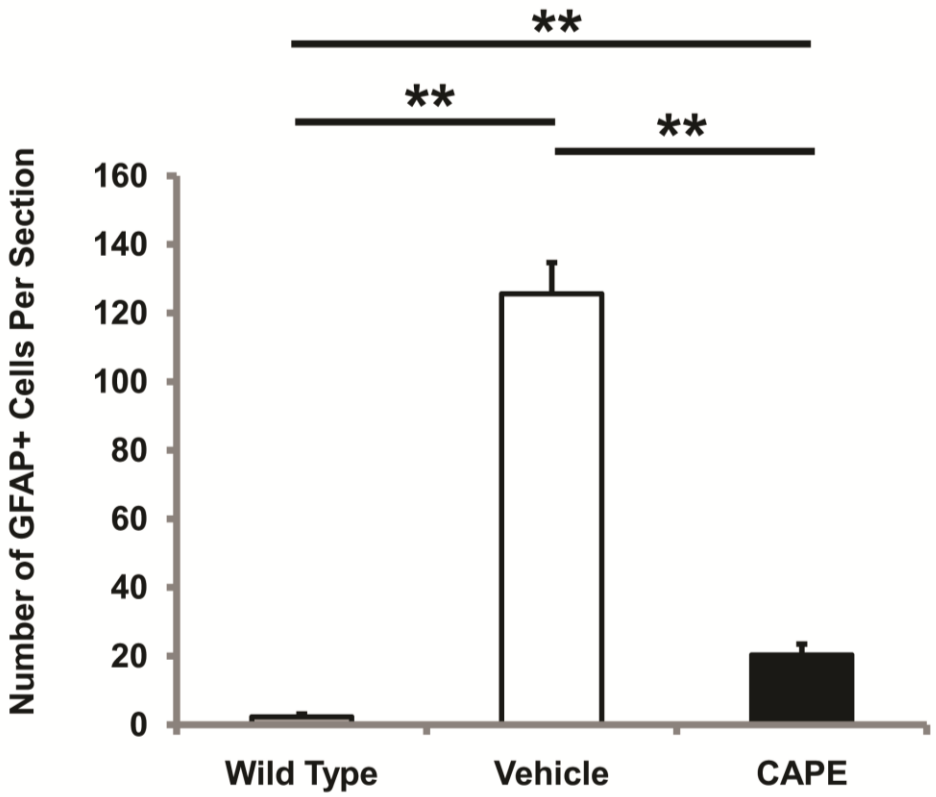

Figure 2.8B. CAPE reduced the number of activated astrocytes in lumbar spinal cords of symptomatic SOD1^{G93A} mouse.

For 7 days, mice were given CAPE or vehicle. Lumbar spinal cord removal and processing were performed as previously described in Experimental Procedures. Wild type control mice were also analyzed. Digitized images of stained sections were quantitated and demonstrated lower numbers of GFAP-positive cells in the spinal cord with CAPE treatment as compared to vehicle. Values represent the mean ± SEM. Statistical analysis was performed using one-way ANOVA. **, $p < 0.01$; n = 4, WT; n = 8, vehicle, n = 9, CAPE.

2.5.7. Administration of CAPE to SOD1^{G93A} mice with disease onset decreased CD11b expression in spinal cords

For further examination of glial activation in spinal cords after CAPE treatment, expression of a marker of activated microglia, CD11b, which is induced by inflammation (Boillee *et al.*, 2006), was detected via Western blotting at 3 days (Fig 2.9A) and 7 days (Fig 2.9B) after SOD1^{G93A} mice were given 10 mg/kg CAPE. At 3 days post-CAPE treatment of symptomatic mice, representative immunoblots (Fig 2.9Aa) and subsequent band density measurements (Fig 2.9Ab) revealed no differences in CD11b expression in all groups (group averages ± SEM: 0.266 ± 0.065 for wild type, n = 4 ; 0.276 ± 0.046 for vehicle, n = 3; 0.298 ± 0.0074 for CAPE, n = 3). However, after 7 days of post-onset CAPE treatment, representative immunoblot (Fig 2.9Ba) and band density measurements (Fig 2.9Bb) showed there was a significant increase in CD11b expression in the spinal cord of vehicle mice (0.669 ± 0.057 for vehicle, n = 3, *** $p < 0.005$ versus wild type and CAPE) when compared to CAPE-treated animals (0.248 ± 0.036, n = 3), whose CD11b expression was found to be at a similar level to wild type mice (0.288 ± 0.024 , n = 3) after 7 days.

a.

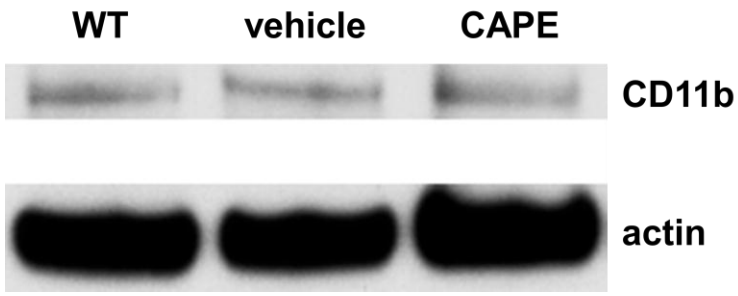

b.

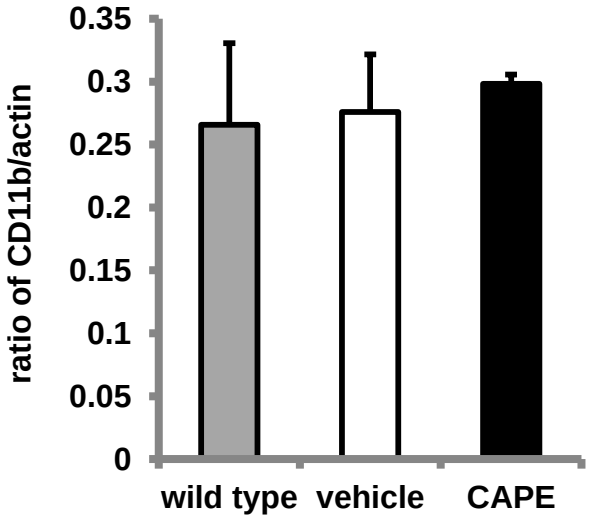

Figure 2.9A. No difference in CD11b-immunoreactivity was observed at 3 days post-onset with CAPE treatment.

Lumbar spinal cords were removed and processed at 3 days post-onset for Western blot as described in Experimental Procedures. Unchanged actin in all groups served as an internal loading control. (a) The representative immunoblots and (b) band densities that were measured showed no change in spinal cord CD11b expression after 3 days of disease onset diagnosis with or without 10 mg/kg CAPE treatment. WT (wild type), n = 4; vehicle, n = 3; CAPE, n = 3.

a.

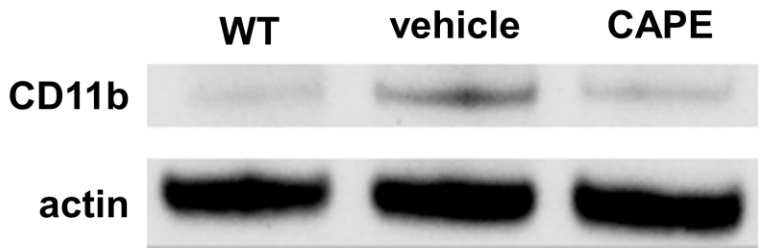

b.

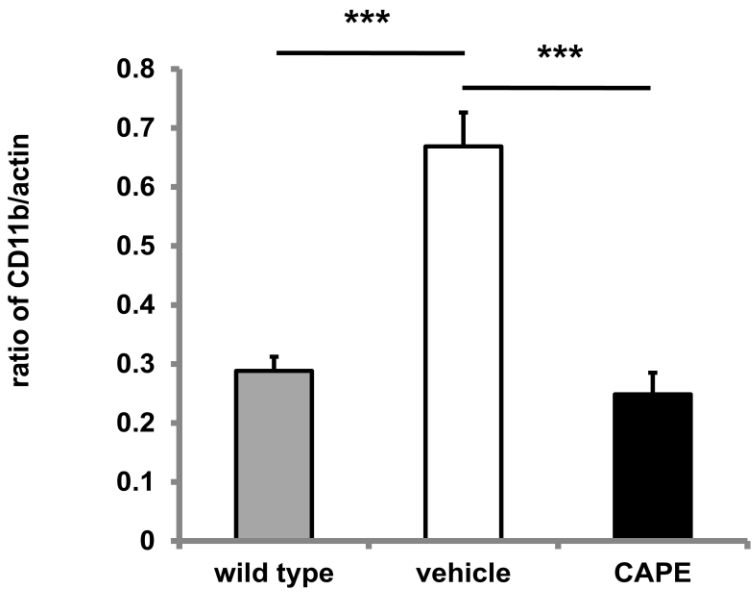

Figure 2.9B. 7-day treatment with CAPE reduced expression of CD11b in spinal cords of symptomatic SOD1^{G93A} mice.

Spinal cords were removed for CD11b immunoblot as described in Experimental Procedures. Actin expression was unchanged in all groups and served as an internal loading control. (a) Representative immunoblots and (b) band quantitation demonstrated a decrease in spinal cord CD11b expression after 7-day CAPE treatment as compared to vehicle. WT (wild type), n = 3; vehicle, n = 3; CAPE, n = 3. *** $p < 0.005$.

2.5.8. SOD1^{G93A} mice with disease onset and treated with CAPE demonstrated reduced microglial activation in lumbar spinal cords

CAPE's neuroprotection was further observed at the cellular level by examining the presence of activation of microglia in the spinal cord. Because CD11b is not specific to microglia, immunohistochemical analysis with a microglia-specific marker, Iba-1 (Ito *et al.*, 2001) was used. Microglial activation closely paralleled astrocyte GFAP-immunoreactivity (See previous Fig 2.8A and 2.8B) in lumbar spinal cords with or without CAPE treatment for 7 days (Fig 2.10A).

The number of activated microglia in lumbar spinal cords of SOD1^{G93A} mice was markedly decreased by CAPE treatment (44.8 ± 1.8, $p < 0.01$ vs. vehicle) in comparison to animals without CAPE (84.5 ± 4.3) as confirmed by immunostaining with Iba-1 (Fig 2.10B). For comparison, age-matched, wild type littermates given CAPE for 7 days exhibited no activated microglia with Iba-1 immunoreactivity in the spinal cord lumbar area (representative slide not shown). As observed with the number of GFAP-positive cells in lumbar spinal cord, the number of Iba-1-positive cells in CAPE-treated mice was still significantly higher compared to wild type controls (0.00 ± 0.0; Fig 2.10B).

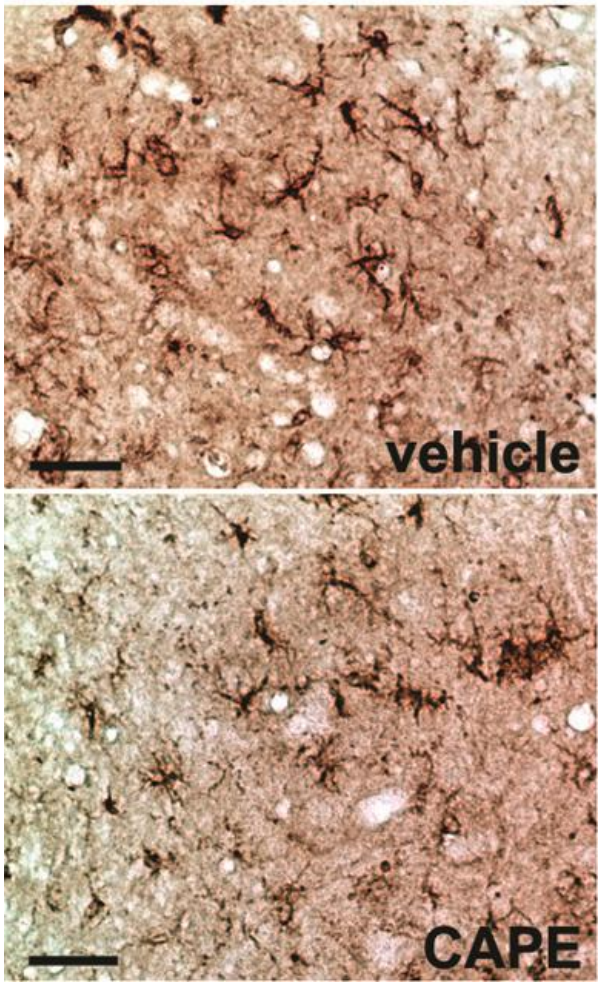

Figure 2.10A. CAPE reduced the presence of activated microglia in lumbar spinal cords of symptomatic SOD1^{G93A} mice.

Lumbar spinal cords of mice were analyzed for activated microglia by immunohistochemical staining with antibodies to Iba-1 at post-onset day 7 of the study. Representative sections of spinal cord revealed diminished immunostaining of activated microglia in the lumbar area in mice given CAPE versus their vehicle counterparts. Wild type controls did not show any Iba-1-positive staining (representative section not shown). Scale bars: 50 µm.

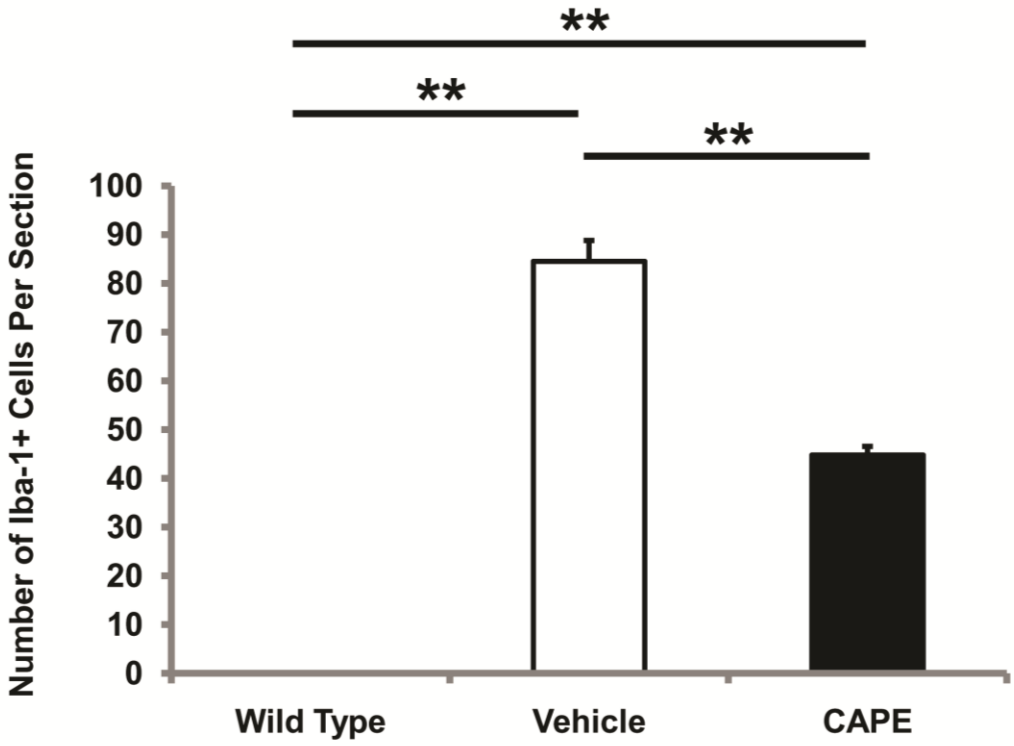

Figure 2.10B. CAPE reduced the number of activated microglia in lumbar spinal cords of symptomatic SOD1^{G93A} mice.

Lumbar spinal cords of mice were analyzed for activated microglia by immunohistochemical staining with antibodies to Iba-1 at post-onset day 7 of the study. Digitized images covering the entire cross-sectional area from 5 – 6 lumbar spinal regions from each mouse in the study were quantitated for staining, which revealed diminished numbers of Iba-1-positive cells in the spinal cords of CAPE-treated animals versus vehicle. Values represent the mean ± SEM. Statistical analysis was performed using one-way ANOVA. **, $p < 0.01$; n = 4, WT; n = 6, vehicle, n = 8 CAPE.

2.5.9. CAPE treatment of symptomatic SOD1^{G93A} mice resulted in decreased expression of cleaved α-II spectrin in spinal cords

Because the activity of the Ca^{2+}-activated protease, calpain, was found to be increased in the spinal cord of SOD1^{G93A} mice (Stifanese *et al.*, 2010), the effect of CAPE treatment on the calpain system in SOD1^{G93A} mice was explored by measuring expression of a known cleavage target of calpain, α-II spectrin (Strong, 1999). After 3 days post-onset, expression of cleaved α-II spectrin was significantly decreased in symptomatic mice receiving CAPE treatment (0.31 ± 0.006, n = 3; *** $p < 0.005$) and wild type controls (0.38 ± 0.03, *** $p < 0.005$) as compared to mice without CAPE (0.61 ± 0.06, n = 3) as demonstrated in a representative immunoblot (Fig 2.11a) and quantified band density measurements (Fig 2.11b). Actin levels were unchanged in all groups.

a.

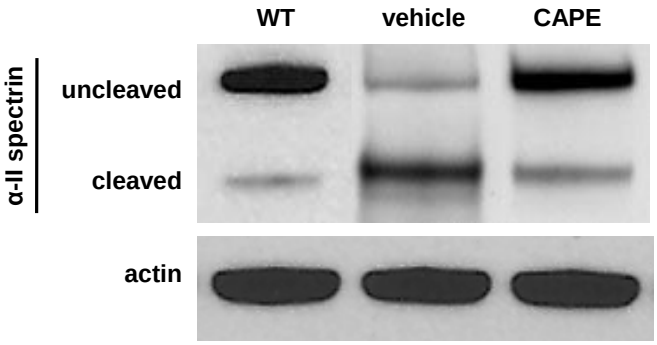

b.

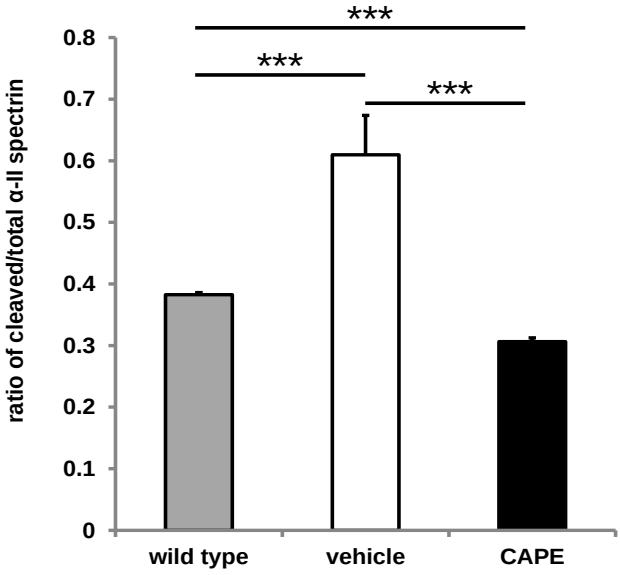

Figure 2.11. CAPE treatment for 3 days decreased α-II spectrin cleavage in symptomatic SOD1^{G93A} mice.

SOD1^{G93A} mice were given 10 mg/kg CAPE or vehicle for 3 days and spinal cords were removed for Western blot as described in Experimental Procedures. Actin expression was unchanged in all groups and used as an internal loading control. (a) Representative immunoblots and (b) quantitation of bands revealed a decrease in cleaved α-II spectrin expression at 3 days post-onset when CAPE treatment was given. Wild type, n = 5; vehicle, n = 3; CAPE, n = 3. *** $p < 0.005$. Data are group averages ± SEM.

2.5.10. CAPE treatment decreased expression of cleaved caspase-12 in spinal cords of SOD1^{G93A} mice with disease onset

Endoplasmic reticulum (ER) stress is posited to be implicated in the motor neuron death observed in SOD1^{G93A} mouse spinal cord (Wootz *et al.*, 2004, 2006). In order to examine the effect of CAPE treatment on a component of the ER stress cascade, caspase-12 (Wootz *et al.*, 2004), spinal cords that were removed from symptomatic SOD1^{G93A} mice were analyzed via Western blot. After 3 days following disease onset, there was a significant decrease in cleaved caspase-12 expression in SOD1^{G93A} mice given CAPE treatment for 3 days (0.62 ± 0.004, n = 3, *** $p < 0.005$) and wild type controls (0.42 ± 0.005, *** $p < 0.005$) versus their vehicle-treated counterparts (0.80 ± 0.02, n = 3) as shown in representative blots (Fig 2.12a) and quantitative analyses of band densities (Fig 2.12b). Levels of actin were unchanged regardless of CAPE and genotype.

a.

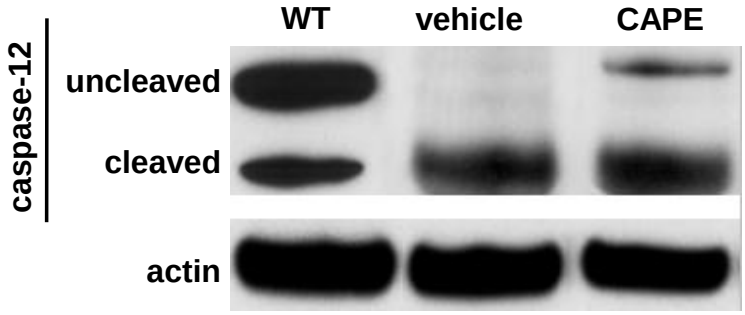

b.

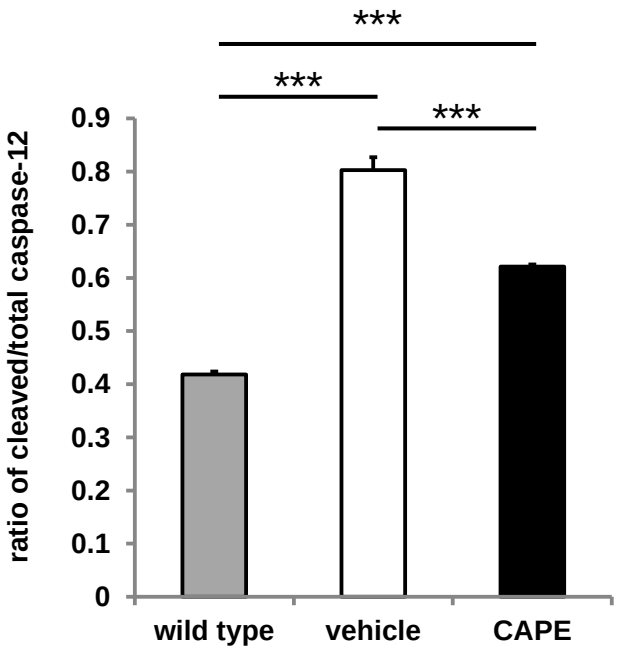

Figure 2.12. CAPE treatment had no effect on cleaved caspase-12 expression in SOD1^{G93A} mice at 3 days post-onset.

SOD1^{G93A} mice were given 10 mg/kg CAPE or vehicle for 3 days and spinal cords were removed for Western blot as described in Experimental Procedures. Unchanged actin expression in all groups served as an internal loading control. (a) Representative immunoblots and (b) quantification of band densities showed no difference in caspase-12 cleavage with or without CAPE treatment for 3 days. Wild type, n = 5; vehicle, n = 3; CAPE, n = 3. *** $p < 0.005$. Data are group averages ± SEM.

2.6. Discussion

This preclinical study sought to validate a candidate small molecule for ALS therapy by employing experimental systems approximating a clinical treatment scenario. Most importantly for clinical translation, the effectiveness of CAPE was examined when administered after disease symptoms developed in the well-established $SOD1^{G93A}$ mouse model of ALS (Gurney *et al*., 1994). The results from this study demonstrate that post-onset, daily oral administration of CAPE at a dose of 10 mg/kg was effective in delaying disease progression and prolonging survival. These findings are consistent with previous studies from this laboratory demonstrating potent neuroprotective activity of CAPE both *in vivo* and *in vitro* in various neurodegenerative disease models (Wei *et al*., 2004; Ma *et al*., 2006; Wei *et al*., 2008). Taken together, the present findings and previous *in vitro* and *in vivo* studies from this laboratory suggest that CAPE has high potential as a therapeutic compound for neurodegenerative diseases.

In the vast majority of sporadic ALS cases the etiology is unknown; although, pathological data from human patients as well as mouse models suggest that disease sequelae are promoted by accumulation of tissue derived toxins that disrupt homeostatic functions. Implicated toxins and pathologic processes are glutamate excitotoxicity, reactive oxygen species, mitochondrial injury, inflammation propagated by neighboring cells (for example, glia), dysfunctional axonal transport, endoplasmic reticulum stress, vascular dysfunction, proteosome inhibition, synaptic defects, loss of barrier function between peripheral and central nervous tissues, and toxic peptide conformations

(Ilieva *et al*., 2009). It is not currently known which of these processes are primary to disease onset and progression and which are secondary events due to disease state; thus, hindering development of disease-targeted therapies. This lack of a clear understanding of ALS pathophysiology may partially explain the many failures in the clinic of therapeutic modalities that demonstrated clear potential in preclinical testing (Gurney *et al*., 1998).

Although the uncertainties regarding the molecular basis of ALS hinder development of disease modifying therapies, it is formally possible that agents, such as CAPE, which block major neurodegenerative pathways resulting from the initial insult(s), will be efficacious in preventing disease progression. In fact, the extension of post-onset lifespan correlated with a significantly greater number of surviving motor neurons in the lumbar spinal cord after 7 days of CAPE treatment. Also observed was a decreased number of activated microglia and astrocytes in the lumbar region of the spinal cord, suggesting that CAPE may exert some of its protective effects through repressing inflammatory and cell death processes. This was corroborated by reduced levels of activated p38 MAPK, which is part of an important signal transduction pathway that contributes to neuronal death and inflammation (Cuenda *et al*., 2007) in spinal cords of CAPE-treated $SOD1^{G93A}$ mice (Dewil *et al*., 2007).

Current evidence suggests that p38 mitogen activated protein kinase (MAPK) may be involved in motor neuron cell death in the$SOD1^{G93A}$ mouse (Bendotti *et al.*, 2004; Wengenack *et al.*, 2004; Dewil *et al.*, 2007). Activated (phosphorylated) p38 MAPK was upregulated in spinal cords of $SOD1^{G93A}$ mice

(Tortarolo *et al.*, 2003; Bendotti *et al*., 2004; Wengenack *et al.*, 2004) and human ALS patients (Hu *et al.*, 2003). Furthermore, chemical inhibition of the p38 MAPK pathway increased motor neuron survival and reduced microglial activation in $SOD1^{G93A}$ mouse spinal cord (Dewil *et al.*, 2007), suggesting the dual pathogenic role of the p38 MAPK pathway in ALS motor neuron cell death and neuroinflammation. In our previous studies, CAPE protected against glutamate excitoxicity and reduced p38 phosphorylation (Wei *et al.*, 2008). Previous studies from this laboratory reported that CAPE was able to attenuate the increase in phospho-p38 levels observed in glutamate-induced cerebellar granule neuronal death (Wei *et al.*, 2008), demonstrating reduction of phospho-p38 played a key role in CAPE-induced neuroprotection against glutamate neurotoxicity (excitotoxicity). Additionally, glutamate-induced transient activation of p38 MAPK in microglia has been also strongly linked to glutamate neurotoxicity in mixed neuronal cultures, indicating the involvement of phosphor-p38 in neuronal death-related inflammation (Tikka *et al.*, 2001). Since it has been confirmed that excitotoxicity plays an important role in ALS pathogenesis, CAPE-induced decreases in phospho-p38 levels in symptomatic $SOD1^{G93A}$ mice may play an important role in attenuation of the neuroinflammatory events and motor neuron death observed in ALS and disease progression.

The onset of motor neuron excitotoxic death and oxidative stress has been proposed to induce neuroinflammatory responses, such as elevations in pro-inflammatory cytokines in the CNS (Almer *et al*., 2001; Wu *et al*., 2006) and astrocyte (Yamanaka *et al*., 2008) and microglia activation (Boillee *et al*., 2006b),

which are thought to play key roles in ALS progression and motor neuron death and are pathogenic hallmarks of this disease (Rowland and Shneider, 2001).

The anti-inflammatory and anti-cell death effects of CAPE observed in this study and posited to occur via downregulation of phospho-p38 in the SOD1^{G93A} mouse model were predicted based on similar properties in other neurodegenerative models (Wei *et al*., 2004; Noelker *et al*., 2005; Ma *et al*., 2006), which share many common molecular and cellular pathogenic events with ALS such as free radical production (Bossy-Wetzel *et al*., 2004). Thus, the motor neuron protection, anti-inflammation, and attenuated glial activation observed in CAPE-treated SOD1^{G93A} mice may also involve a reduction in free radical generation and other anti-oxidative damage mechanisms.

Calpain activity has been observed to be increased in the SOD1^{G93A} mouse (Wootz *et al.*, 2006; Stifanese *et al.*, 2010) due to increased levels of calcium in the cytosol caused by excitotoxicity (Roy *et al.*, 1998; Tradewell and Durham, 2010). Activated calpains target and cleave cytoskeletal proteins, such as α-II spectrin; calpain cleavage activity results in the accumulation of α-II spectrin and formation of inclusions located in motor neurons (Stifanese *et al.*, 2010). Inhibition of calpain via expression of its endogenous inhibitor, calpastatin, slowed degeneration of SOD1^{G93A} motor neurons (Tradewell and Durham, 2010). CAPE treatment of symptomatic SOD1^{G93A} mice resulted in the decreased expression of a cleaved calpain target, α-II spectrin, in the spinal cord, suggesting that CAPE's neuroprotection involves inhibition of calpain activation. Additionally, α-II spectrin was also shown to be a substrate for caspase-3

cleavage (Siman *et al.*, 1989; Wang *et al.*, 1998; Roberts-Lewis and Siman, 1993). Thus, CAPE's blockage of α-II spectrin cleavage may be via inhibition of both calpain and caspase-3 activity.

Endoplasmic reticular (ER) stress is also thought to play a role in the motor neuron degeneration observed in ALS. Found in association with ER stress were elevated levels of cleaved and activated caspase-12 (Nagata *et al.*, 2007). In ALS, ER stress is thought to be caused by excitotoxicity-induced oxidative damage (Ilieva *et al.*, 2007). CAPE treatment of $SOD1^{G93A}$ mice with disease onset resulted in decreased levels of cleaved caspase-12 in the spinal cord. Because caspase-12 activation and cleavage is an event downstream from excitotoxicity, oxidative damage, and ER stress, it may be possible that CAPE is able to exert its neuroprotection via anti-excitotoxic, anti-oxidative, or anti-ER stress mechanisms.

The neurologic benefit of CAPE treatment may be a result of the compound's ability to simultaneously modulate multiple pathways, such anti-inflammation and anti-neuron cell death, thereby, providing a more effective blockade of disease progression. Previous potential candidates ALS treatments, such as Coenzyme Q_{10} (an anti-oxidant), topiramate (an anti-epileptic drug that blocks glutamate excitoxicity) and celecoxib (a non-steroidal anti-inflammatory drug), target individual pathways and had no beneficial effect in ALS patients despite promising results when used with animal models (Cudkowicz *et al*., 2003, 2006; Kaufmann*et al*., 2009). It is plausible that the ineffectiveness of these compounds in the more complex human disease relates to their capacity to

mainly modulate a single pathogenic mechanism. However, it should be noted that although CAPE acts very fast after it is administrated immediately after onset, its neuroprotective efficacy is not as strong as we expected. Our observations found that after seven to fourteen-day's significant improvement in mouse behavior, mice deteriorate very quickly. Our hypothesis is that after 7 – 14 days of treatment, CAPE may lose its ability to block several pathways known to contribute to neuronal death, resulting in neurons dying by alternative death pathways. This phenomenon is very common in *in vitro* neuroprotective studies. Currently, there is no treatment able to completely abolish cell death. Additionally, although CAPE has multiple capabilities, including anti-inflammatory, anti-oxidant, and anti-cell death functions, CAPE may be unable to exert effects on currently unknown neurodegenerative events contributing to disease progression as the definitive spectrum of neuronal death pathways has yet to be elucidated in ALS and the G93A mouse model, allowing for motor neuron cell death to continue via alternative, short-cut pathways to those blocked by CAPE.

CHAPTER 3: EXPLORATORY STUDY - Adipose-derived Stem Cell Conditioned Media Extends Survival of a Mouse Model of Amyotrophic Lateral Sclerosis

3.1. Rationale

Caffeic acid phenethyl ester (CAPE) treatment was previously found by this laboratory to be neuroprotective in a neonatal rat model of hypoxia-ischemia (Wei *et al,.* 2004). CAPE's protective abilities were related to its anti-inflammatory, anti-oxidant, and anti-cell death properties. The previous chapters centered upon the use of one compound (CAPE) with two etiologically and neuropathologically different animal models of neurodegeneration, the MPTP and $SOD1^{G93A}$ mice. These data provide evidence that if two diseases share multiple downstream pathways and a compound is able to target those downstream pathways, then the compound will be effective against progression of both diseases.

Recent studies by this laboratory have demonstrated that adipose-derived stem cell conditioned media (ASC-CM) is neuroprotective in an *in vivo* model of neurodegenerative disease, a neonatal rat model of hypoxia-ischemia (Wei *et al.,* 2009). This pilot study was designed to determine the effects of ASC-CM treatment in a genetic animal model of neuronal death, the $SOD1^{G93A}$ mouse, as ASC-CM was found to be neuroprotective in an injury-induced animal model of neuronal death, the hypoxia-ischemia neonatal rat (Wei *et al.*, 2009).

3.2 Introduction

For a complete review, please see Section 2.3.1. Amyotrophic Lateral Sclerosis of Chapter 2.

3.3. Experimental Procedures

For all protocols, please refer to Section 2.4. Experimental Procedures of Chapter 2.

3.3.1. Animal Treatment Protocol

Adipose-derived stem cell media (ASC-CM) was made as previously described (Wei *et al.*, 2009) and injected intraperitoneally (i.p.) at a volume of 200 µL, once daily. Animals in the vehicle group Basal Media Eagle (BME) alone were given an equivalent injection volume as ASC-CM-treated mice. Mice received one daily dose of ASC-CM or vehicle until a humane endpoint near death (survival studies) or for 3 or 7 days after disease onset (biochemical and immunohistochemical studies).

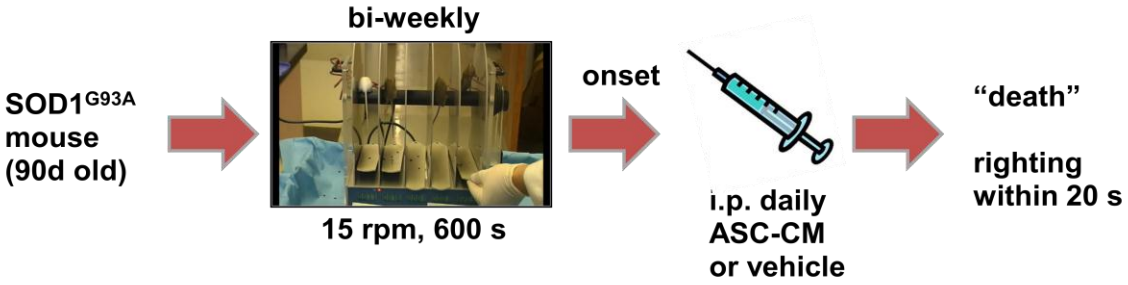

Figure 3.1. Diagram of the Animal Treatment Protocol.

3.4. Results

3.4.1. Post-onset ASC-CM treatment of SOD1^{G93A} mice significantly diminished symptomatic progression and extended life span

SOD1^{G93A} mice were given ASC-CM treatment from disease onset until a humane time point near death (death endpoint). The length of time from disease onset until death was measured and reported as days of post-onset survival (Fig 3.2A). The SOD1^{G93A} mice given ASC-CM had increased post-onset survival times (31.6 ± 4.1 days, n = 5; *** $p < 0.005$) as compared to vehicle-treated mice (16.1 ± 1.6 days, n = 7). This increase in survival translated into an extension of SOD1^{G93A} mice lifespans (Fig 3.2B). ASC-CM-treated mice had significantly longer lifespans (138.8 ± 3.1 days, n = 5) versus the vehicle counterparts (124.4 ± 1.5 days, n = 7).

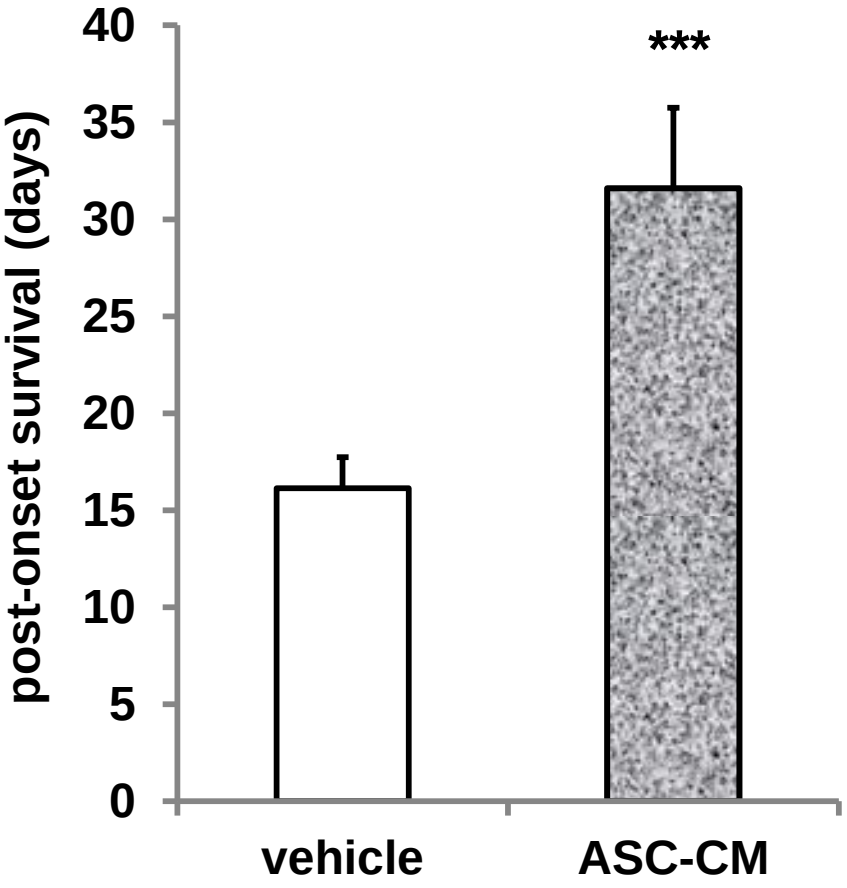

Figure 3.2A. Treatment with ASC-CM extends post-onset survival of SOD1^{G93A} mice.

Male and female symptomatic SOD1^{G93A} mice were given daily ASC-CM treatment or vehicle until the death endpoint. Duration of disease is reported as days of post-onset survival and measured by the number of days between disease onset and a humane endpoint near death. Mice with disease onset who were treated daily with ASC-CM (n = 7) had a significant extension of survival time as compared to SOD1^{G93A} mice without ASC-CM (n = 5). The calculated averages (± SEM) of post-onset survival were significantly increased in mice given ASC-CM compared to vehicle. Statistical analysis was performed using one-way ANOVA. ***, $p < 0.005$ vs. vehicle.

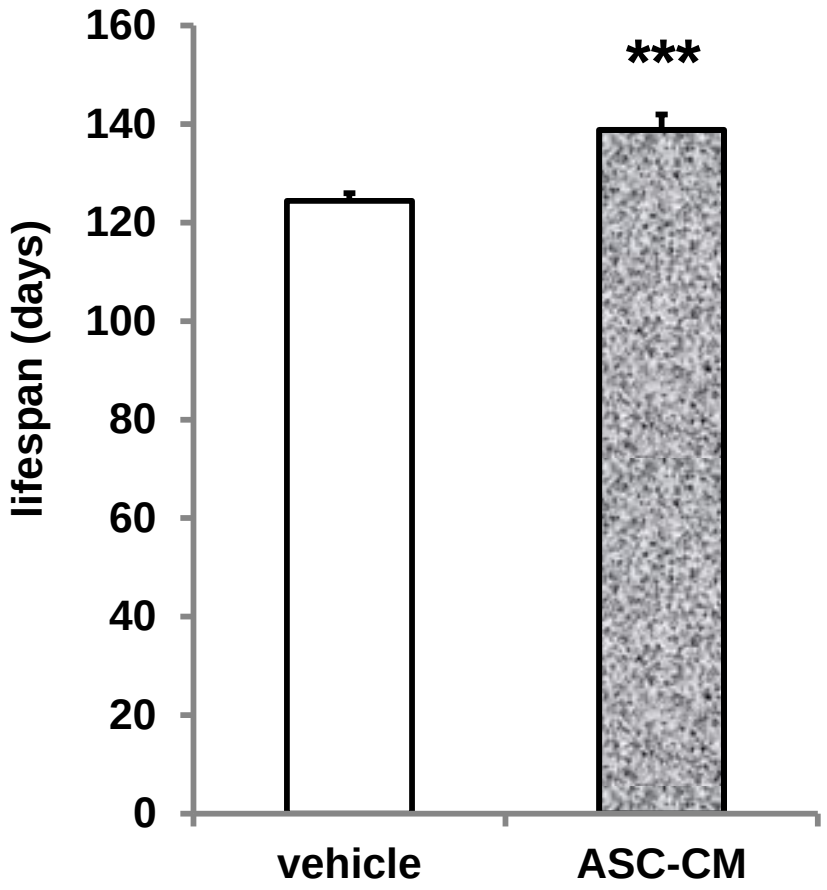

Figure 3.2B. ASC-CM treatment lengthens the lifespan of SOD1^{G93A} mice with disease onset.

Male and female SOD1^{G93A} mice with disease onset were treated with ASC-CM or vehicle until the death endpoint. The number of days between birth and a humane endpoint near death were measured in days of lifespan . ASC-CM-treated mice with disease onset (n = 5) had a significant lifespan extension when compared to SOD1^{G93A} mice with no ASC-CM treatment (n = 7). Extended post-onset survival times of ASC-CM-treated mice resulted in the marked lengthening of lifespan relative to vehicle mice. ***, $p < 0.005$ vs. vehicle.

3.4.2. A greater number of motor neurons in the lumbar spinal cord survived with ASC-CM treatment

It was determined whether the extended survival of ASC-CM-treated SOD1^{G93A} mice correlated with prevention of motor neuron loss. Motor neuron number changes at 7 days following onset were evaluated in cross-sections of lumbar spinal cords of the SOD1^{G93A} mice (Fig 3.3A). Vehicle-treated mice exhibited a marked (*** $p < 0.005$) loss of ventral horn motor neurons in the lumbar region versus wild type littermates (group means: 7.8 ± 0.84 and 21.9 ± 0.79, respectively; Fig 3.3B). The loss of motor neurons was prevented at this time point by ASC-CM treatment (15.9 ± 2.0, $p < 0.01$ vs. vehicle); however, there was still significant motor neuron loss ($p < 0.05$) compared to age-matched, wild type mice, although this loss is not as severe as in the vehicle group (Fig 3.3B). MAP2-immunoreactive neuronal processes were observed and clearly defined throughout the tissue sections from wild type and ASC-CM-treated mice. In contrast, there was very little to no presence of MAP2-positive neuronal processes visible in vehicle-treated SOD1^{G93A} mice spinal cord (Fig 3.3A).

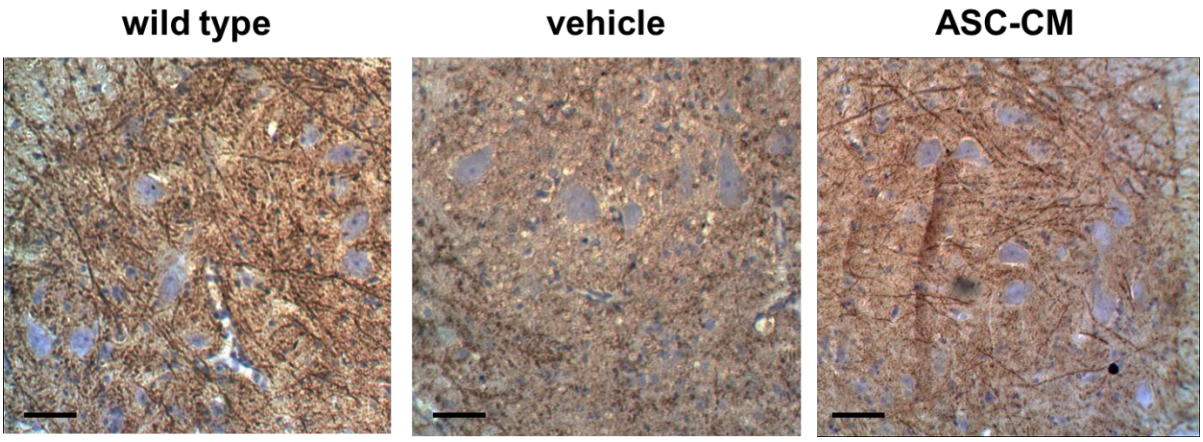

Figure 3.3A. ASC-CM 7-day treatment of SOD1^{G93A} mice with disease resulted in a greater number of motor neurons present in lumbar spinal.

Symptomatic SOD1^{G93A} mice were given ASC-CM or vehicle for 7 days. Motor neurons in the lumbar spinal cord area were identified by immunoreactivity to MAP2 antibody and hematoxylin nuclear counterstaining as described in Chapter 2's Experimental Procedures section. Representative images of stained lumbar spinal cord sections showed an increase in the presence of MAP2-positive neurons in lumbar spinal cord of SOD1^{G93A} mice treated with ASC-CM compared to vehicle. Scale bars: 100 µm.

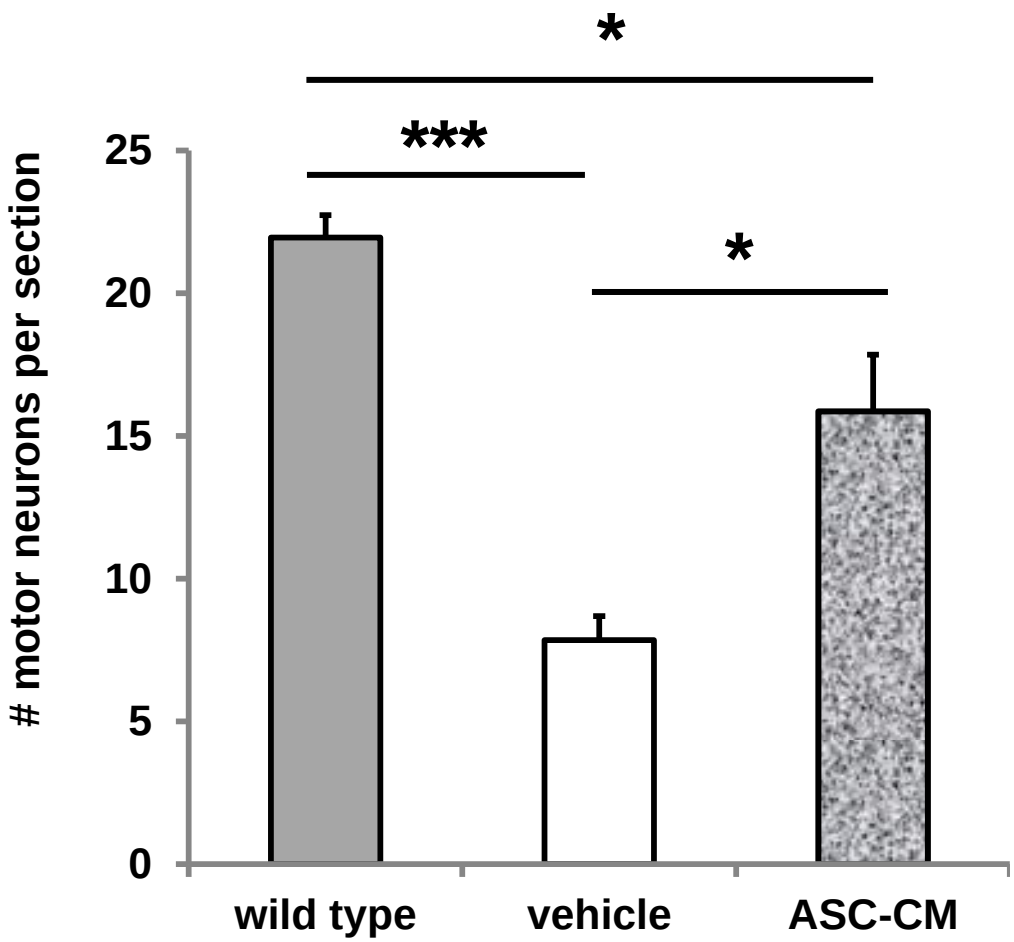

Figure 3.3B. A greater number of motor neurons were observed in lumbar spinal cords of SOD1^{G93A} mice treated with ASC-CM for 7 days.

Symptomatic SOD1^{G93A} mice were treated with or without ASC-CM for 7 days. Digitized images covering the entire cross-sectional area from 6 – 8 lumbar spinal regions from each mouse in the study were quantitated for MAP2 immunoreactivity and hematoxylin nuclear counterstain. With ASC-CM treatment, a higher number of motor neurons was observed in SOD1^{G93A} mice with disease onset (n = 5) versus vehicle (n = 5). Wild type control data were generated from 4 mice. Experimental group data are presented as averages ($\pm$ SEM) and statistical analyses were performed using one-way ANOVA. * $p < 0.05$; ***, $p < 0.005$.

3.4.3. Administration of ASC-CM had no effect on mouse SOD1$^{wild\ type}$ and mutant human SOD1^{G93A} expression in spinal cords of SOD1^{G93A} mice

Studies have shown that the transgene copy number (copies of the transgene with the G → A at position 93, human mutant form of SOD1) affects survival of the SOD1^{G93A} mouse (Alexander *et al.*, 2004b). In order to determine if ASC-CM has an effect on SOD1 gene expression, immunoblot analyses were performed on spinal cord homogenates after 7 days of ASC-CM treatment (Fig 3.4a). Band density measurements showed that levels of both wild type endogenous mouse SOD1 (mSOD1^{WT}) and mutated human SOD1 (hSOD1^{G93A}) expressed exhibited no differences with or without 7-day ASC-CM treatment (Fig 3.4b). “Wild type/WT” mice express wild type endogenous mouse SOD1 (mSOD1^{WT}) but do not carry the mutated human SOD1 (hSOD1^{G93A}) transgene; “vehicle” and “ASC-CM” mice are the experimentally-treated SOD1^{G93A} transgenic mice that express wild type endogenous mouse SOD1 (mSOD1^{WT}) in addition to the mutated human SOD1 (hSOD1^{G93A}) transgene. Actin levels remained unchanged and served as an internal loading control for endogenous mouse SOD1 (mSOD1^{WT}). There were differences in endogenous mouse SOD1 (mSOD1^{WT}) levels, which then served as an internal control for mutated human SOD1 (hSOD1^{G93A}) expression.

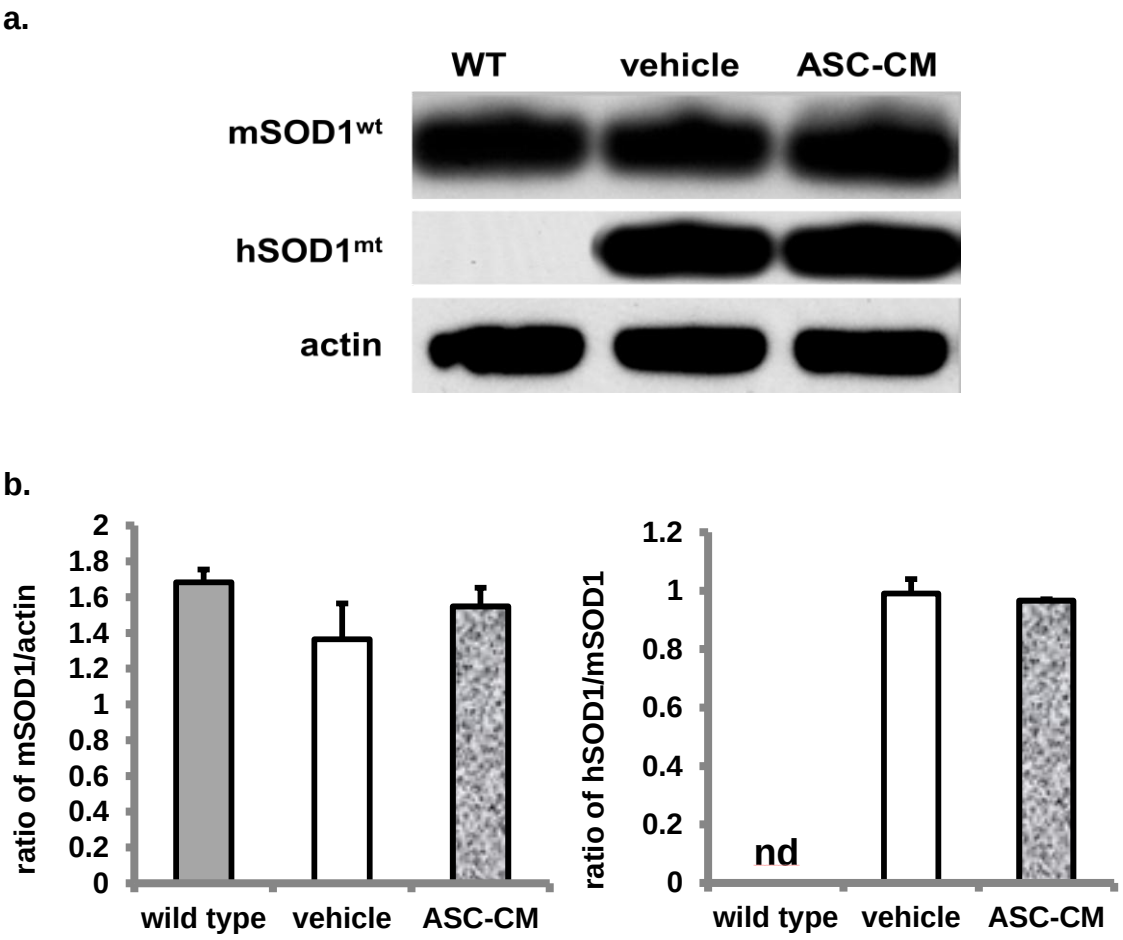

Figure 3.4. Treatment with ASC-CM did not affect expression of endogenous mouse wild type SOD1 and mutated human SOD1 transgene in spinal cord.

Wild type control ("WT") and SOD1^{G93A} mice ("vehicle" and "ASC-CM") spinal cords were prepared as detailed in Chapter 2's Experimental Procedures. Levels of actin were unchanged and used as an internal loading control for endogenous mouse wild type SOD1 ("mSOD1^{WT}"). There was no difference in mSOD1^{WT} levels, which was the loading control for mutated human SOD1 ("hSOD1^{G93A}"). After 7 days of ASC-CM treatment, there was no change in expression of either endogenous mouse wild type SOD1 or human SOD1 carrying the G93A mutation in symptomatic SOD1^{G93A} mice. n = 3 per group.

3.4.4. Daily ASC-CM treatment decreased phosphorylation of p38 MAP kinase in spinal cords of SOD1^{G93A} mice

It has been demonstrated that motor neuron loss occurs partly through the action of activated inflammatory cells in the surrounding area (Boillee *et al*., 2006a). In order to determine if the protection of motor neurons following ASC-CM treatment is due to inflammatory pathway inhibition, levels of phosphorylated p38 in spinal cords were evaluated at 3 days (Fig 3.5A) and 7 days (Fig 3.5B) following disease onset and with or without ASC-CM administration during that time period. In agreement with other reports using the SOD1^{G93A} mouse (Hu *et al*., 2003; Dewil *et al*., 2007), p38 phosphorylation was elevated in SOD1^{G93A} mice after disease onset at both 3 days (0.84 ± 0.0092, $p < 0.005$ vs. wild type and ASC-CM; Fig 3.5Ab) and 7 days post-onset (1.3 ± 0.17, $p < 0.01$ vs. wild type; Fig 3.5Bb). Levels of phospho-p38 protein in the spinal cords were significantly decreased with ASC-CM treatment for 3 days (0.69 ± 0.023, $p < 0.005$ vs. vehicle and wild type; Fig 3.5Ab) and for 7 days (0.56 ± 0.23, $p < 0.05$ vs. vehicle; Fig 3.5Bb) as compared to the vehicle groups. These phospho-p38 levels observed in ASC-CM-treated animals were still higher than wild type controls at 3 days (0.38 ± 0.062, $p < 0.005$ vs. ASC-CM group; Fig 3.5Bb).

a.

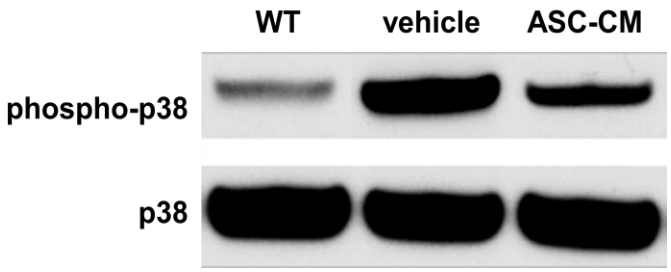

b.

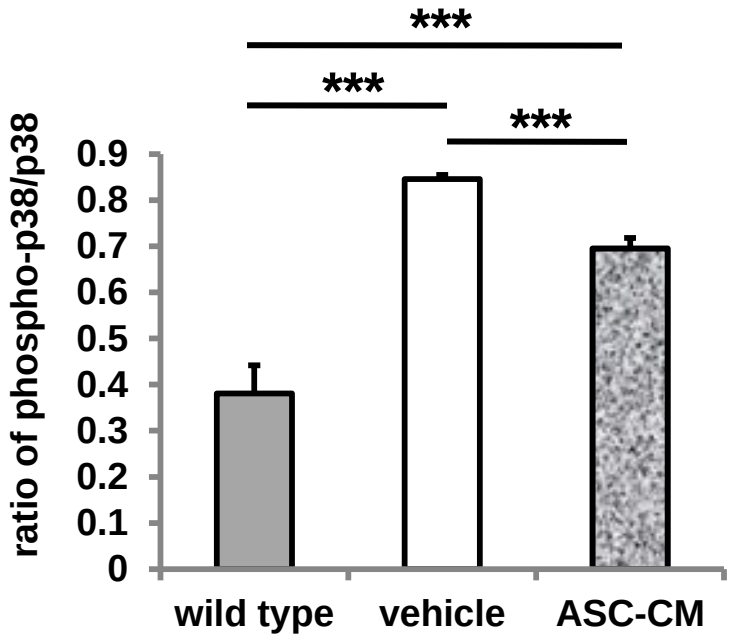

Figure 3.5A. Reduced phosphorylation of p38 in spinal cords of SOD1^{G93A} mice with disease onset was observed after 3 days of ASC-CM treatment.

SOD1^{G93A} mice with onset received ASC-CM or vehicle for 3 days and spinal cords were prepared for Western blot as described in Experimental Procedures. (a) Representative Western blots and (b) quantitation of band density showed reduced phosphorylated-p38 expression in spinal cords of SOD1^{G93A} mice given ASC-CM versus vehicle. Unchanged total p38 expression served as an internal loading control. Values are the mean density ± SEM. One-way ANOVA was used for statistical analysis. ***, $p < 0.005$; n = 3 per group.

a.

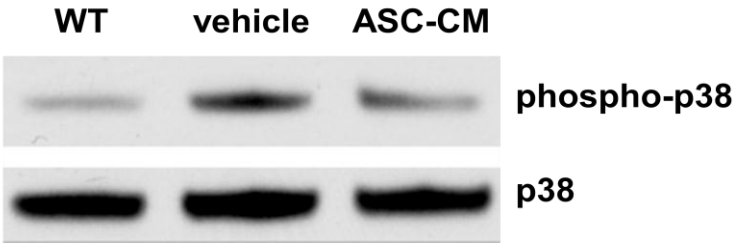

b.

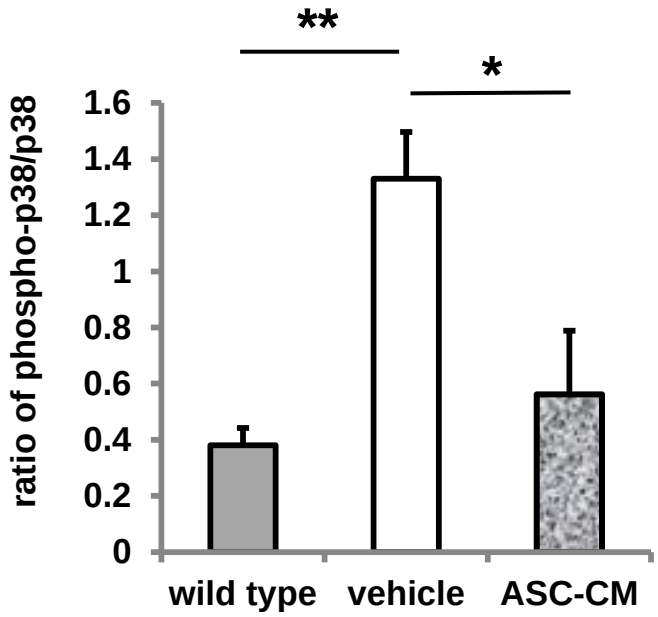

Figure 3.5B. Decreased levels of phospho-p38 in spinal cords of symptomatic SOD1^{G93A} mice were observed after 7 days of ASC-CM treatment.

Symptomatic SOD1^{G93A} mice were given ASC-CM or vehicle for 7 days and spinal cords were harvested for Western blotting as described in Experimental Procedures in Chapter 2. (a) Representative immunoblots and (b) densitometric quantitation demonstrated reduced phosphorylated p38 expression with ASC-CM treatment as compared to vehicle-treated animals. Unchanged total p38 levels served as an internal loading control. Values represent the mean density ± SEM. Statistical analysis was performed using one-way ANOVA. * $p < 0.05$; ** $p < 0.01$; n = 3 per group.

3.4.5. A reduction in GFAP expression was observed in the spinal cords of symptomatic SOD1^{G93A} mice treated with ASC-CM

Because treatment with ASC-CM was showing significant neuroprotection of motor neurons potentially via anti-inflammatory mechanisms thus far, glial activation after treatment with ASC-CM was examined to further explore this possibility. Expression of GFAP was measured in the spinal cords of SOD1^{G93A} mice after 3 days of treatment with ASC-CM or vehicle. Representative immunoblots demonstrated that there is significantly reduced GFAP expression with ASC-CM treatment (0.89 ± 0.027) versus vehicle (1.2 ± 0.020; *** $p < 0.005$; Fig 3.6a). The GFAP levels observed in the ASC-CM-treated group were comparable to that of the wild type controls (0.95 ± 0.034).

a.

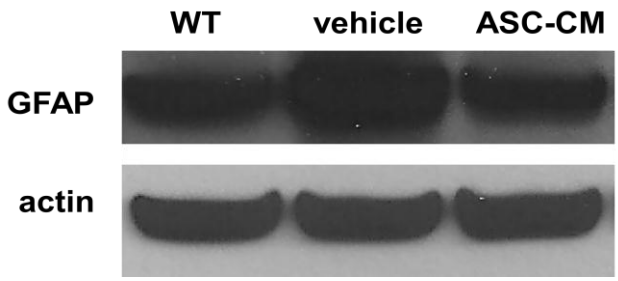

b.

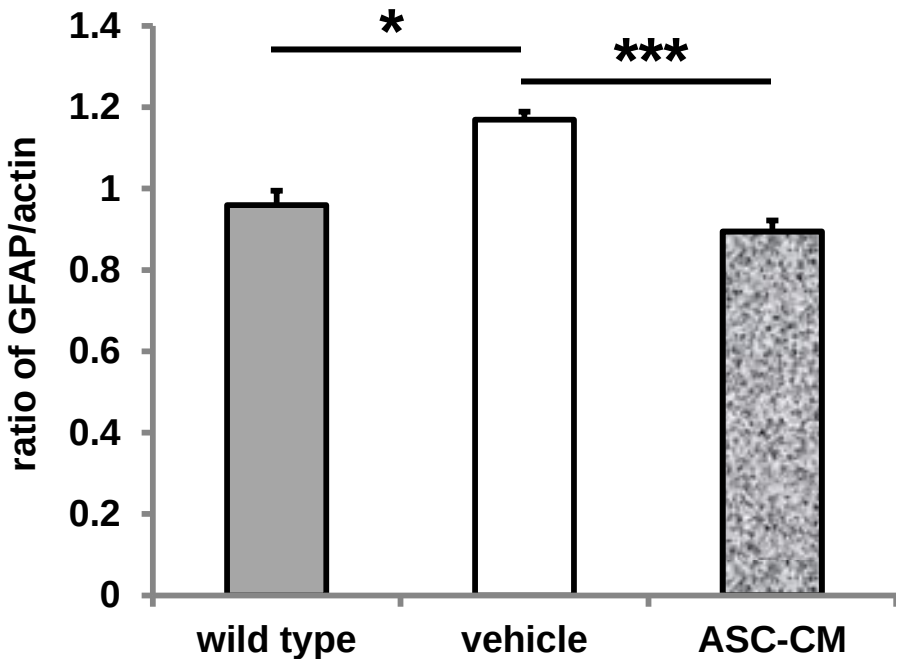

Figure 3.6. 3-day treatment with ASC-CM showed reduced GFAP expression in spinal cords of symptomatic SOD1^{G93A} mice.

SOD1^{G93A} mice with disease onset were given ASC-CM or vehicle for 3 days. Spinal cords were removed for immunoblot as described in Experimental Procedures. Actin expression remained unchanged in all groups and served as an internal loading control. (a) Representative immunoblots and (b) band quantitation demonstrated a decrease in spinal cord GFAP expression after 3-day ASC-CM treatment as compared to vehicle. Experiments were completed in triplicate with n = 3 per group. * $p < 0.05$; *** $p < 0.005$.

3.4.6. Administration of ASC-CM to SOD1^{G93A} mice with disease onset decreased CD11b expression in spinal cords

In order to further investigate glial activation after ASC-CM treatment, spinal cords were prepared for Western blot and examined for expression of CD11b, a glial marker found to be induced by neuroinflammation (Boillee *et al.*, 2006). CD11b expression was observed at 3 days (Fig 3.7A) and 7 days (Fig 3.7B) after ASC-CM or vehicle treatment. After 3 days of ASC-CM treatment of symptomatic SOD1^{G93A} mice, representative immunoblots (Fig 3.7Aa) and measurements of band densities (Fig 3.7Ab) demonstrated no differences in CD11b expression in all groups (group averages ± SEM: 0.27 ± 0.065 for wild type; 0.28 ± 0.050 for vehicle; 0.24 ± 0.067 for ASC-CM). However, after 7 days of ASC-CM treatment, representative immunoblots (Fig 3.8Ba) and band density quantitation (Fig 3.8Bb) demonstrated a significant increase in CD11b expression in the spinal cord of vehicle mice (0.83 ± 0.049 for vehicle, *** $p < 0.005$ versus wild type and ASC-CM) when compared to ASC-CM-treated animals (0.50 ± 0.078), whose CD11b expression level was at a similar level to wild type mice (0.46 ± 0.023) after 7 days.

a.

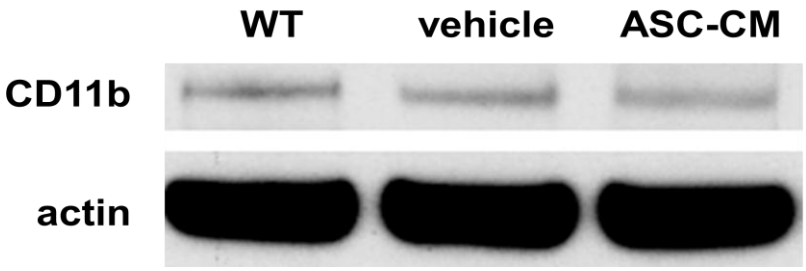

b.

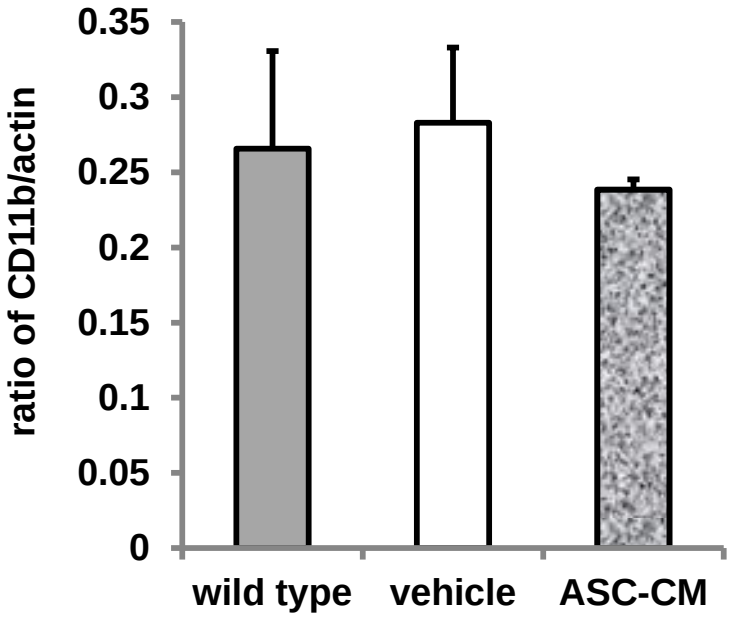

Figure 3.7A. 3 days of ASC-CM treatment had no effect on CD11b expression in spinal cords of symptomatic SOD1^{G93A} mice.

SOD1^{G93A} mice were given 3 days of ASC-CM treatment or vehicle upon disease onset. Spinal cords were processed Western blot as described in Experimental Procedures. Unchanged actin in all groups served as an internal loading control. (a) The representative immunoblots and (b) band densities that were measured showed no change in spinal cord CD11b expression after 3 days of ASC-CM treatment. WT (wild type), n = 3; vehicle, n = 4; ASC-CM, n = 4.

a.

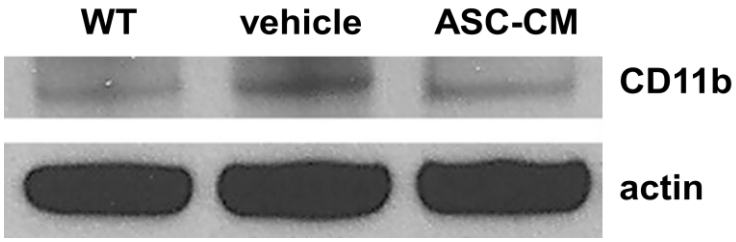

b.

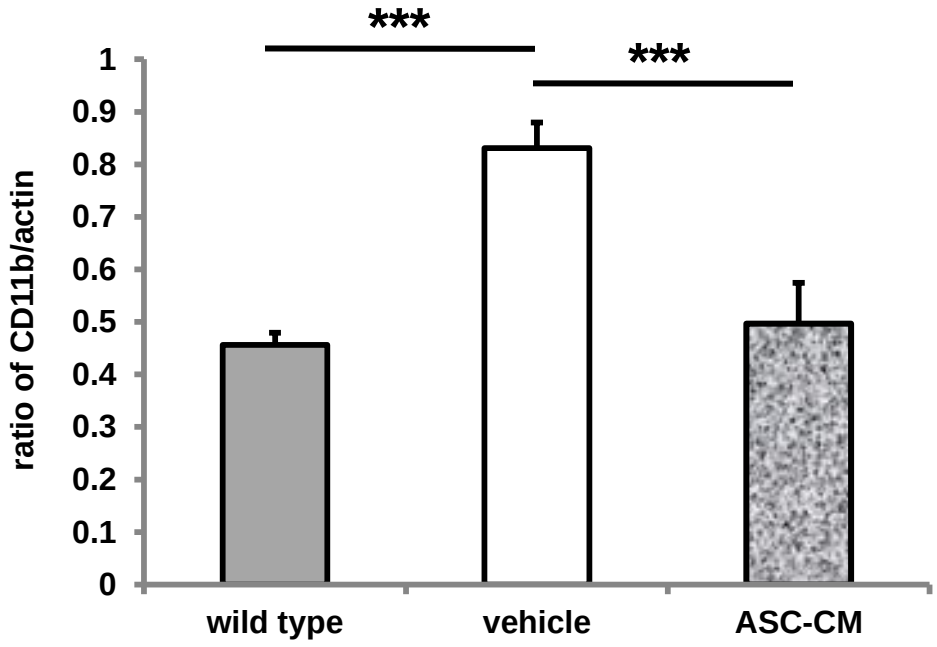

Figure 3.7B. ASC-CM treatment for 7 days reduced expression of CD11b in spinal cords of SOD1^{G93A} mice with disease onset.

For 7 days, symptomatic SOD1^{G93A} mice were given ASC-CM or vehicle. Spinal cords were removed for immunoblot as described in Experimental Procedures. Unchanged actin expression served as an internal loading control. (a) Representative immunoblots and (b) band quantitation demonstrated a decrease in spinal cord CD11b expression after 7 days of ASC-CM treatment as compared to vehicle. WT (wild type), n = 3; vehicle, n = 3; ASC-CM, n = 3. *** $p < 0.005$.

3.4.7. ASC-CM treatment of symptomatic SOD1^{G93A} mice resulted in decreased expression of α-II spectrin in spinal cords

Activity of the Ca^{2+}-activated protease, calpain, was increased in SOD1^{G93A} mice spinal cords (Stifanese *et al.*, 2010). ASC-CM's effect on the calpain system in SOD1^{G93A} mice was determined by measuring expression of α-II spectrin, a known cleavage target of calpain (Strong, 1999). After 3 days following disease onset, cleaved α-II spectrin expression was significantly decreased in SOD1^{G93A} mice receiving ASC-CM treatment (0.17 ± 0.03, n = 4; *** $p < 0.005$) and wild type controls (0.16 ± 0.01, *** $p < 0.005$) as compared to mice given vehicle (0.99 ± 0.003, n = 3), which was demonstrated in a representative immunoblot (Fig 3.8a) and quantified band density measurements (Fig 3.8b). Levels of actin remained unchanged for all groups and were used as internal loading controls.

a.

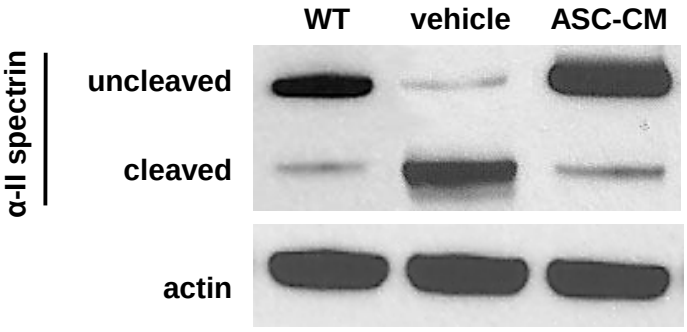

b.

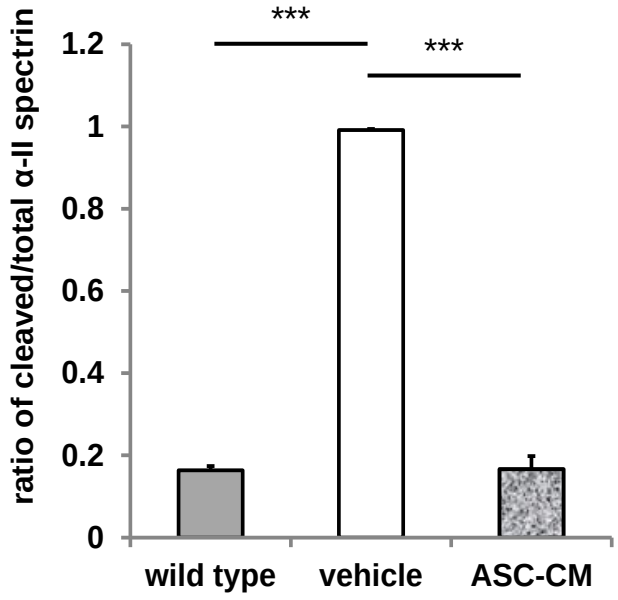

Figure 3.8. ASC-CM treatment for 3 days decreased α-II spectrin cleavage in symptomatic SOD1^{G93A} mice.

SOD1^{G93A} mice were given ASC-CM or vehicle for 3 days and Western blot analysis was done as described in Chapter 2's Experimental Procedures. Unchanged actin expression served as an internal loading control. (a) Representative immunoblots and (b) quantitation of band densities revealed a decrease in cleaved α-II spectrin expression at 3 days post-onset when ASC-CM treatment was given. Wild type, n = 5; vehicle, n = 3; ASC-CM, n = 4. *** $p <$ 0.005.

3.4.8. ASC-CM treatment had no effect on caspase-12 cleavage in spinal cords of SOD1^{G93A} mice with disease onset

Because ER stress is thought to play a role in motor neuron death in SOD1^{G93A} mouse spinal cord (Wootz *et al.*, 2004, 2006), spinal cords were examined for the effect of ASC-CM treatment on caspase-12, an ER stress pathway component (Wootz *et al.*, 2004). Spinal cords were removed from symptomatic SOD1^{G93A} mice and analyzed via Western blot. At 3 days after disease onset, there was a significant decrease in cleaved caspase-12 expression in symptomatic SOD1^{G93A} mice injected with ASC-CM for 3 days (0.47 ± 0.09, * $p < 0.05$) and wild type controls (0.53 ± 0.006, *** $p < 0.005$) versus their vehicle-treated counterparts (0.74 ± 0.01) as shown in representative blots (Fig 3.9a) and quantitative analyses of band densities (Fig 3.9b). Actin levels were not changed regardless of CAPE treatment and genotype and used as an internal control.

a.

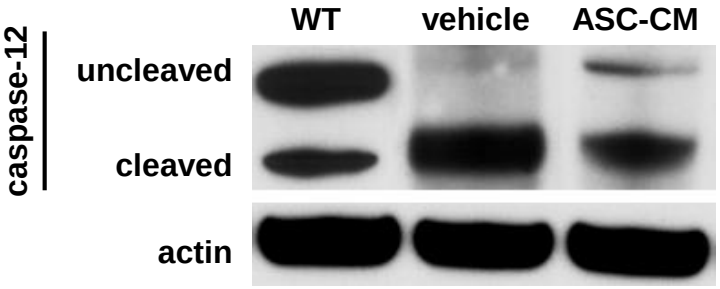

b.

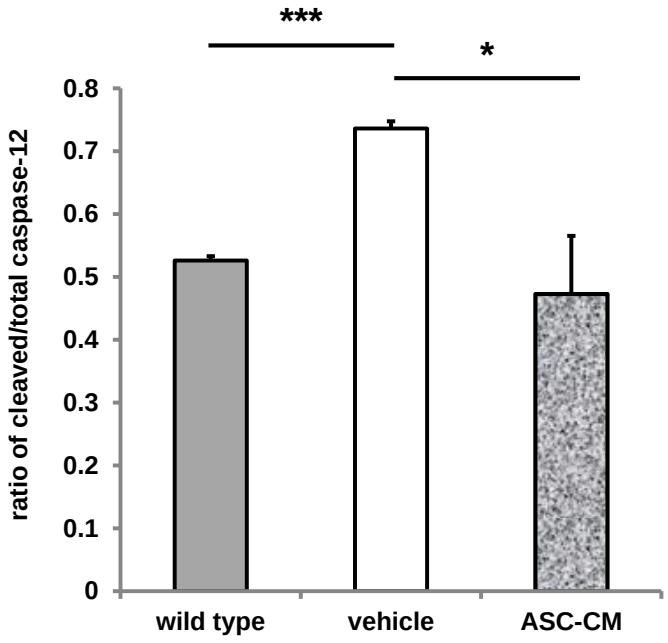

Figure 3.9. ASC-CM treatment for 3 days decreased caspase-12 cleavage in symptomatic SOD1^{G93A} mice.

SOD1^{G93A} mice were given ASC-CM or vehicle for 3 days and spinal cords were removed for Western blot as described in Chapter 2's Experimental Procedures. Actin expression was unchanged in all groups and used as an internal loading control. (a) Representative immunoblots and (b) band density quantitation showed no difference in caspase-12 cleavage with or without ASC-CM treatment. n = 4 per group; * $p < 0.05$; *** $p < 0.005$. Data are group averages ± SEM.

3.5 Discussion

This exploratory study was designed to confirm the effects of a biologically-derived reagent on an ALS animal model that is clinically relevant such that treatment was applied after disease onset was established in the widely used $SOD1^{G93A}$ mouse model (Gurney *et al.*, 1994). The data collected from this pilot study demonstrate the effectiveness of ASC-CM treatment in prolonging post-onset survival and extending the lifespan of the symptomatic $SOD1^{G93A}$ mouse. These results are in agreement with previous studies from this laboratory demonstrating that treatment with ASC-CM is beneficial and protective of neurons *in vivo* during neuronal injury or challenge, such as in the hypoxic-ischemic rat neonatal brain (Wei *et al.*, 2009). The findings from this exploratory study and the previous *in vivo* studies suggest that ASC-CM has potential as a therapeutic for neuronal degeneration.

Although the etiology of sporadic ALS is currently unknown, through the use of animal models and correlation with neuropathological findings from human ALS patients, several key mechanisms of neuronal death have been proposed to disrupt normal motor neuron function and lead to their degeneration. Current studies implicate glutamate-induced excitotoxicity, mitochondrial dysfunction, oxidative stress, neuroinflammation, aberrant axonal transport systems, endoplasmic reticulum (ER) stress, inhibition of proteosomal function, compromised blood-brain barrier, and abnormal protein aggregation (Ilieva *et al.*, 2009). There is much debate as to which processes contribute towards disease etiology and which events are secondary to the established disease state. This

presents ALS drug development with difficulties as neuropathology-specific targeting of treatment may be ineffective.

Despite the mechanistic uncertainties underlying events leading to ALS neuropathologic changes, treatments like ASC-CM may prove to be beneficial as they are able to block or modify several neuronal death pathways due to the heterogeneity in their composition. ASC-CM has been found to contain a multitude of neurotrophic factors such as insulin-like growth factor (IGF-1) and brain-derived neurotrophic factor (BDNF), which could be beneficial for the diseased motor neuron (Wei *et al.*, 2009). After 7 days of treatment with ASC-CM, symptomatic $SOD1^{G93A}$ mice had significant prolongation of post-onset survival times, which translated into an overall extension of lifespan. Additionally, this lengthened of post-onset lifespan following ASC-CM administration was correlated with markedly higher numbers of surviving motor neurons in the lumbar area of the spinal cord. Further examinations at the cellular level determined that the increase in motor neuron survival after ASC-CM treatment was accompanied by decreased expression of glial activation markers and reductions in levels of phosphorylated p38 MAP kinase, which are important components of the neuroinflammation pathway (Cuende *et al.*, 2007) contributing to neuronal death in the spinal cords of $SOD1^{G93A}$ mice (Dewil *et al.*, 2007). Other pilot data from this study show lower levels of cleaved α-II spectrin, which is a known substrate of both calpains and caspase-3 (Simon *et al.*, 1989; Wang *et al.*, 1998). Decreased cleavage of α-II spectrin in the spinal cords of ASC-CM-treated $SOD1^{G93A}$ mice may indicate that this biologically-derived reagent has

protective effects against glutamate-induced apoptotic mediators (Wootz *et al.*, 2006; Stifanese *et al.*, 2010; Tradewell and Durham, 2010). A reduction in cleaved caspase-12 expression was also observed in the spinal cords of $SOD1^{G93A}$ mice given ASC-CM treatment, suggesting that treatment with this biological agent may be effective in reducing ER stress associated with ALS (Nagata *et al.,* 2007).

Taken together, this exploratory study demonstrated that ASC-CM provides significant neuroprotection in the $SOD1^{G93A}$ mouse model of ALS. This protective ability may reside in the individual actions of its neurotrophic components working separately or in concert towards the preservation of motor neurons in the spinal cord as well as attenuation of the neuropathogenic mechanisms underlying motor neuron death and disease progression.

CHAPTER 4: General Conclusions

4.1 Summary

The study in Chapter 1 reports that oral administration of CAPE in mice prevents MPTP-induced neuronal death and the loss of striatal DA, accompanied by inhibition of MPTP-induced expression of caspase-1 and iNOS *in vivo.* Additionally, in contrast to minocycline treatment (Tipton and Singer, 1993), CAPE administration directly blocks MPP^+-induced neurotoxicity *in vitro* and this action may mediate inhibition of MPP^+-induced release of cytochrome *c* and AIF from mitochondria. Collectively, these data provide evidence that CAPE, an active component isolated from *propolis*, has robust neuroprotective activity in the MPTP mouse model of Parkinson's disease. Therefore, CAPE may prove effective in altering or preventing the induction of or slowing the progression of Parkinson's disease and related neurodegenerative disorders, such as amyotrophic lateral sclerosis.

The study in Chapter 2 presents the potential for a treatment with a small molecule compound that acts on multiple pathways (i.e., neuroinflammation, ER stress, and cell death) that are putatively involved in and converge towards ALS progression. Importantly, these effects were evident when CAPE was administered upon symptom onset in the $SOD1^{G93A}$ mouse, which is highly correlative to the stage of presentation and disease diagnosis in human patients. Data from the current and previous studies from this laboratory suggest that CAPE could be a potent pharmacological therapy for ALS and PD as well as

other diseases of the brain and spinal cord with shared neuronal death pathways and the ensuing neuropathogenic consequences.

The pilot study in Chapter 3 provides evidence for the potential of using a biologically-derived reagent for the treatment for ALS as the neuroprotective effects of ASC-CM were demonstrated in its ability to significantly prolong the survival of a clinically-relevant animal model of ALS as well as its actions on multiple pathways posited to be involved in ALS disease progression. Exploratory data from these experiments in combination with previous studies from this laboratory suggest that ASC-CM may be effective for the treatment of ALS and other neuronal death-related disorders.

REFERENCES

Agid Y. 1991. Parkinson's disease: pathophysiology. Lancet 337:1321-1324.

Alexander GM, Erwin KL, Byers N, Deitch JS, Augelli BJ, Blankenhorn EP, Heiman-Patterson TD. 2004. Effect of transgene copy number on survival in the G93A SOD1 transgenic mouse model of ALS. Molec Brain Res 130:7-15.

Almer G, Guegan C, Teismann P, Naini A, Rosoklija G, Hays AP, Chen C, Przedborski S. 2001. Increased expression of the pro-inflammatory enzyme cyclooxygenase-2 in amyotrophic lateral sclerosis. Ann Neurol 49: 76-185.

Ankarcrona M, Dypbukt JM, Bonfoco E, Zhivotovsky B, Orrenius S, Lipton SA, Nicotera P. 1995. Glutamate-induced neuronal death: a succession of necrosis or apoptosis depending on mitochondrial function. Neuron 15:961-973.

Antal A, Bandini F, Keri S, Bodis-Wollner I. 1998. Visuo-cognitive dysfunctions in Parkinson's disease. Clin Nueurosci 5:147-152.

Aubin N, Curet O, Deffois A, Carter C. 1998. Aspirin and salicylate protect against MPTP-induced dopamine depletion in mice. J Neurochem 71:1635-1642.

Aygun FO, Akcam FZ, Kaya O, Ceyhan BM, Sutcu R. 2011. Caffeic acid phenethyl ester modulates gentamicin-induced oxidative nephrotoxicity in kidney of rats. Biol Trace Elem Res [Epub ahead of print].

Balcar VJ and Johnston GAR. 1972. The structural specificity of the high affinity uptake of L-glutamate and L-aspartate by rat brain slices. J Neurochem 19:2657-2666.

Balcar VJ, Johnston GAR, Twitchin B. 1977. Stereospecificity of the inhibition of L-glutamate and L-aspartate high affinity uptake in rat brain slices by threo-3-hydroxy-aspartate. J Neurocehm 28:1145-1146.

Baldereschi M, Di Carlo A, Rocca WA, Vanni P, Maggi S, Perissinotto E, Grigoletto F, Amaducci L, Inzitari D. 2000. Parkinson's disease and parkinsonism in a longitudinal study: two-fold higher incidence in men. ILSA Working Group. Italian Longitudinal Study on Aging. Neurology 55:1358-1363.

Baranano DE, Rao M, Ferris CD, Snyder SH. 2002. Biliverdin reductase: a major physiologic cytoprotectant. Proc Natl Acad Sci USA 99:16093-16098.

Berry C, La Vecchia C, Nicotera P. 2010. Paraquat and Parkinson's disease. Cell Death Differ 17:1115-1125.

Beal MF. 1998. Excitotoxicity and nitric oxide in Parkinson's disease pathogenesis. Ann Neurol S110-S114.

Beck KD, Knusel B, Pasinetti G, Michel PP, Zawadzka H, Goldstein M, Hefti F. 1991. Tyrosine hydroxylase mRNA expression by dopaminergic neurons in culture: effect of 1-methyl-4-phenylpyridinium treatment. J Neurochem 57:527-532.

Bendotti C, Atzori C, Piva R, Tortarolo M, Strong MJ, DeBiasi S, Mighetli A. 2004. Activated p38MAPK is a novel component of the intracellular inclusions found in human amyotrophic lateral sclerosis and mutant SOD1 transgenic mice. J Neuropathol Exp Neurol 63:113-119.

Betarbet R, Sherer TB, MacKenzie G, Garcia-Osuna M, Panov AV, Greenamyre JT. 2000. Chronic systemic pesticide exposure reproduces features of Parkinson's disease. Nat Neurosci 3:1301-1306.

Bezard E, Imbert C, Gross CE. 1998. Experimental models of Parkinson's disease: from the static to the dynamic. Rev Neurosci 9:71-90.

Bezard E and Przedborski S. 2011. A Tale on Animal Models of Parkinson's Disease. Mov Disord 26:993-1002.

Biedler JL, Roffler-Tarlov S, Schachner M, Freedman LS. 1978. Multiple neurotransmitter synthesis by human neuroblastoma cell lines and clones. Cancer Res 38:3751-3757.

Blandini F, Nappi G, Tassorelli C, Martignoni E. 2000. Functional changes of the basal ganglia circuitry in Parkinson's disease. Prog Neurobiol 62:63-88.

Blandini F, Armentero MT, Fancellu R, Blaugrund E, Nappi G. 2004. Neuroprotective effect of rasagiline in a rodent model of Parkinson's diease. Exp Neurol 187:455-459.

Blin O, Desnuelle C, Rascol OBorg M, Peyro Saint Paul H, Azulay JP, Bille F, Figarella D, Coulom F, Pellissier JF. 1994. Mitochondrial respiratory failure in skeletal muscle from patients with Parkinson's disease and multiple system atrophy. J Neurol Sci 125:95-101.

Blum-Degen D, Muller T, Kuhn W. 1995. Interleukin-1 beta and interleukin-6 are elevated in the cerebrospinal fluid of Alzheimer's and de novo Parkinson's disease patients. Neurosci Lett 202:17-20.

Bocchetta A, Piccardi MP, Del Zompo M, Pintus S, Corsini GU. 1985. 1-methyl-4-phenyl-1,2,3,6-tetrahydropyridine: Correspondence of its binding sites to monoamine oxidase in rat brain, and inhibition of dopamine oxidative deamination *in vivo* and *in vitro*. J Neurochem 45:673-676.

Boillee S, Vande Velde C, Cleveland DW. 2006a. ALS: A disease of motor neurons and their nonneuronal neighbors. Neuron 52:39-59.

Boillee S, Yamanaka K, Lobsiger CS, Copeland NG, Jenkins NA, Kassiotis G, Kollias G, Cleveland DW. 2006b. Onset and progression in inherited ALS determined by motor neurons and microglia. Science 312:1389-1392.

Boka G, Anglade P, Wallach D, Javoy-Agid F, Agid Y, Hirsch EC. 1994. Immunocytchemical analysis of tumor necrosis factor and its receptors in Parkinson's disease. Neurosci Letter 172:151-154.

Bonifati V, Rizzu P, van Baren MJ, Schaap O, Breedveld GJ, Krieger E, Dekker MC, Squitieri F, Ibanez P, Joosse M, van Dongen JW, Vanacore N, van Swieten JC, Brice A, Meco G, van Duijn Cm, Oostra BA, Heutink P. 2003. Mutations in the DJ-1 gene associated with autosomal recessive early-onset parkinsonism. Science 299:256-259.

Bonsi P, Cuomo D, Picconi B, Sciamanna G, Tscherter A, Tolu M, Bernardi G, Calabresi P, Pisani A. 2007. Striatal metabotropic glutamate receptors as a target for pharmacotherapy in Parkinson's disease. Amino Acids 32:189-195.

Borland MK, Trimmer PA, Rubinstein JD, Keeney PM, Mohanakumar KP, Liu L, Bennett JP. 2008. Chronic, low-dose rotenone reproduces Lewy neuritis found in early stages of Parkinson's disease, reduces mitochondrial movement and slowly kills differentiated SH-SY5Y neural cells. Mol Neurodegener 3:21-33.

Bossy-Wetzel E, Schwarzenbacher R, Lipton SA. 2004. Molecular pathways to neurodegeneration. Nat Med 10:S2-S9.

Bruijn LI, Houseweart MK, Kato S, Anderson KL, Anderson SD, Ohama E, Reaume AG, Scott RW, Cleveland DW. 1998. Aggregation and motor neuron toxicity of an ALS-linked SOD1 mutant independent from wild type SOD1. Science 281:1851-1854.

Bruijn LI, Miller TM, Cleveland DW. 2004. Unraveling the mechanisms involved in motor neuron degeneration in ALS. Annu Rev Neurosci 27:723-749.

Cannon JR and Greenamyre JT. 2010. Neurotoxic *in vivo* models of Parkinson's disease: recent advances. Prog Brain Res 184:17-33.

Carlsson A, Lindquist M, Mangusson T. 1957. 3,4-dihydroxyphenylalanine and 5-hydroxytryptophan as reserpine antagonists. Nature 180:1200.

Carrasco E and Werner P. 2002. Selective destruction of dopaminergic neurons by low concentrations of 6-OHDA and MPP+: protection by acetylsalicylic acid aspirin. Parkinsonism Relat Disord 8:407-411.

Cassarino DS, Fall CP, Smith TS, Bennett JP Jr. 1998. Pramipexole reduces reactive oxygen species production in vivo and in vitro and inhibits the mitochondrial permeability transition produced by parkinsonian neurotoxin methylpyridinium ion. J Neurochem 71:295-301.

Chan CS, Gertler TS, Surmeier DJ. 2009. Calcium homeostasis, selective vulnerability and Parkinson's disease. Trends Neurosci 32:249-256.

Chau KY, Ching HL, Schapira AH, Cooper JM. 2009. Relationship between alpha synuclein phosphorylation, proteasomal inhibition and cell death: Relevance to Parkinson's disease pathogenesis. J Neurochem 110:1005-1013.

Chen K, Gunter K, Maines MD. 2000. Neurons overexpressing heme oxygenase-1 resist oxidative stress-mediated cell death. J Neurochem 75:304-312.

Choi HK, Won L, Roback D, Wainer BH, Heller A. 1992. Specific modulation of dopamine expression in neuronal hybrid cells by primary cells from different brain regions. Proc Natl Acad Sci USA 89:8943-8947.

Chu, C. T., Zhu, J. H., Cao, G., Signore, A., Wang, S., Chen, J. 2005. Apoptosis inducing factor mediates caspase-independent 1-methyl-4-phenylpyridinium toxicity in dopaminergic cells. J Neurochem 94:1685-1695.

Chun HS, Gibson GE, DeGiorgio LA, Zhang H, Kidd VJ, Son JH. 2001. Dopaminergic cell death induced by MPP(+), oxidant and specific neurotoxicants shares the common molecular mechanism. J Neurochem 76:1010-1021.

Clements JD, Lester RA, Tong G, Jahr CE, Westbrook GL. 1992. The time course of glutamate in the synaptic cleft. Science 258:1498-1501.

Collier TJ, Steece-Collier K, McGuire S, Sortwell CE. 2003. Cellular models to study dopaminergic injury responses. Ann NY Acad Sci 991:140-151.

Cudkowicz ME, Shefner JM, Schoenfeld DA, Brown RH Jr, Johnson H, Qureshi M, Jacobs M, Rothstein JD, Appel SH, Pascuzzi RM, Heiman-Patterson TD, Donofrio PD, David WS, Russell JA, Tandan R, Pioro EP, Felice KJ, Rosenfeld J, Mandler RN, Sachs GM, Bradley WG, Raynor EM, Baquis GD, Belsh JM, Novella S, Goldstein J, Hulihan J. 2003. A randomized, placebo-controlled trial of topiramate in amyotrophic lateral sclerosis. Neurology 61:456-464.

Cudkowicz ME, Shefner JM, Schoenfeld DA, Zhang H, Andreasson KI, Rothstein JD, Drachman DB. 2006. Trial of celecoxib in amyotrophic lateral sclerosis. Ann Neurol 60:22-31.

Cuenda A and Rousseau S. 2007. P38 MAP-kinases pathway regulation, function and role in human diseases. Biochim Biophys Acta 1773:1358-1375.

Dauer W, Kholodilov N, Vila M, Trillat AC, Goodchild R, Larsen KE, Staal R, Tieu K, Schmitz Y, Yuan CA, Rocha M, Jackson-Lewis V, Hersch S, Sulzer D, Przedborski S, Burke R, Hen Rene. 2002. Resistance of α-synuclein null mice to the parkinsonian neurotoxin MPTP. Proc Natl Acad Sci USA 99:14524-14529.

Dauer W and Przedborski S. 2003. Parkinson's Disease: Mechanisms and Models. Neuron 39:889-909.

Davies K. 1995. Oxidative stress: the paradox of aerobic life. Biochem Soc Symp 61:1-31.

Dawson TM and Dawson VL. 2003. Molecular pathways of neurodegeneration in Parkinson's disease. Science 302:819-822.

Day BJ, Patel M, Calavetta L, Chang LY, Stamler JS. 1999. A mechanism of paraquat toxicity involving nitric oxide synthase. Proc Natl Acad Sci USA 96:12760-12765.

Dehmer T, Lindenau J, Haid S, Dichgans J, Schulz JB. 2000. Deficiency of inducible nitric oxide synthase protects against MPTP toxicity in vivo. J Neurochem 74**:**2213-2216.

Deumens R, Blokland A, Prickaerts J. 2002. Modeling Parkinson's disease in rats: an evaluation of 6-OHDA lesions of the nigrostriatal pathway. Exp Neurol 175:303-317.

Dewil M, dela Cruz VF, Van Den Bosch L, Robberecht W. 2007. Inhibition of p38 mitogen activated protein kinase activation and mutant SOD1(G93A)-induced motor neuron death. Neurobiol Dis 26:332-341.

Dingledine R, Borges K, Bowie D, Traynelis SF. 1999. The glutamate receptor ion channels. Pharmacol Rev 51:7-61.

Dinkova-Kostova AT, Holtzclaw WD, Cole RN, Itoh K, Wakabayashi N, Katoh Y, Yamamoto M, Talalay P. 2002. Direct evidence that sulfhydryl groups of Keap1 are the sensors regulating induction of phase 2 enzymes that protect against carcinogens and oxidants. Proc Natl Acad Sci USA 99:11908-11913.

Di Monte DA. 2001. The role of environmental agents in Parkinson's disease. Clin Neurosci Res 1:419-426.

Dodge JC, Haidet AM, Yang W, Passini MA, Hester M, Clarke J, Roskelley EM, Treleaven CM, Rizo L, Martin H, Kim SH, Kaspar R, Taksir TV, Griffiths DA, Cheng SH, Shihabuddin LS, Kaspar BK. 2008. Delivery of AAV-IGF-1 to the CNS extends survival in ALS mice through modification of aberrant glial cell activity. Mol Ther 16:1056-1064.

Driver-Dunckley E, Samanta J, Stacy M. 2003. Pathological gambling associated with dopamine agonist therapy in Parkinson's disease. Neurology 61:422-423.

Du Y, Dodel RC, Bales KR, Jemmerson R, Hamilton-Byrd E, Paul SM. 1997. Involvement of a caspase-3-like cysteine protease in 1-methyl-4-phenylpyridinium-mediated apoptosis of cultured cerebellar granule neurons. J Neurochem 69:1382-1388.

Du Y, Ma Z, Lin S, Dodel RC, Gao F, Bales KR, Triarhou LC, Chernet E, Perry KW, Nelson DL, Luecke S, Phebus LA, Bymaster FP, Paul SM. 2001. Minocycline prevents nigrostriatal dopaminergic neurodegeneration in the MPTP model of Parkinson's disease. Proc Natl Acad Sci U S A 98:14669-14674.

Edmondson DE, Mattevi A, Binda C, Li M, Hubalek F. 2004. Structure and mechanism of monoamine oxidase. Curr Med Chem 11:1983-1993.

Edmondson DE, Binda C, Mattevi A. 2007. Structural insights into the mechanism of amine oxidation by monoamine oxidases A and B. Arch Biochem Biophys 464:269-276.

El-Agnaf OM, Jakes R, Curran MD, Middleton D, Ingenito R, Bianchi E, Pessi A, Neill D, Wallace A. 1998. Aggregates from mutant and wild type alpha-synuclein proteins and NAC peptide produce apoptotic cell death in human neuroblastoma cells by formation of beta-sheet and amyloid-like filaments. FEBS Lett 440:71-75.

Evans AH, Strafella AP, Weintraub D, Stacy M. 2009. Impulsive and compulsive behaviors in Parkinson’s disease. Mov Disord 24:1561-1570.

Eyles JM. 1955. James Parkinson (1755-1824). Nature 176:580-581.

Fahn S and Przedborski S. 2010. Parkinsonism. In: Rowland LP, Pedley Ta, eds. Merritt’s Neurology. 12th ed. New York: Lippincott Williams and Wilkins, 751-769.

Fearnley JM and Lees AJ. 1991. Ageing and Parkinson’s disease: substantia nigra regional selectivity. Brain 114:2283-2301.

Ferrante RJ, Schulz JB, Kowall NW, Beal MF. 1997. Systemic administration of rotenone produces selective damage in the striatum and globus pallidus, but not in the substantia nigra. Brain Res 753:157-162.

Finotti N, Castagna L, Moretti A, Marzatico F. 2000. Reduction of lipid peroxidation in different rat brain areas after cabergoline treatment. Pharmacol Res 42:287-291.

Floyd RA. 1999. Antioxidants, oxidative stress, and degenerative neurological disorders. Proc Soc Exp Biol Med 222:236-245.

Garbuzova-Davis S, Saporta S, Haller E, Kolomey I, Bennett SP, Potter H, Sanberg PR. 2007. Evidence of compromised blood-spinal cord barrier in early and late symptomatic SOD1 mice modeling ALS. PLoS One 11:e1205.

Gash DM, Rutland K, Hudson NL, Sullivan PG, Bing G, Cass WA, Pandya JD, Liu M, Choi DY, Hunter RL, Gerhardt GA, Smith CD, Slevin JT, Prince TS. 2008. Trichloroethylene: Parkinsonism and complex 1 mitochondrial neurotoxicity. Ann Neurol 63:184-192.

George JM. 2002. The synucleins. Genome Biol 3:REVIEWS3002.

Gerlach M, Riederer P, Przuntek H, Youdim MB. 1991. MPTP mechanisms of neurotoxicity and their implications for Parkinson's disease. Eur J Pharmacol 208:273-286.

German DC, Manaye K, Smith WK, Woodward DJ, Saper CB. 1989. Midbrain dopaminergic cell loss in Parkinson's disease: computer visualization. Ann Neurol 26:507-514.

Giasson BI, Forman MS, Higuchi M, Golbe LI, Graves CL, Kotzbauer PT, Trojanowski JQ, Lee VM. 2003. Initiation and synergistic fibrillization of tau and alpha-synuclein. Science 300:636-640.

Gocer H and Gulcin I. 2011. Caffeic acid phenethyl ester (CAPE): correlation of structure and antioxidant properties. Int J Food Sci Nutr [Epub ahead of print].

Gokce A, Oktar S, Yonden Z, Aydin M, Ilhan S, Ozkan OV, Davarci M, Yalcinkaya FR. 2009. Protective effect of caffeic acid phenethyl ester on cyclosporine A-induced nephrotoxicity in rats. Ren Fail 31:843-847.

Gomez C, Reiriz J, Pique M, Ferrer I, Ambrosio S. 2001. Low concentrations of 1-methyl-4-phenylpyridinium ion induce caspase-mediated apoptosis in human SH-SY5Y neuroblastoma cells. J Neurosci Res 63:421-428.

Gomez-Santos C, Ferrer I, Reiriz J, Vinals F, Barrachina M, Ambrosio S. 2002. MPP+ increases alpha-synuclein expression and ERK/MAP-kinase phosphorylation in human neuroblastoma SH-SY5Y cells. Brain Res 935:23-39.

Grace AA and Bunney BS. 1983. Intracellular and extracellular electrophysiology of nigral dopaminergic neurons – 2. Action potential generating mechanisms and morphological correlates. Neuroscience 10:317-331.

Grace AA and Bunney BS. 1984. The control of firing pattern in the nigral dopamine neurons: single spike firing. J Neurosci 4:2866-2876.

Graham DG. 1978. Oxidative pathways for catecholamines in the genesis of neuromelanin and cytotoxic quinines. Mol Pharmacol 14:633-643.

Greenamyre JT and Porter RH. 1994. Anatomy and physiology of glutamate in the CNS. Neurology 44:S7-S13.

Greenamyre JT, Sherer TB, Betarbet R, Panov AV. 2001. Complex I and Parkinson's disease. IUBMB Life 52:135-141.

Grossman SD, Rosenberg LJ, Wrathall JR. 2001. Temporal-spatial pattern of acute neuronal and legal loss after spinal cord contusion. Exp Neurol 168:273-282.

Grunberger D, Banerjee R, Eisinger K, Oltz EM, Efros L, Caldwell M, Estevez V, Nakanishi K. 1988. Preferential cytotoxicity on tumor cells by caffeic acid phenethyl ester isolated from propolis. Experientia 44:230-232.

Guegan C, Vila M, Rosoklija G, Hays AP, Przedborski S. 2001. Recruitment of the mitochondrial-dependent apoptotic pathway in amyotrophic lateral sclerosis. J Neurosci 21:6569-6576.

Gurney ME, Pu H, Chiu Y, Dal Canto MC, Polchow CY, Alexander DD, Caliendo J, Hentati A, Kwon YW. Deng HX, Chen W, Zhai P, Sufit RL, Siddique T. 1994. Motor neuron degeneration in mice that express a human Cu,Zn superoxide dismutase mutation. Science 264:1772-1775.

Gurney ME, Cutting, FB, Zhai P, Doble A, Taylor CP, Andrus PK, Hall ED. 1996. Benefit of vitamine E, riluzole, and gabapentin in a transgenic model of familial amyotrophic lateral sclerosis. Ann Neurol 39:147-157.

Gurney ME, Fleck TJ, Himes CS, Hall ED. 1998. Riluzole preserves motor function in a transgenic model of familial amyotrophic lateral sclerosis. Neurology 50:62-66.

Hageman G, van der Hoek J, van Hout M, van der Laan G, Steur EJ, de Bruin W, Herholz K. 1999. Parkinsonism, pyramidal signs, polyneuropathy, and cognitive decline after long-term occupational solvent exposure. J Neurol 246:198-206.

Hall ED, Oostveen JA, Gurney ME. 1998. Relationship of microglial and astrocytic activation to disease onset and progression in a transgenic model of familial ALS. Glia 23:249-256.

He Y, Appel S, Le W. 2001. Minocycline inhibits microglial activation and protects nigral cells after 6-hydroxydopamine injection into mouse striatum. Brain Res 909:187-193.

Heikkila RE, Hess A, Duvoisin RC. 1984. Dopaminergic neurotoxicity of 1-mthyl-4phenyl-1,2,5,6,-tetrahydropyridine in mice. Science 224:1451-1453.

Hertz CA. 2007. ER stress signaling and the BCL-2 family of proteins: From adaptation to irreversible cellular damage. Antioxid Redox Signal 9:2345-2355.

Heyer EJ, Chung EY, Van Woert M, Parise J. 1986. Characterization of dopamine receptors on neurons grown in primary dissociated cell culture from ventral mesencephalon of mouse. Brain Res 377:54-62.

Hickey P and Stacy M. 2011. Available and emerging treatments for Parkinson's disease: a review. Drug Des Dev Ther 5:241-254.

Hirsch E, Graybiel AM, Agid YA. 1988. Melanized dopaminergic neurons are differentially susceptible to degeneration in Parkinson's disease. Nature 334:345-348.

Hoehn MM. 1992. The natural history of Parkinson's disease in the pre-lovedopa and post-levodopa eras. Neurol Clin 10:331-339.

Hu JH, Chernoff K, Pelech S, Krieger C. 2003. Protein kinase and protein phosphatase expression in the central nervous system of G93A mSOD over-expressing mice. J Neurochem 85:422-431.

Hung HC and Lee EH. 1998. MPTP produces differential oxidative stress and antioxidative responses in the nigrostriatal and mesolimbic dopaminergic pathways. Free Radic Biol Med 24:76-84.

Hunot S, Dugas N, Faucheux B, Hartmann A, Tardieu M, Debre P, Agid Y, Dugas B, Hirsch EC. 1999. FcepsilonRII/CD23 is expressed in Parkinson's disease and induces, in vitro, production of nitric oxide and tumor necrosis factor-alpha in glial cells. J Neurosci 19:3440-3447.

Ilieva EV, Avala V, Jove M, Dalfo E, Cacabelos D, Povedano M, Bellmunt MJ, Ferrer I, Pamplona R, Porter-Otin M. 2007. Oxidative and endoplasmic reticulum stress interplay in sporadic amyotrophic lateral sclerosis. Brain 130:3111-3123.

Ilieva H, Polymenidou M, Cleveland DW. 2009. Non-cell autonomous toxicity in neurodegenerative disorders: ALS and beyond. J Cell Biol 187:761-772.

Iraz M, Ozerol E, Gulec M, Tasdemir S, Idiz N, Fadillioglu E, Naziroglu M, Akyol O. 2006. Protective effect of caffeic acid phenethyl ester (CAPE) administration on cisplatin-induced oxidative damage to liver in rat. Cell Biochem Funct 24:357-361.

Itoh K, Wakabayashi N, Katoh Y, Ishii T, Igarashi K, Engel JD, Yamamoto M. 1999. Keap1 represses nuclear activation of antioxidant responsive elements by Nrf2 through binding to the amino-terminal Neh2 domain. Genes Devel 13:76-86.

Ito D, Tanaka K, Suzuki S, Dembo T, Fukuuchi Y. 2001. Enhanced expression of Iba1, ionized calcium-binding adapter molecule 1, after transient focal cerebral ischemia in rat brain. Stroke 32:1208-1215.

Javoy F, Sotelo C, Herbert A, Agid Y. 1976. Specificity of dopaminergic neuronal degeneration induced by intracerebral injection of 6-hydroxydopamine in the nigrostriatal dopamine system. Brain Res 102:210-215.

Jellinger KA. 2009. Formation and development of Lewy pathology: A critical update. J Neurol 256S:270-279.

Johnson KA, Conn PJ, Niswender CM. 2009. Glutamate receptors as therapeutic targets for Parkinson's disease. CNS Neurol Disord Drug Targets 8:475-491.

Kaufmann P, Thompson JL, Levy G, Buchsbaum R, Shefner J, Krivickas LS, Katz J, Rollins Y, Barohn RJ, Jackson CE, Tiryaki E, Lomen-Hoerth C, Armon C, Tandan R, Rudnicki SA, Rezania K, Sufit R, Pestronk A, Novella SP, Heiman-Patterson T, Kasarskis EJ, Pioro EP, Montes J, Arbing R, Vecchio D, Barsdorf A, Mitsumoto H, Levin B. 2009. Phase II trial of CoQ10 for ALS finds insufficient evidence to justify phase III. Ann Neurol 66:235-244.

Kim WG, Mohney RP, Wilson B, Jeohn GH, Liu B, Hong JS. 2000. Regional difference in susceptibility to lipopolysaccharide-induced neurotoxicity in the rat brain: role of microglia. J Neurosci 20:6309-6316.

Kindt MV, Heikkila RE, Nicklas WJ. 1987. Mitochondrial and metabolic toxicity of 1-methyl-1,2,3,6-tetrahydropyridine. J Pharmacol Exp Ther 242:858-863.

Kitada T, Asakawa S, Hattori N, Matsumine H, Yamamura Y, Minoshima S, Yokochi M, Mizuno Y, Shimizu N. 1998. Mutations in the parkin gene cause autosomal recessive juvenile parkinsonism. Nature 392:605-608.

Klevenyi P, Andreassen O, Ferrante RJ Schleicher JR Jr, Friedlander RM, Beal MF. 1999. Transgenic mice expressing a dominant negative mutant interleukin-1beta converting enzyme show resistance to MPTP neurotoxicity. Neuroreport 10**:**635-638.

Knott C, Stern G, Wilkin GP. 2000. Inflammatory regulators in Parkinson's disease: iNOS, lipocortin-1, and cyclooxygenases-1 and -2. Mol Cell Neurosci 16**:**724-739.

Kohutnicka M, Lewandowska E, Kurkowska-Jastrzebska I, Czonkowski A, Czonkowska A. 1998. Microglial and astrocytic involvement in a murine model of Parkinson’s disease induced by 1-methyl-4-phenyl-1,2,3,6-tetrahydropyridine (MPTP). Immunopharmacol 39:167-180.

Kondo T, Ito T, Sugita Y. 1994. Bromocriptine scavenges methamphetamine-induced hydroxyl radicals and attenuates dopamine depletion in mouse straitum. Ann N Y Acad Sci 738:222-229.

Kowall NW, Hantraye P, Brouillet E, Beal MF, McKee AC, Ferrante RJ. 2000. MPTP induces alpha-synuclein aggregation in the substantia nigra of baboons. Neuroreport 11:211-213.

Kupsch A, Sautter J, Gotz ME, Breithaupt W, Schwarz J, Youdim MB, Riederer P, Gerlach M, Oertel WH. 2001. Monoamine oxidase-inhibition and MPTP-induced neurotoxicity in the non-human primate: comparison of rasagiline (TVP 1012) with selegiline. J Nerural Transm 108:985-1009.

Kurkowska-Jastrzebska I, Wronska A, Mohutnicka M. 1999. The inflammatory reaction following 1-methyl-4-phenyl-1,2,3,6-tetrahydropyridine intoxication in mouse. Exp Neurol 156:50-61.

Kurkowska-Jastrzebska I, Babiuch M, Joniec I, Przybykowski A, Czonkowski A, Czonkowska A. 2002. Indomethacin protects against neurodegeneration caused by MPTP intoxication in mice. Int Immunopharmacol 2:1213-1218.

Langston JW, Ballard P, Tetrud JW, Irwin I. 1983. Chronic Parkinsonism in humans due to a product of meperidine-analog synthesis. Science 219:979-980.

Langston JW and Irwin I. 1986. MPTP: current concepts and controversies. Clin Nueropharmacol 9:485-507.

Langston JW, Forno LS, Tetrud J, Reeves AG, Kaplan JA, Karluk D. 1999. Evidence of active nerve clel degeneration in the substantia nigra of humans years after 1-methyl-4-phenyl-1,2,3,6-tetrahydropyridine exposure. Ann Neurol 46:598-605.

Le WD, Xie WJ, Appel SH. 1999. Protective role of heme oxygenase-1 in oxidative stress-induced neuronal injury. J Neurosci Res 56:652-658.

Lee MK, Stirling W, Xu Y, Xu X, Qui D, Mandir AS, Dawson TM, Copeland NG, Jenkins NA, Price DL. 2002. Human alpha-synuclein-harboring familial Parkinson's disease-linked Ala-53 → Thr mutation causes neurodegenerative disease with alpha-synuclein aggregation in transgenic mice. Proc Natl Acad Sci USA 99:8968-8973.

Leenders K L and Oertel WH. 2001. Parkinson's disease: clincial signs and symptoms, neural mechanisms, positron emission tomography, and therapeutic interventsions. Neural Plast 8**:**99-110.

Li Q and Verma IM. 2002. NF-kappaB regulation in the immune system. Nat Rev Immunol 2:725-734.

Liberatore GT, Jackson-Lewis V, Vukosavic S, Mandir AS, Vila M, McAuliffe WG, Dawson VL, Dawson TM, Przedborski S. 1999. Inducible nitric oxide synthase stimulates dopaminergic neurodegeneration in the MPTP model of Parkinson disease. Nat Med 5**:**1403-1409.

Liou HH, Tasi MAC, Chen CJ, Jeng JS, Chang YC, Chen SY, Chen RC. 1997. Environmental risk factors and Parkinson's disease: a case-control study in Taiwan. Neurology 48:1583-1588.

Liu SF and Malik AB. 2006. NF-κB activation as a pathological mechanism of septic shock and inflammation. Am J Physiol 290:L622-L645.

Lotharius J, Dugan LL, O'Malley KL. 1999. Distinct mechanisms underlie neurotoxin-mediated cell death in cultured dopaminergic neurons. J Neurosci 19:1284-1293.

Luthman J, Fredriksson A, Sundstrom E, Jonsson G, Archer T. 1989. Selective lesion of central dopamine or noradrenaline neuron systems in the neonatal rat: motor behavior and monoamine alterations at adult stage. Behav Brain Res 33:267-277.

Lyons KE and Pahwa R. 2006. Conversion from sustained release carbidopa/levodopa to carbidopa/levodopa/entacapone (stalevo) in Parkinson disease patients. Clin Neuropharmacol 29:73-76.

Ma Z, Wei X, Fontanilla C, Noelker C, Dodel R, Hampel H, Du Y. 2006. Caffeic acid phenethyl ester blocks free radical generation and 6-hydroxydopamine-induced neurotoxicity. Life Sci 79**:**1307-1311.

Maguire-Zeiss KA. 2008. alpha-Synuclein: A therapeutic target for Parkinson's disease? Pharmacol Res 58:271-280.

Malgouris C, Daniel M, Doble A. 1994. Neuroprotective effects of riluzole on N-methyl-D-aspartate or veratridine-induced neurotoxicity in rat hippocampal slices. Neurosci Lett 177:95-99.

Manning-Bog AB, McCormack AL, Li J, Uversky VN, Fink AL, Di Monte DA. 2002. The herbicide paraquat causes up-regulation and aggregation of alpha-synuclein in mice: paraquat and alpha-synuclein. J Biol Chem 277:1641-1644.

Marsden CD. 1990. Parkinson's disease. Lancet 335:948-952.

Martin D, Thompson MA, Nadler JV. 1993. The neuroprotective agent riluzole inhibits release of glutamate and aspartate from slices of hippocampal area CA1. Eur J Pharmacol 250:473-476.

Martin ER, Scott WK, Nance MA, Watts RL, Hubble JP, Koller WC, Lyons K, Pahwa R, Stern MB, Colcher A, Hiner BC, Jankovic J, Ondo WG, Allen FH Jr, Goetz CG, Small GW, Masterman D, Mastaglia F, Laing NG, Stajich JM, Ribble RC, Booze MW, Rogala A, Hauser MA, Zhang F, Gibson RA, Middleton LT, Roses AD, Haines JL, Scott BL, Pericak-Vance MA, Vance JM. 2001. Association of single-nucleotide polymorphisms of the tau gene with late-onset Parkinson disease. JAMA 286:2245-2250.

Mattiazzi M, D'Aurelio M, Gajewski CD, Martushova K, Kiaei M, Beal MF, Manfredi G. 2002. Mutated human SOD1 causes dysfunction of oxidative phosphorylation in mitochondria of transgenic mice. J Biol Chem 277:292626-29633.

McCormack JG, Halestrap AP, Denton RM. 1990. Role of calcium ions in regulation of mammalian intramitochondrial metabolism. Physiol Rev 70:391-425.

McCormack AL, Thiruchelvam M, Manning-Bog, AB, Thiffault C, Langston JW, Cory-Slechta DA, Di Monte DA. 2002. Environmental risk factors and Parkinson's disease: selective degeneration of nigral dopaminergic neurons caused by the herbicide paraquat. Neurobiol Dis 10:119-127.

McGeer PL, Itagaki S, Boyes BE, McGeer EG. 1988. Reactive microglia are positive for HLA-DR in the substantia nigra of Parkinson's and Alzheimer's disease brains. Neurology 38:1285-1291.

Merello M, Starkstein S, Petracca G, Cataneo EA, Manes F, Leiguarda R. 1996. Drug-induced parkinsonism in schizophrenic patients: motor response and psychiatric changes after acute challenge with L-Dopa and apomorphine. Clin Neuropharmacol 19:439-443.

Michaluart P, Masferrer JL, Carothers AM, Subbaramaiah K, Sweifel BS, Koboldt C, Mestre JR, Grunberger D, Sacks PG, Tanabe T, Dannenberg AJ. 1999. Inhibitory effects of caffeic acid phenethyl ester on the activity and expression of cyclooxygenase-2 in human oral epithelial cells and in a rat model of inflammation. Cancer Res 59:2347-2352.

Michel PP and Hefti F. 1990. Toxicity of 6-hydroxydopamine and dopamine for dopaminergic neurons in culture. J Neurosci Res 26:428-435.

Mirza B, Hadberg H, Thomsen P, Moos T. 2000. The absence of reactive astrocytosis is indiciative of a unique inflammatory process in Parkinson's disease. Neuroscience 95:425-432.

Mitsumoto Y, Watanabe A, Mori A, Koga N. 1998. Spontaneous regeneration of nigrostriatal dopaminergic neurons in MPTP-treated C57BL/6 mice. Biochem Biophys Res Commun 248:660–663.

Mogi M, Harada M, Kondo T, Riederer P, Inagaki H, Minami M, Nagatsu T. 1994a. Interleukin-1 beta, interleukin-6, epidermal growth factor and transforming growth factor-alpha are elevated in the brain from parkinsonian patients. Neurosci Lett 180:147-150.

Mogi M, Harada M, Riederer P, Narabayashi H, Fujita K, Nagatsu T. 1994b. Tumor necrosis factor-alpha (TNF-α) increases both in the brain and in the cerebrospinal fluid from parkinsonian patients. Neurosci Lett 165:208-210.

Mogi M, Togari A, Ogawa M, Ikeguchi K, Shizuma N, Fan D, Nakano I, Nagatsu T. 1998. Effects of repeated systemic administration of 1-methyl-4-phenyl-1,2,3,6-tetrahydropyridine (MPTP) to mice on internleukin-1beta and nerve growth factor in the striatum. Neurosci Lett 250:25-28.

Mohanakumar KP, Muralikrishnan D, Thomas B. 2000. Neuroprotection by sodium salicylate against 1-methyl-4-phenyl-1,2,3,6-tetrahydropyridine-induced neurotoxicity. Brain Res 864:281-290.

Morris AD, Brux MD, Lond MB. 1955. James Parkinson: Born April 11, 1755. Lancet 265:761-763.

Muller T, Blum-Degen D, Przuntek H, Kuhn W. 1998. Interleukin-6 levels in cerebrospinal fluid inversely correlate to severity of Parkinson's disease. Acta Neurol Scand 98:142-144.

Mytilineou C and Cohen G. 1985. Deprenyl protects dopamine neurons from the neurotoxic effect of 1-methyl-4-phenylpyridinium ion. J Neurochem 45:1951-1953.

Nagai T, Inoue R, Inoue H, Suzuki N. 2003. Preparations and antioxidant properties of water extract of propolis. Food Chem 80:29-33.

Nagata T, Ilieva H, Murakami T, Shiote M, Narai H, Ohta Y, Hayashi T, Shoji M, Abe K. 2007. Increased ER stress during motor neuron degeneration in a transgenic mouse model of amyotrophic lateral sclerosis, Neurol Res 29:767-771.

Nagatsu T, Mogi M, Ichinose H, Togari A. 2000. Cytokines in Parkinson's disease. J Neural Transm 58S:143-151.

Natarajan K, Singh S, Burke TR Jr, Grunberger D, Aggarwal BB. 1996. Caffeic acid phenethyl ester is a potent and specific inhibitor of activation of nuclear transcription factor NF-κB. Proc Natl Acad Sci USA 93:9090-9095.

National Institute of Neurological Disorders and Stroke (NINDS). Parkinson's Disease: Hope Through Research. http://ninds.nih.gov/disorders/parkinsons_disease. Accessed September 2011.

Nicklas WJ, Yougster SK, Kindt MV, Heikkila RE. 1987. MPTP, MPP+ and mitochondrial function. Life Sci 40:721-729.

Nishibayashi S, Asanuma M, Kohno M, Gomez-Vargas M, Ogawa N. 1996. Scavenging effects of dopamine agonists on nitric oxide radicals. J Neurochem 67:2208-2211.

Noelker C, Bacher M, Gocke P, Wei X, Klockgether T, Du Y, Dodel R. 2005. The flavanoide caffeic acid phenethyl ester blocks 6-hydroxydopamine-induced neurotoxicity. Neurosci Lett 383:39-43.

Offen D, Beart PM, Cheung NS, Pascoe CJ, Hochman A, Gorodin S, Melamed E, Bernard R, Bernard O. 1998. Transgenic mice expressing human Bcl-2 in their neurons are resistant to 6-hydroxydopamine and 1-methyl-4-phenyl-1,2,3,6- tetrahydropyridine neurotoxicity. Proc Natl Acad Sci U S A 95**:**5789-5794.

Ogawa N, Tanaka K, Asanuma M, Kawai M, Masumizu T, Kohno M, Mori A. 1994. Bromocriptine protects mice against 6-hydroxydopamine and scavenges hydroxyl free radicals in vitro. Brain Res 657:207-213.

Olanow CW and Prusiner SB. 2009. Is Parkinson's disease a prion disorder? Proc Natl Acad Sci USA 106:12571-12572.

Orban Z, Mitsiades N, Burke TR, Tsokos M, Chrousos GP. 2000. Caffeic acid phenethyl ester induces leukocyte apoptosis, modulates nuclear factor-kappa B and suppresses acute inflammation. Neuroimmunomod 7:99-105.

Orth M and Tabrizi SJ. 2003. Models of Parkinson's disease. Mov Disord 18:729-737.

Otterbein LE, Saores MP, Yamashita K, Bach FH. 2003. Heme oxygenase-1: unleashing the protective properties of heme. Trends Immunol 24:449-455.

Pakkenberg B, Moller A, Gundersen HJG, Mouritzen Dam A, Pakkenberg H. 1991. The absolute number of nerve cells in substantia nigra in normal subjects and in patients with Parkinson's disease estimated with an unbiased stereological method. J Neurol Neurosurg Psych 54:30-33.

Parker WD Jr, Boyson SJ, Parks JK. 1989. Abnormalities of the electron transport chain in idiopathic Parkinson's disease. Ann Neurol 26:719-723.

Parkinson J. 1817. An Essay on the Shaking Palsy. London: Sherwood, Neely and Jones.

Petroske E, Meredith GE, Callen S, Totterdell S, Lau YS. 2001. Mouse model of Parkinsonism: a comparison between subacute MPTP and chronic MPTP/probenecid treatment. Neuroscience 106:589–601.

Polymeropoulos MH, Lavedan C, Leroy E, Ide SE, Dehejia A, Dutra A, Pike B, Root H, Rubenstein J, Boyer R, Stenroos ES, Chandrasekharappa S, Athanassiadou A, Papapetropoulos T, Johnson WG, Lazzarini AM, Duvoisin RC, Di Iorio G, Golbe LI, Nussbaum RL. 1997. Mutation in the alpha-synuclein gene identified in families with Parkinson's disease. Science 276:2045-2047.

Presgraves SP, Ahmed T, Borwege S, Joyce JN. 2004. Terminally differentiated SH-SY5Y cells provide a model system for studying neuroprotective effects of dopamine agonists. Neurotox Res 5:579-598.

Przedborski S, Levivier M, Jiang H, Ferreira M, Jackson-Lewis V, Donaldson D, Togosaki DM. 1995. Dose-dependent lesions of the dopaminergic nigrostriatal pathway induced by intrastriatal injection of 6-hydroxydopamine. Neuroscience 67:631-647.

Przedborski S, Burke R, Hen R. 2002. Resistance of alpha-synuclein null mice to the parkinsonian neurotoxin MPTP. Proc Natl Acad Sci USA 99:14524-14529.

Quinn NP. 1998. Classification of fluctuations in patients with Parkinson's disease. Neurology 51**:**S25-29.

Raivich G, Jones LL, Werner A, Bluthmann H, Doetschmann T, Kreutzberg GW. 1999a. Molecular signals for glial activation: pro- and anti-inflammatory cytokines in the injured brain. Acta Neurochir 73S:21-30.

Raivich G, Bohatschek M, Kloss CU, Werner A, Jones LL, Kreutzberg GW. 1999b. Neuroglial activation repertoire in the injured brain: graded response, molecular mechanisms and cues to physiological function. Brain Res Brain Res Rev 30:77-105.

Richardson JR, Quan Y, Sherer TB, Greenamyre JT, Miller GW. 2005. Paraquat neurotoxicity is distinct from that of MPTP and rotenone. Toxicol Sci 88:193-201.

Ricaurte GA, Langston JW, DeLanney LE, Irwin I, Peroutka SJ, Forno LS. 1986. Fate of nigrostriatal neurons in young mature mice given 1-methyl-4-phenyl-1,2,3,6-tetrahydropyridine: a neurochemical and morphological reassessment. Brain Res 376:117-124.

Roberts-Lewis JM and Siman R. 1993. Spectrin proteolysis in the hippocampus: a biochemical marker for neuronal injury and neuroprotection. Ann NY Acad Sci 679:78-86.

Rodriguez MC, Obeso JA, Olanow CW. 1998. Subthalamic nucleus-mediated excitotoxicity in Parkinson’s disease: a target for neuroprotection. Ann Neurol 44:S175-S188.

Rosen DR, Siddique T, Patterson D, Figlewicz DA, Sapp P, Hentati A, Donaldson D, Goto J, O'Regan JP, Deng HX, Rahmani Z, Krizus A, McKenna-Yasek D, Cayabyab A, Gaston SM, Berger R, Tanzi TE, Halperin JJ, Herzfeldt B, Van Den Bergh R, Hung WY, Bird T, Deng G, Mulder DW, Smyth C, Laing NG, Soriano E, Pericak-Vance MA, Haines J, Rouleau GA, Gusella JS, Horvitz HR, Brown Jr, RH. 1993. Mutations in Cu/Zn superoxide dismutase gene are associated with familial amyotrophic lateral sclerosis. Nature 362:59-62.

Rothstein JD and Kuncl RW. 1995. Neuroprotective strategies in a model of chronic glutamate-mediated motor neuron toxicity. J Neurochem 65:643-651.

Rothstein JD, Dykes-Hoberg M, Pardo CA, Bristol LA, Jin L, Kuncl RW, Kanai Y, Hediger MA, Wang Y, Schielke JP, Welty DF. 1996. Knockout of glutamate transporters reveals a major role for astroglial transport in excitotoxicity and clearance of glutamate. Neuron 16:675-686.

Rothstein JD, Patel S, Regan MR, Haenggeli C, Huang YH, Bergles DE, Jin L, Dykes Hoberg M, Vidensky S, Chung DS, Toan SV, Bruijn LI, Su ZZ, Gupta P, Fisher PB. 2005. Beta-lactam antibiotics offer neuroprotection by increasing glutamate transporter expression. Nature 433:73-77.

Rothstein JD. 2009. Current hypotheses for the underlying biology of amyotrophic lateral sclerosis. Ann Neurol **65**:S3-S9.

Rowland LP and Shneider NA. 2001. Amyotrophic lateral sclerosis. N Engl J Med 344:1688-1700.

Roy J, Minotti S, Dong L, Figlewicz DA, Durham HD. 1998. Glutamate potentiates the toxicity of mutant Cu/Zn-superoxide dismutase in motor neurons by postsynaptic calcium-dependent mechanisms. J Neurosci 18:9673-9684.

Russo A, Longo R, Vanella A. 2002. Antioxidant activity of propolis: role of caffeic acid phenethyl ester and galangin. Fitoterapia 73:S21-S29.

Sado M, Yamasaki Y, Iwanaga T, Onaka Y, Ibuki T, Nishihara S, Mizuguchi H, Momota H, Kishibuchi R, Hashimoto T, Wada D, Kitagawa H, Watanabe TK. 2009. Protective effect against Parkinson's disease-related insults through the activation of XBP1. Brain Res 1257:16-24.

Sanchez-Ramos J, Barrett JN, Goldstein M, Weiner WJ, Hefti F. 1986. 1-Methyl-4-phenylpyridinium (MPP+) but not 1-methyl-4-phenyl-1,2,3,6-tetrahydropyridine (MPTP) selectively destroys dopaminergic neurons in culures of dissociated rat mesencephalic neurons. Neurosci Lett 72:215-220.

Sasaki Y, Ohsawa K, Kanazawa H, Kohsaka S, Imai Y. 2001. Iba1 is an actin-cross-linking protein in macrophages/microglia. Biochem Biophys Res Comm 286:292-297.

Sato M, Horinouchi T, Sakurai M, Murakami N, Sato S, Kato M. 2003. Cyclosporin A reduces delayed motor neuron death after spinal cord ischemia in rabbits. Ann Thorac Surg 75:1294-1299.

Scapagnini G, Foresti R, Calabrese V, Giuffrida Stella AM, Green CJ, Motterlini R. 2002. Caffeic acid phenethyl ester and curcumin: a novel class of heme oxygenase-1 inducers. Molec Pharmacol 61:554-561.

Scapagnini G, Sonya V, Nader AG, Calogero C, Zella D, Fabio G. 2011. Modulation of Nrf2/ARE pathway by food polyphenols: a nutritional neuroprotective strategy for cognitive and neurodegenerative disorders. Mol Neurobiol 44:192-201.

Schapira AH, Cooper JM, Dexter D, Clark JB, Jenner P, Marsden CD. 1990. Mitochondrial complex I deficiency in Parkinson's disease. J Neurochem 54:823-827.

Scherman D, Desnos C, Darchen F, Pollak P, Javoy-Agid F, Agid Y. 1989. Striatal dopamine deficiency in Parkinson's disease: role of aging. Ann Neurol 26:551-557.

Schule B, Reijo Pera RA, Langston JW. 2009. Can cellular models revolutionize drug discovery in Parkinson's disease? Biochim Biophys Acta 1792:1043-1051.

Schwarting RK and Huston JP. 1996. The unilateral 6-hydroxydopamine lesion model in behavioral brain research. Analysis of functional deficits, recovery and treatments. Prog Neurobiol 50:275-331.

Scott S, Kranz JE, Cole J, Lincecum JM, Thompson K, Kelly N, Bostrom A, Theodoss J, Al-Nakhala BM, Vieira FG, Ramasubbu J, Heywood JA. 2008. Design, power, and interpretation of studies in the standard murine model of ALS. Amyotr Lat Scler 9:4-15.

Sejvar JJ, Holman RC, Bresee JS, Kochanek KD, Schonberger LB. 2005. Amyotrophic lateral sclerosis mortality in the United States, 1979-2001. Neuroepidemiology 25:144-152.

Shang T, Uihlein AV, Asten JV, Kalyanaraman B, Hillard CJ. 2003. 1-Methyl-4-phenylpyridinium accumulates in cerebellar granule neurons via organic cation transporter 3. J Neurochem 85**:**358-367.

Sherer TB, Trimmer PA, Borland K, Parks JK, Bennett JP Jr, Tuttle JB. 2001. Chronic reduction in complex I function alters calcium signaling in SH-SY5Y neuroblastoma cells. Brain Res 891:94-105.

Sherer TB, Kim JH, Betarbet R, Greenamyre JT. 2003. Subcutaneous rotenone exposure causes highly selective dopaminergic degeneration and alpha-synuclein aggregation. Exp Neurol 179:9-16.

Sian J, Dexter DT, Lees AJ, Daniel S, Agid Y, Javoy-Agid F, Jenner P, Marsden CD. 1994. Alterations in glutathione levels in Parkinson's disease and other neurodegenerative disorders affecting basal ganglia. Ann Neurol 36:348-355.

Siderowf A and Stern M. 2003. Update on Parkinson disease. Ann Intern Med 138:651-658.

Siman R, Noszek JC, Kegerise C. 1989. Calpain I activation is specifically related to excitatory amino acid induction of hippocampal damage. J Neurosci 9:1579-1590.

Son S and Lewis BA. 2002. Free radical scavenging and antioxidative activity of caffeic acid amide and ester analogues: structure-activity relationship. J Agric Food Chem 50:468-472.

Song DD and Haber SN. 2000. Striatal responses to partial dopaminergic lesion: evidence for compensatory sprouting. J Neurosci 20:5102–5114.

Spencer JPE. 2008. Flavonoids: modulators of brain function? Brit J Nutr 99:ES60-ES77.

Stacey M and Galbreath A. 2008. Optimizing long-term therapy for Parkinson disease: levodopa, dopamine agonists, and treatment-associated dyskinesia. Clin Neuropharmacol 31:51-56.

Stacy M. 2009. Medical treatment of Parkinson disease. Neurol Clin 27:605-631.

Tipton KF, Boyce S, O'Sullivan J, Davey GP, Healy J (2004) Monoamine oxidases: certainties and uncertainties. Curr Med Chem 11:1965-1982.

Stavrovskaya IG and Kristal BS. 2004. The powerhouse takes control of the cell: Is the mitochondrial permeability transition a viable therapeutic target against neuronal dysfunction and death? Free Rad Biol Med 38:687-697.

Stifanese R, Averna M De TR, Pedrazzi M, Beccaria F, Salamino F, Milanese M, Bonanno G, Pontremoli S, Melloni E. 2010. Adaptive modifications in the calpain/calpstatin system in brain cells after persistent alteration in Ca^{2+} homeostasis. J Biol Chem 285:631-643.

Stocke R, Yamamoto Y, McDonagh AF, Glazer AN, Ames BN. 1987. Bilirubin is an antioxidant of possible physiological importance. Science 235:1043-1046.

Strong MJ. 1999. Neurofilament metabolism in sporadic amyotrophic lateral sclerosis. J Neurol Sci 169:170-177.

Su ZZ, Grunberger D, Fisher PB. 1991. Suppression of adenovirus type 5 E1A-mediated transformation and expression of the transformed phenotype by caffeic acid phenethyl ester (CAPE). Mol Carcinog 4:231-242.

Su ZZ, Lin J, Grunberger D, Fisher PB. 1994. Growth suppression and toxicity induced by caffeic acid phenethyl ester (CAPE) in type 5 adenovirus-transformed rat embryo cells correlate directly with transformation progression. Cancer Res 54:1865-1870.

Swerdlow RH, Parks JK, Miller Sw, Tuttle JB, Trimmer PA, Sheehan JP, Bennett JP Jr, Davis RE, Parker WD Jr. 1996. Origin and functional consequences of the complex I defect in Parkinson's disease. Ann Neurol 40:663-671.

Takada M, Sugimoto T, Hattori T. 1988. Cerebellar Purkinje cell: Another neuronal basis of MPTP-induced parkinsonism. Soc Neurosci Abstr 14:1026.

Talpade DJ, Greene JG, Higgins DS Jr, Greenamyre JT. 2000. In vivo labeling of mitochondrial complex I (NADH:ubiquinone oxidoreductase) in rat brain using [(3)H]dihydrorotenone. J Neurochem 75:2611-2621.

Tan J, Ma Z, Han L, Du R, Zhao L, Wei X, Hou D, Johnstone BH, Farlow MR, Du Y. 2005. Caffeic acid phenethyl ester possesses potent cardioprotective effects in a rabbit model of acute myocardial ischemia-reperfusion injury. Am J Physiol Heart Circ Physiol 289:H2265-H2271.

Tandan R and Bradley WG. 1985. Amyotrophic lateral sclerosis: Part 1. Clinical features, pathology, and ethical issues in management. Ann Neurol 18:271-280.

Tanner CM, Ross GW, Jewell SA, Hauser RA, Jankovic J, Factor SA, Bressman S, Deligtisch A, Marras C, Lyons KE, Bhudhikanok GS, Roucoux DF, Meng C, Abbott RD, Langston JW. 2009. Occupation and risk of parkinsonism: A multicenter case-control study. Arch Neurol 66:1106-1113.

Teismann P and Ferger B. 2001. Inhibition of the cyclooxygenase isoenzymes COX-1 and COX-2 provide neuroprotection in the MPTP-mouse model of Parkinson's disease. Synapse 39:167-174.

Tikka T, Fiebich BL, Goldsteins G, Keinanen R, Koistinaho J. 2001. Minocycline, a tetracycline derivative, is neuroprotective against excitotoxicity by inhibiting activation and proliferation of microglia. J Neurosci 21**:**2580-2588.

Tipton KF and Singer TP. 1993. Advances in our understanding of the mechanisms of the neurotoxicity of MPTP and related compounds. J Neurochem 61**:**1191-1206.

Tolwani RJ, Jakowec MW, Petzinger GM, Green S, Waggie K. 1999. Experimental models of Parkinson's disease: insights from many models. Lab Anim Sci 49**:**363-371.

Tortarolo M, Veglianese P, Calvaresi N, Botturi A, Rossi C, Giorgini A, Migheli A, Bendotti C. 2003. Persistent activation of p38 mitogen-activated protein kinase in a mouse model of familial amyotrophic lateral sclerosis correlates with disease progression. Mol Cell Neurosci 23:180-192.

Tradewell ML and Durham HD. 2010. Calpastatin reduces toxicity of SOD1G93A in a culture model of amyotrophic lateral sclerosis. Neuroreport 21:976-979.

Turner BJ and Talbot K. 2008. Transgenics, toxicity and therapeutics in rodent models of mutant SOD1-mediated familial ALS. Prog Neurobiol 85:94-134.

Ungerstedt U. 1968. 6-Hydroxydopamine induced degeneration of central monoamine neurons. Eur J PHarmacol 5:107-110.

Ungerstedt U and Arbuthnott GW. 1970. Quantitative recording of rotational behavior in rats after 6-hydroxydopamine lesions of the nigrostriatal dopamine system. Brain Res 24:485-493.

US Census Bureau. US interim projections by age, sex, race, and hispanic origin: 2000-2050. http://www.census.gov/population/www/projections/usinterimproj. Accessed September 2011.

Valko M, Leibfritz D, Moncol J, Cronin MT, Mazur M, Telser J. 2007. Free radicals and antioxidants in normal physiological functions and human disease. Int J Biochem Cell Biol 39:44-84.

Veech GA, Dennis J, Keeney PM, Fall CP, Swerdlow RH, Parker WD Jr, Bennet JP Jr. 2000. Disrupted mitochondrial electron transport function increases expression of anti-apoptotic bcl-2 and bcl-X(L) proteins in SH-SY5Y neuroblastoma and in Parkinson disease cybrid cells through oxidative stress. J Neurosci Res 61:693-700.

Venton BJ, Zhang H, Garris PA, Phillips PE, Sulzer D, Wightman RM. 2003. Real-time decoding of dopamine concentration changes in the caudate-putamen during tonic and phasic firing. J Neurochem 87:1284-1295.

Vila M, Vuksavic S, Jackson-Lewis V, Neystat M, Jakowec M, Przedborski S. 2000. Alpha-synuclein up-regulation in substantia nigra dopaminergic neurons following administration of the parkinsonian toxin MPTP. J Neurochem 74:721-729.

Vila M and Przedborski S. 2003. Targeting programmed cell death in neurodegenerative diseases. Nat Rev Neurosci 4:365-375.

Viswanath V, Wu Y, Boonplueang R, Chen S, Stevenson FF, Yantiri F, Yang L, Beal MF, Andersen JK. 2001. Caspase-9 activation results in downstream caspase-8 activation and bid cleavage in 1-methyl-4-phenyl-1,2,3,6-tetrahydropyridine-induced Parkinson's disease. J Neurosci 21:9519-9528.

Von Coelln R, Kugler S, Bahr M, Weller M, Dichgans J, Schulz JB. 2001. Rescue from death but not from functional impairment: caspase inhibition protects dopaminergic cells against 6-hydroxydopamine-induced apoptosis but not against the loss of their terminals. J Neurochem 77:263-273.

Voskuhl RR, Peterson RS, Song B, Ao Y, Morales LBJ, Tiwari-Woodruff S, Sofroniew MV. 2009. Reactive astrocytes form scar-like perivascular barriers to leukocytes during adaptive immune inflammation of the CNS. J Neurosci 29:11511-11522.

Wakabayashi N, Dinkova-Kostova AT, Holtzclaw WD, Kang MI, Kobayashi A, Yamamoto M, Kensler TW, Talalay P. 2004. Protection against electrophile and oxidant stress by induction of the phase 2 response: fate of cysteines of the Keap1 sensor modified by inducers. Proc Natl Acad Sci USA 101:2040-2045.

Wang KK, Posmantur R, Nath R, McGinnis K, Whitton M, Talanian RV, Glantz SB, Morrow JS. 1998. Simultaneous degradation of alphaII- and betaII-spectrin by caspase 3 (CPP32) in apoptotic cells. J Biol Chem 273:22490-22497.

Wang R and Zhang D. 2005. Memantine prolongs survival in an amyotrophic lateral sclerosis mouse model. Eur J Neurosci 22:2376-2380.

Wang X, Stavchansky S, Kerwin SM, Bowman PD. 2010. Structure-activity relationships in the cytoprotective effect of caffeic acid phenethyl ester (CAPE) and fluorinated derivatives: effects on heme oxygenase-1 induction and antioxidant activities. Eur J Pharmacol 635:16-22.

Wei X, Zhao L, Ma Z, Holtzman DM, Yan C, Dodel RC, Hampel H, Oertel W, Farlow MR, Du Y. 2004. Caffeic acid phenethyl ester prevents neonatal hypoxic-ischaemic brain injury. Brain 127**:**2629-2635.

Wei X, Ma Z, Fontanilla CV, Zhao L, Xu ZC, Taggliabraci V, Johnstone BH, Dodel RC, Farlow MR, Du Y. 2008. Caffeic acid phenethyl ester prevents cerebellar granule neurons (CGNs) against glutamate-induced neurotoxicity. Neuroscience 155:1098-1105.

Wei X, Du Z, Zhao L, Feng D, Wei G, He Y, Tan J, Lee WH, Hampel H, Dodel R, Johnstone BH, March KL, Farlow MR, Du Y. 2009. IFATS collection: the conditioned media of adipose stromal cells protect against hypoxia-ischemia-induced brain damage in neonatal rats. Stem Cells 27:478-488.

Weintraub D, Siderowf AD, Potenza MN, Goveas J, Morales KH, Duda JE, Moberg PJ, Stern MB. 2006. Association of dopamine agonist use with impulse control disorders in Parkinson disease. Arch Neurol 63:969-973.

Weintraub D, Koester J, Potenza MN, Siderowf AD, Stacy M, Voon V, Whetteckey J, Wunderlich GR, Lang AE. 2010. Impulse control disorders in Parkinson disease: a cross-sectional study of 3090 patients.

Wengenack TM, Holasek SS, Montano CM, Gregor D, Curran GL, Poduslo JF. 2004. Activation of programmed cell death markers in ventral horn motor neurons during early presymptomatic stages of amyotrophic lateral sclerosis in a transgenic mouse model. Brain Res 1027:73-86.

Wichers M, Aguilera M, Kenis G, Krabbendam L, Myin-Germeys I, Jacobs N, Peeters F, Derom C, Vlietinck R, Mengelers R, Delespaul P, Van Os J. 2007. The catechol-O-methyl transferase Val158Met polymorphism and experience of reward in the flow of daily life. Neuropsychopharm 33:3030-3036.

Windle WF and Cammermayer J. 1958. Functional and structural observations on chronically reserpinized monkeys. Science 127:1503-1504.

Wootz H, Hansson I, Korhonen L, Napankangas U, Lindholm D. 2004. Caspase-12 cleavage and increased oxidative stress during motoneuron degeneration in transgenice mouse model of ALS. Biochem Biophys Res Commun 322:281-286.

Wootz H, Hansson I, Korhonen L, Lindholm D. 2006. XIAP decreases caspase-12 cleavage and calpain activity in spinal cord of ALS transgenic mie. Exp Cell Res 312:1890-1898.

Wu DC, Jackson-Lewis V, Vila M, Tieu K, Teismann P, Vadseth C, Choi DK, Ischiropoulos H, Przedborski S. 2002. Blockade of microglial activation is neuroprotective in the 1-methyl-4-phenyl-1,2,3,6-tetrahydropyridine mouse model of Parkinson disease. J Neurosci 22:1763-1771.

Wu DC, Re DB, Nagai M, Ischiropoulos H, Przedborski S. 2006. The inflammatory NADPH oxidase enzyme modulates motor neuron degeneration in amyotrophic lateral sclerosis in mice. Proc Natl Acad Sci USA 103:12132-12137.

Yamanaka K, Chun SJ, Boillee S, Fujimori-Tonou N, Yamashita H, Gutmann DH, Takahashi R, Misawa H, Cleveland DW. 2008. Astrocytes as determinants of disease progression in inherited amyotrophic lateral sclerosis. Nat Neurosci 11:251-253.

Yildiz Y, Serter M, Ek RO, Ergin K, Cecen S, Demir EM, Yenisey C. 2009. Protective effects of caffeic acid phenethyl ester on intestinal ischemia-reperfusion injury. Dig Dis Sci 54:738-744.

Yokoyama H, Kuroiwa Y, Kasahara J, and Araki T. 2011. Neuropharcological approach against MPTP (1-methyl-4-phenyl-1,2,3,6-tetrahydrophyridine)-induced mouse model of Parkinson's disease. Acta Neurobiol Exper 71:269-280.

Yoshioka M, Tanaka K, Miyazaki I, Fujita N, Higashi Y, Asanuma M, Ogawa N. 2002. The dopamine agonist cabergoline provides neuroprotection by activation of the glutathione system and scavenging free radicals. Neurosci Res 43:259-267.

Young AMJ, Crowder JM, Bradford HF. 1988. Potentiation by kainite of excitatory amino acid release in striatum: Complementary *in vivo* and *in vitro* experiments. J Neurochem 50:337-345.

CURRICULUM VITAE

Christine V. Fontanilla

EDUCATION

1993 – 1997	**Bachelor of Science:** Biology **Bachelor of Arts:** Chemistry Minor: Psychology Indiana University, Bloomington, IN
1998 – 2000	**Master of Science:** Cell Biology, Neurobiology & Anatomy Loyola University Chicago, Maywood, IL
2005 – 2012	**Doctor of Philosophy:** Medical Neuroscience Minor: Anatomy Indiana University School of Medicine, Indianapolis, IN

FELLOWSHIPS

2000 – 2001	IUSM Graduate Fellowship for First-Year Students
2005 – 2006	Scottish Rite Fellowship for Neurobiology Graduate Students
2006 – 2007	IUSM Minor in Aging Fellowship
Fall 2010	The Institute on Teaching and Mentoring Fellowship

AWARDS

Fall 1999	28th Autumn Immunology Conference Loyola Travel Award
2009 – 2011	AAAS/Science Full Membership sponsored by IUSM

TEACHING EXPERIENCE

2010	Graduate Teaching Assistant for G717: Biomedical Science III Cellular Basis of Systems Biology Indiana University School of Medicine, Indianapolis, IN

SERVICES

Fall 2002	Indiana University Brain Awareness Week Representative
2005 – 2006	Medical Neurosciences Program Student Representative
Spring 2009	Indiana University School of Medicine Statehouse Day Student Representative

PROFESSIONAL MEMBERSHIPS

2006 – 2012	Society for Neuroscience
2009 – 2012	American Association for the Advancement of Science

ORAL PRESENTATIONS

1999	"Anti-interleukin-6 antibody treatment following burn trauma with prior acute ethanol exposure." 28th Autumn Immunology Conference. Chicago, IL. November 1999.

POSTER PRESENTATIONS

2002 "Effects of concurrent access to and deprivation of ethanol and saccharine on the expression of a deprivation effect in alcohol-preferring (P) rats." 25th Annual Scientific Meeting of the Research Society on Alcoholism. San Francisco, CA. July 2002.

2007 "Caffeic acid phenethyl ester treatment in a mouse model of ALS." 37th Annual Meeting of the Society for Neuroscience. San Diego, CA. November 2007.

2008 "Treatment with adipose stem cell conditioned media in a mouse model of amyotrophic lateral sclerosis." 38th Annual Meeting of the Society for Neuroscience. Washington, D.C. November 2008.

PUBLICATIONS

Fontanilla CV, Faunce DE, Gregory MS, Colantoni A, Messingham KAN, Duffner LA, Kovacs EJ (2000) Anti-interleukin-6 antibody treatment restores cell mediated immune function in mice with acute alcohol exposure before burn trauma. *Alcohol: Clinical and Experimental Research* 24:1392-1399.

Colantoni A, Duffner LA, De Maria N, **Fontanilla CV**, Messingham KAN, Van Thiel DH, Kovacs EJ (2000) Dose-dependent effect of ethanol on hepatic oxidative stress and IL-6 production following burn injury in the mouse. *Alcohol: Clinical and Experimental Research* 24:1443-1448.

Durbin EA, Gregory MS, Messingham KAN, **Fontanilla CV**, Duffner LA, Kovacs EJ (2000) The role of interleukin-6 in interferon-gamma production in thermally-injured mice. *Cytokine* 12(11):1669-1675.

Messingham KAN, **Fontanilla CV**, Colantoni A, Duffner LA, Kovacs EJ (2000) Cellular immunity after alcohol exposure and burn injury: dose and time dependence. *Alcohol* 22:35-44.

Choudhry M, Messingham KAN, Namak S, Colantoni A, **Fontanilla CV**, Duffner LA, Sayeed MM, Kovacs EJ (2000) Ethanol exacerbates T cell dysfunction after thermal injury. *Alcohol* 21:239-243.

Ma Z, Wei X, **Fontanilla CV**, Noelker C, Dodel R, Farlow M, Du Y (2006) Caffeic acid phenethyl ester blocks free radical generation and 6-hydroxydopamine-induced neurotoxicity. *Life Sciences* 79:1307-1311.

Wei X, Chen X, **Fontanilla C**, Dodel R, Hampel H, Farlow M, Du Y (2007) C/T conversion alters Interleukin-1A promoter function in a human astrocyte cell line**.** *Life Sciences* 80:1152-1156.

Wei X, Ma Z, **Fontanilla CV**, Zhao L, Xu ZC, Taggliabraci V, Johnstone BH, Dodel RC, Farlow MR, Du Y (2008) Caffeic acid phenethyl ester prevents cerebellar granule neurons (CGNs) against glutamate-induced neurotoxicity. *Neuroscience* 155:1098-1105.

Gu H, Wei X, Monnot AD, **Fontanilla CV**, Behl M, Farlow MR, Zheng W, Du Y (2011) Lead exposure increases levels of β-amyloid in the brain and CSF and inhibits LRP1 expression in APP transgenic mice. *Neuroscience Letters* 490:16-20.

Fontanilla CV, Ma Z, Wei X, Klotsche J, Zhao L, Wisniowski P, Lee W, Dodel RC, Farlow MR, Oertel WH, Du Y (2011) Caffeic acid phenethyl ester prevents 1-methyl-4-phenyl-1,2,3,6-tetrahydropyridine-induced neurodegeneration. *Neuroscience* 188:135-41.

Fontanilla CV, Wei X, Zhao L, Johnstone B, Pascuzzi RM, Farlow MR, Du Y (2012) Caffeic acid phenethyl ester extends survival of a mouse model of amyotrophic lateral sclerosis. *Neuroscience*, *Epub ahead of print*.

Ma Z, **Fontanilla CV**, Tan J, Wei X, Tu P, Du Y. Minocycline protects neurons against glial cells-mediated bilirubin neurotoxicity. *Neurochemistry International*, *Submitted*.

Fontanilla CV, Wei X, Cheng P, Pascuzzi RM, Farlow MR, Du Y. Adipose-derived stem cell conditioned media delays disease progression of the SOD1-G93A mouse model of amyotrophic lateral sclerosis. *In Preparation.*

ABSTRACTS

Messingham KAN, Colantoni A, **Fontanilla CV**, Heinrich SA, Kovacs EJ. The effect of estrogen on IL-6-mediated immune suppression in male mice following ethanol exposure and burn injury. 24th Annual RSA Scientific Meeting. Montreal, Quebec, Canada. June 2001.

Kovacs EJ, **Fontanilla CV**, Colantoni A, Messingham KAN. Effects of ethanol on post-injury immunity are dose and time dependent. 24th Annual RSA Scientific Meeting. Montreal, Quebec, Canada. June 2001.

Messingham KAN, **Fontanilla CV**, Duffner LA, Kovacs EJ. Estrogen treatment restores immunity in male mice given alcohol prior to burn injury via suppression of IL-6 production. 29th Autumn Immunology Conference. Chicago, IL. November 2000.

Kovacs EJ, Messingham KAN, Durbin EA, **Fontanilla CV**, Kopf M, Duffner LA. Improved survival and immunity in interluekin-6 (IL-6) deficient mice subjected to burn trauma. 3rd Joint Meeting of the ICS/ISICR. Amsterdam, Netherlands. November 2000.

Messingham KAN, **Fontanilla CV**, Duffner LA, Kovacs EJ. Estrogen improves cellular immune function in male mice subjected to burn injury with prior ethanol. 34th Annual Meeting for the Society for Leukocyte Biology. Cambridge, MA. October 2000.

Messingham KAN, **Fontanilla CV**, Colantoni A, Emanuele MA, Duffner LA, Kovacs EJ. The role of gonadal steroids in controlling IL-6 production and immune function after thermal injury with prior ethanol exposure. 7th Annual Conference of the International Cytokine Society. Hilton Head, SC. December 1999.

Colantoni A, Duffner LA, De Maria N, **Fontanilla CV**, Messingham KAN, Van Thiel DH, Emanuele MA, Kovacs EJ. Effect of ethanol on hepatic production of interleukin-6 following burn injury. 7th Annual Conference of the International Cytokine Society. Hilton Head, SC. December 1999.

Fontanilla CV, Messingham KAN, Duffner LA, Colantoni A, Kovacs EJ. Anti-IL-6 antibody treatment following burn trauma with prior alcohol exposure. 28th Autumn Immunology Conference. Chicago, IL. November 1999.

Messingham KAN, **Fontanilla CV**, Colantoni A, Emanuele MA, Duffner LA, Kovacs EJ. Estrogen control of IL-6 production restores immune function after thermal injury. 28th Autumn Immunology Conference. Chicago, IL. November 1999.

Colantoni A, Duffner LA, **Fontanilla CV**, Messingham KAN, Van Thiel DH, Kovacs EJ. Dose dependent effect of alcohol on hepatic production of IL-6 following burn injury in a mouse model. 28th Autumn Immunology Conference. Chicago, IL. November 1999.

Rodd-Henricks ZA, **Fontanilla CV**, Bell RL, Kuc KA, Murphy JM, McBride WJ, Lumeng L, Li TK. Effects of concurrent access to and deprivation of ethanol and saccharine on the expression of a deprivation effect in alcohol-preferring (P) rats. 25th Annual Scientific Meeting of the Research Society on Alcoholism. San Francisco, CA. July 2002.

Fontanilla CV, Wei G, He Y, Farlow MR, Du Y. Caffeic acid phenethyl ester treatment in a mouse model of ALS. 37th Annual Meeting of the Society for Neuroscience. San Diego, CA. November 2007.

Fontanilla CV, Cheng P, Farlow MR, Pascuzzi R, Du Y. Treatment with adipose stem cell conditioned media in a mouse model of amyotrophic lateral sclerosis." 38th Annual Meeting of the Society for Neuroscience. Washington, D.C. November 2008.